Max-Planck-Institut für Kolloid- und Grenzflächenforschung

Lignin Valorization: Extraction, Characterization and Applications

Dissertation

Zur Erlangung des akademischen Grades
„Doctor rerum naturalium“
(Dr.rer.nat.)
in der Wissenschaftsdisziplin „Kolloidchemie“

Eingereicht an der
Mathematisch-Naturwissenschaftlichen Fakultät
der Universität Potsdam

von

Micaela Graglia

Potsdam, September 2016

Published online at the
Institutional Repository of the University of Potsdam:
URN urn:nbn:de:kobv:517-opus4-104863
http://nbn-resolving.de/urn:nbn:de:kobv:517-opus4-104863

Table of Contents

1. INTRODUCTION

1.1 Motivation

Our current lifestyle requires the consumption of a huge amount of energy, fuel and chemicals. Approximately 82 % of world energy,[1] 97 % of fuel consumed in the USA[2] and most of the materials we use derive from fossil feedstock, namely crude oil, coal and natural gas. Although it took millions of years for such resources to be accumulated, it has been estimated that their depletion will occur within 230 years. Once out of stock, fossil reserves will not be regenerated and therefore they are considered non-renewable.[3] Moreover, their global distribution is not homogeneous: the OPEC (Organization of the exporting countries) estimated that 80 % of the world's crude oil reserves come from just six politically unstable countries,[4] which causes massively fluctuating feedstock prices and an unbalanced geopolitical economy. Such political issues, together with the continuous growth of global consumption and the increasing social pressure for a more sustainable lifestyle, are shifting the global attention towards possible alternatives to petroleum.[5] Aside from a wide range of short term solutions, such as the decrease of consumption and the improvement of domestic and industrial energy efficiency, chemists have the responsibility to find valid alternatives to the classical fossil feedstock for the production of fuel and materials. Remarkable progress in the production of energy has been obtained by the use of solar, hydroelectric, wind and geothermal power. Biomasses, defined as "biological material coming from living organism",[6] represent an additional alternative source to oil for the production of both fuel and materials. Biomass such as plants, trees, algae, industrial and domestic organic waste as well as residues of agriculture or dedicated crops, are inexhaustible because they can be replaced by newly grown biomass. Therefore, they are considered to be renewable and sustainable. The use of biomass as a feedstock for materials is not a new concept indeed, as far back as the 1600's BC, Mesoamericans were preparing balls, bands and figurines by processing natural rubber.[7] The use of pitch for the boat-building process was already known to early Egyptian (3rd millennium BC). Later on, in 1911, Worden reported the benefits of nitro-functionalized cellulose to obtain nitrocellulose.[8] In the 20th century the large abundance and the consequently low cost of fossil feedstock led to their massive use for the production of energy and synthetic plastics such as polyethylene, polypropylene and polystyrene. The latter materials significantly improved the quality of our lives. However, the current depletion of fossil raw materials makes the use of alternative feedstock such as biomass necessary, for a partial or total substitution of petroleum derivatives in fuel and material production.[9] The current

and future challenge for the scientific community is the development of processing methods for renewable feedstocks which afford the achievement of more sustainable products. In this regard, the integration of biomass into the biorefinery industry, which means the production of different bio-products utilizing the various components of the biomass, represents the main goal (Fig.1.1).

Figure 1.1 *Schematic concept of a biorefinery*

Classical examples of modern biorefineries include the production of lactic acid by fermentation, during bioethanol synthesis or the glycerol generation, which is obtained as byproduct of the biodiesel production.[5] In line with the previous examples, most of the biorefinery processes are still connected with the use of raw materials that come from crops dedicated to food and animal feed production,[10] causing ethical and social issues. For this reason, the attention is shifting from these so called "first generation biofuels" to "second generation biofuels", which rely on the use of non-edible biomass, such as lignocellulose (LgC).

Lignocellulosic material makes up the cell wall of plants and can be found in forest residues, discarded food crops and in municipal and industrial wastes. LgC is an aggregate made of a carbohydrate fraction (cellulose and hemicellulose) and a polyphenolic fraction (lignin), which should be isolated from each other in order to be better valorized. The production of levulinic acid and hydroxymethylfurfural from the carbohydrate fraction of LgC already poses as a case of lignocellulose valorization scaled up to industry.[11] Currently, vanillin is the only commercial product obtained from the polyphenolic component of LgC.[12] Lignin is the most abundant aromatic source on the earth, cheap and widely available; however 98 %

of it is still burned to power mills in paper industry, which is the main source of lignin as a byproduct of the paper production. In the next section, lignin's structure and the role of lignin in plants will be discussed in detail.

1.2 Lignocellulosic biomass

1.2.1 Cell wall structure in plants

Lignocellulosic biomass is a complex material synthesized by plants during the formation of the cell wall. LgC is a semi-rigid structure external to the cytoplasmic membrane, which protects the cytoplasm from physical, chemical and microbiological stress and facilitates the transports of water and nutrients.[13] Lignocellulose constitutes of polysaccharide polymers such as cellulose and hemicellulose, as a percentage of the bulk material between 40-50 % and 20-35 % respectively,[14] as well as of the aromatic polymer lignin (ca. 15-30 %).[15] Minor quantities of proteins and several inorganic and pectic substances are also present. The amount and the proportion of each component depends on the species and the age of the plant, as well as the type of cell within the same plant.[16] The different constituents interact by means of ionic, hydrogen, and covalent bonds as well as hydrophobic forces giving rise to a layered-structure (Fig.1.2). The most external layer, the *middle lamella* made almost only of pectic molecules, is the first layer to be built from the plant. Following that, there is the primary wall, a polysaccharide-rich layer made mainly of cellulose, hemicellulose and pectic polysaccharides. The last and innermost wall to be synthesized is the secondary wall, where most of the lignin is accumulated.[17]

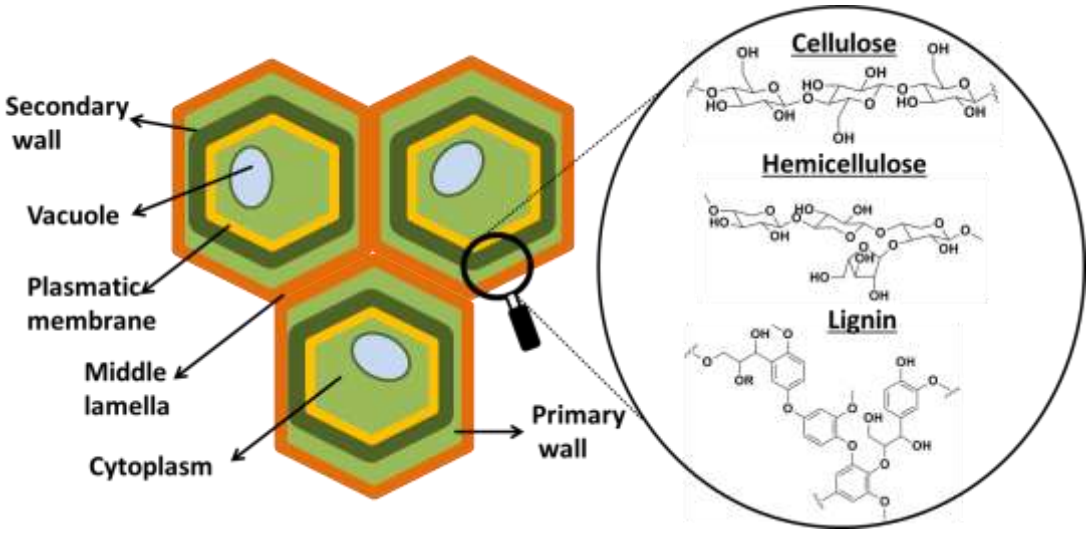

Figure 1.2 *Schematic representation of a plant cell wall. The main components of the primary and secondary wall are highlighted (right)*

1.2.2 Cellulose (C)

Cellulose is a high molecular weight, linear and crystalline homopolymer which provides tensile strength in the primary cell wall.[18] Cellulose is formed by the interconnection of glucose monomers through β-1-4 glycosidic bonds. Unlike starch, within which glucose units are linked by α-1-4 glycosidic bonds, the β-configuration confers a linear conformation. The linearity of cellulose gives rise to a distinct organization in microfibrils, in which every microfibril is surrounded by a matrix made of hemicellulose, pectic substances and lignin, which works as a binder between the components. In native cellulose (cellulose I), two intramolecular and one intermolecular hydrogen bonds enhance the stability and the stiffness of the fibrils, making cellulose insoluble in water and in most organic solvents.[16] Cellulose is biosynthesized by the plasmatic membrane and directly deposited in the primary wall in the form of microfibrills, whereas the matrix is transported by exocytosis from the Golgi membrane.[17]

.1.2.3 Hemicellulose (HmC)

Together with the pectic substances, hemicellulose constitutes the matrix that surrounds cellulose fibrils. HmC is a low molecular weight heteropolymer with an amorphous structure, it is therefore easy to depolymerize. It is composed of hexose and pentose sugars and strongly interacts with cellulose fibrils *via* hydrogen bonds. Hemicellulose monomers can be substituted by small side chain, such as methyl or acetyl groups, as well as by bulkier side groups, such as glucose and mannose. The exact composition of HmC depends on the plant species: for instance xylose is abundant both in hardwood and grass, whereas mannose is more common in softwood wall cell.[16, 19]

1.2.4 Lignin

In the cell wall, lignin fills the space between cellulose and hemicellulose holding the matrix and the fibrils together, as a resistant glue does. Moreover, lignin provides waterproofing and increases the physical and biological strength, bringing rigidity and protection against microbial attack.[20, 21] In the following section, lignin structure and its linkages with the carbohydrate fraction in the lignocellulosic biomass will be analyzed.

1.3 Lignin

1.3.1 Lignin structure

The word "lignin" comes from the Latin word "Lignum", which means wood. Lignin is an aromatic, amorphous and three dimensional heteropolymer (Fig. 1.2), which is present both in vascular plants such as angiosperms and gymnosperms and in non-vascular plants such as algae; in each case, its structure is different depending on the plant species.[22] In order to be studied, lignin is isolated from the other components of lignocellulosic biomass through several possible methods, which will be described in section 1.5. The structure of the isolated lignin is influenced by the extraction process as well as by the plant species; the structure of the extracted lignin is therefore always different from its native form. For this reason, lignin structures currently available in literature are only models that try to describe the yet-unknown pristine form of the polymer.

Lignin is synthesized by the cell at the end of its growth phase. The biosynthesis includes the radical polymerization of three main phenylpropanoid monomers (monolignols), namely coniferyl, sinapyl and p-coumaryl alcohol, which are thus incorporated in the form of guaiacyl (G), syringyl (S) and p-hydroxyphenyl (H) units (Fig.1.3).[21] Monolignols are synthetized in the cytoplasm and transported to the cell wall where the formation of lignin, named lignification, takes place (paragraph 1.3.2). Despite the fact that the monolignols reported in Fig.1.3 are the most abundant in lignin's structure, other less-common monomers are present, and they are all modified forms of hydroxycinnamyl alcohol (Fig.1.3, right).[23]

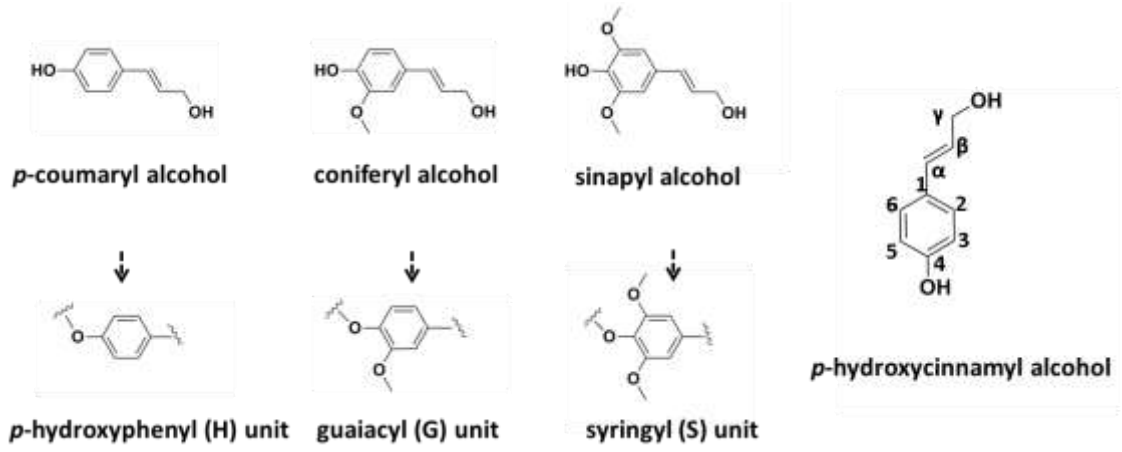

Figure 1.3 Above- *Main three lignin-building-blocks (monolignols).* **Below-** *The corresponding units found in the lignin-structure, p-hydroxyphenyl (H), guaiacyl (G) and syringyl (S) units.* **Right-** *p-hydroxycinnamyl alcohol structure with numbered carbon atoms.*

According to their origin, lignins are classified as softwood (gymnosperms), hardwood (angiosperms) and grass lignin. Softwood lignin is richer in G units, the hardwood form possesses a higher amount of S units, while grass lignin is reported to have an equal amount of G, S and H units.[24] The most important functional groups in the structure are methoxyl, hydroxyl, carboxyl and carbonyl groups highlighted in Fig.1.4.

The complexity of the structure is not only due to the different composition and ratio of monomers, but also to the wide possibility of linkages between them. These bonds fall into eight categories (Fig. 1.4):

- carbon-carbon bonds: β- β´, β-1´, 5-5´;
- carbon-oxygen bonds: β-O-4´, α-O-4´ and 4-O-5´;
- carbon-carbon and carbon-oxygen bonds: β-5´/ α-O-4´, β- β´/ α-O-γ´.

The ether β-O-4 linkage is the dominant one, counting up to 60 % of the total bonds present in the polymer. The linkages between the units give rise to the formation of substructures, among which phenylcoumarans (β-5) and resinols (β- β) are the most abundant.

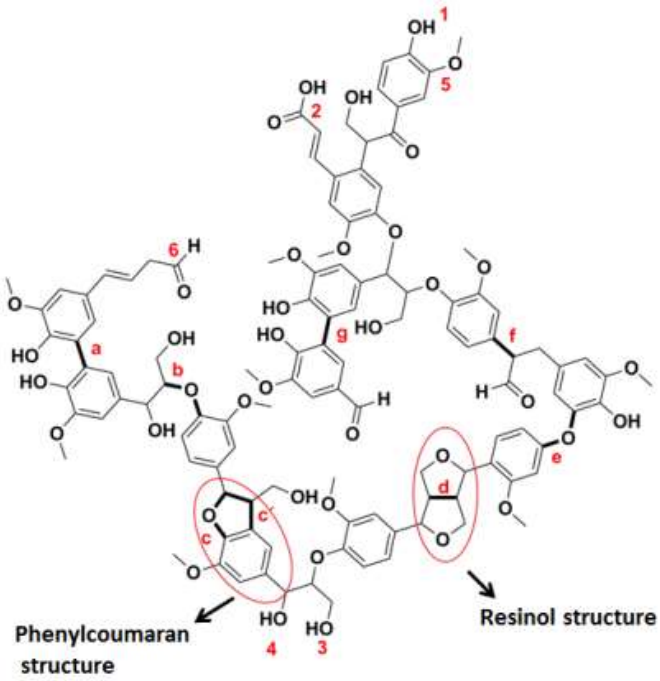

Linkages		Functional groups	
a	5-5´	1	$OH_{phenolic}$
b	β-O-4´	2	carboxyl
c-c´	α-O-4´/ β-5´	3	$OH_{aliphatic}$
d	β-β´	4	OH_{benzyl}
e	4-O-5´	5	methoxyl
f	β-1´	6	carbonyl
g	5-1´		

Figure 1.4 *Model of lignin structure with the main functional groups, linkages and substructures.*

In the plant cell wall, lignin is covalently bonded to the carbohydrate fraction through lignin-carbohydrate complexes (LCCs); the main carbohydrates involved in this process are hemicellulose components. The principal LCCs contain benzyl ethers, esters and phenyl glycosidic bonds, whereas in grass plants ferrulic acid bridges are the most abundant cross linkers (Fig.1.5).[25, 26] Due to the strong

interaction between lignin and carbohydrates, a chemical fractionation method is always required to isolate each of the lignocellulosic components.

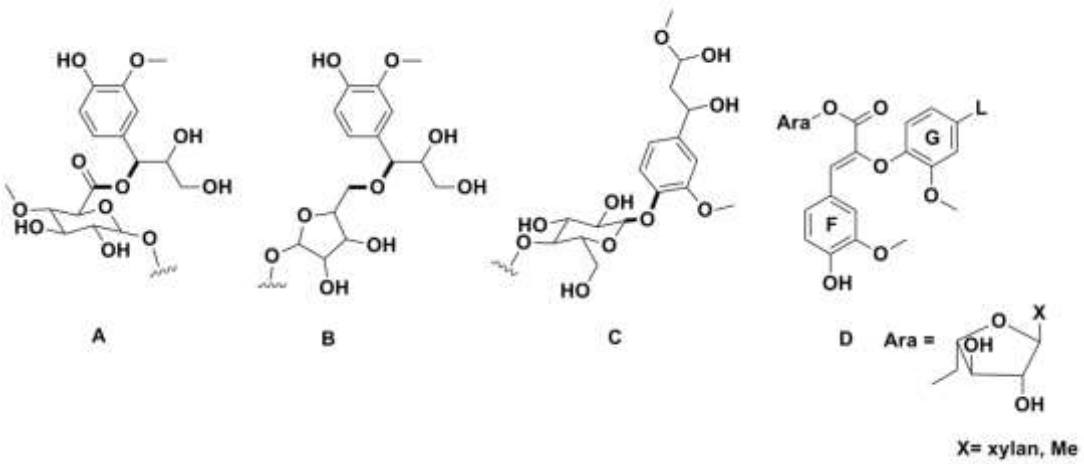

Figure 1.5 *Main types of lignin-carbohydrates complexes (LCCs). Benzyl ester (A), benzyl ether (B), phenyl glycoside (C) and lignin-ferulate complex (D). G, guaicyl unit; F, ferulate (D).*[26]

1.3.2 Biosynthesis of lignin

The biosynthetic process of producing lignin is called "lignification" and refers to the cascade of radical polymerizations, catalyzed by peroxidase and lactase enzymes employing monolignols as building blocks. The latter compounds are synthesized starting from L-phenylalanine and L-Tyrosine, two aromatic amino acids derived from carbohydrates through the Shikimic acid pathway.[27] L-phenylalanine and L-Tyrosine are converted to the corresponding cinnamic acid-derivatives through a series of enzyme-catalyzed steps and finally resulting in the monolignols.[28] This process takes place in the cytosol of the cell and is followed by the transportation of the monomers to the cell wall by passive diffusion, active transport or exocytosis from the Golgi apparatus.[29] In the cell wall matrix, the cinnamyl alcohols are dehydrogenated by a few enzymes, such as laccases and peroxidases, which possess high affinity for cinnamyl alcohol substrates. The peroxidase-catalyzed abstraction of a proton from the phenolic hydroxyl of a monolignol generates a radical structure stabilized by resonance. The monolignol undergoes a random radical coupling initiating the polymerization (Fig. 1.6).[30] A radical monomer reacts with a second phenylpropanoid unit, by radical coupling of carbon-carbon or carbon-oxygen atoms located in different positions of the unit backbone. The reaction product is a dimer called dilignol. It has been calculated that the reaction between two coniferyl alcohol radicals can lead to 15 different dimers, but only five of them are stable enough.[30] The elongation of the chain is caused by a further oxidation of the dimer

and a following reaction with a second component, which can be a mono or dilignol. The branching of the lignin skeleton is developed through the possible nucleophilic addition of several species to the reactive dimer quinone methide, formed as an intermediate during the biosynthetic process. A few examples of addition reactions of water, glucose and coniferyl alcohol to the quinone methide are reported in Fig. 1.6.[30]

Lignification takes place at the corner of the cell wall, and also in the middle lamella provided that the deposition of matrix material and microfibrils of cellulose is finished, thus contributing to the formation of the above mentioned layered-structure.

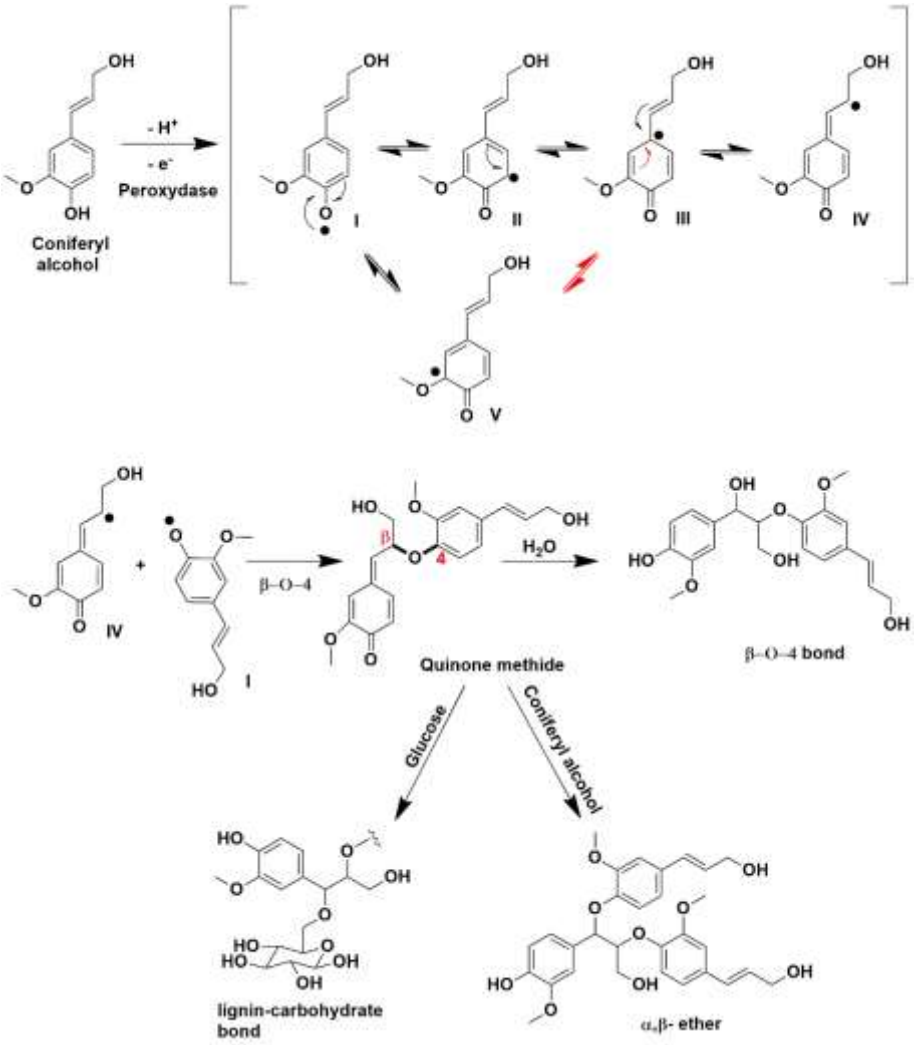

Figure 1.6 ***Above****-Resonance structures of coniferyl alcohol in the radical form.* ***Below****- dimerization of coniferyl alcohol. The coupling of the two coniferyl alcohol radicals leads to the formation of the reactive intermediate quinone methide. Addition of water leads to the consequent aromatization of the ring, producing the dimer. The nucleophilic addition of glucose and coniferyl alcohol to the reactive intermediate increases the branching of the structure.*[30]

1.4 Lignin refinery

As mentioned, lignin is the second most abundant polymer in nature after cellulose and the most abundant aromatic polymer. Lignin has a global distribution and is therefore widely available and cheap. In the 19th century, Payen was the first chemist discovering that the treatment of wood by nitric acid or soda leads to two main fractions, one named cellulose and the other "incrusting material".[31] Later, this material was called lignin and its structure was extensively studied during the 19th and 20th centuries. The aromatic polymer was isolated from the other lignocellulosic components in order to characterize its structure without interference from the carbohydrate fraction. Historically, the main application of lignocellulose (LgC) was the extraction of cellulose for the purpose of paper production. As a result, the paper industry mainly developed LgC pretreatment methods focusing on the isolation of highly pure cellulose.

With an increasing interest towards the possible integration of lignin in the biorefinery industry, several extraction processes have been developed focusing on the direct recovery of lignin. As will be discussed in the following section, the research of milder conditions to isolate lignin with the minimal alteration of the native structure is in constant progress.[32] Indeed, the preservation of a high amount of ether bonds and phenol functionalities makes lignin structure more amenable to further applications, such as a catalytic deconstruction or an additional polymerization.[33] The former process generates a series of low molecular weight and aromatic building blocks, which can be used as starting material for pharmaceuticals or polymers, whereas the second approach can lead to the formation of new biomaterials. In the following section, several lignin-extraction methods will be described considering the advantages of the different pretreatments for the development of lignin refinery.

1.5 Lignin isolation processes

The pretreatment of lignocellulose aims to cleave the covalent bonds between lignin and the carbohydrate fraction. The efficiency of the process derives from the purity, the yield and the degree to which the structure of the isolated lignin is altered.[34] In fact, every extraction method causes a partial cleavage of lignin bonds, influencing the distribution of functional groups and the average molecular weight of the isolated structure. The most amenable linkages to be broken are the ether bonds, whereas the degradation of the C-C bonds requires harsher conditions. During the isolation phase, the lignin structure can be subjected to modifications other than degradation, such as the introduction of additives used during the

process (e.g. sulfite groups in sulfite pulping). Moreover, side recombination reactions, which take place during lignin extraction, cause an increase in structure complexity.[35, 36] Biomass pretreatments are classified as physical, chemical, solvent fractionation and biological processes.[37] Since the topic of this chapter is the influence of chemical and solvent isolation processes on lignin structure, the other two categories of extraction methods will be not discussed here.

1.5.1 Chemical treatments

These isolation methods include acidic and alkaline pretreatment. Depending on the pulping additive, these can also give rise to a sulfur containing lignin. This category of pretreatments includes the main commercial extraction processes, such as lignosulfonate and Kraft treatments.

1.5.1.1 Lignosulfonate process

The sulfite process is the oldest pulping method, industrially applied for the first time by Ekman in 1874 in the context of cellulose isolation for paper production.[38] The process relies on the use of sulfur anions, such as sulfite and bisulfite in combination with several counter ions. Examples of the main commercial counterion sources are calcium, magnesium and ammonium. The pulping liquor is prepared by sulfur combustion in a controlled oxygen atmosphere, thus the obtained sulfur dioxide is reacted with water, giving rise to sulfurous acid. The counter ion source is added to the solution as the corresponding carbonate or hydroxide salt. Depending on the amount of base added, the pH of the process can be adjusted between 1-6[33] and the temperature is kept among 140° and 160° C. The resulting isolated polymer contains up to 5 % sulfur in the form of sulfonate groups, is water soluble, highly cross-linked and includes carbohydrate fractions as impurities. The reaction mechanism (Fig. 1.7) minimizes the cleavage of side chains in comparison with the isolation processes described later. Indeed, the treatment favors the cleavage of α-O-4 linkages rather than β-O-4 linkages. Moreover, the occurrence of condensation events through reaction of the intermediate carbocation with an electron-rich carbon atom leads to a lignosulfonate with high molecular weight (Mw up to 140000 g mol^{-1}) and dispersity index (D, between 4-9).[39] This pulping method requires a complex isolation process of the water soluble lignosulfonate: firstly a complexation with a long-chain alkyl amine to form water insoluble product, then a subsequent organic extraction of the complex, and finally regeneration of lignosulfonate by addition of a base.[40]

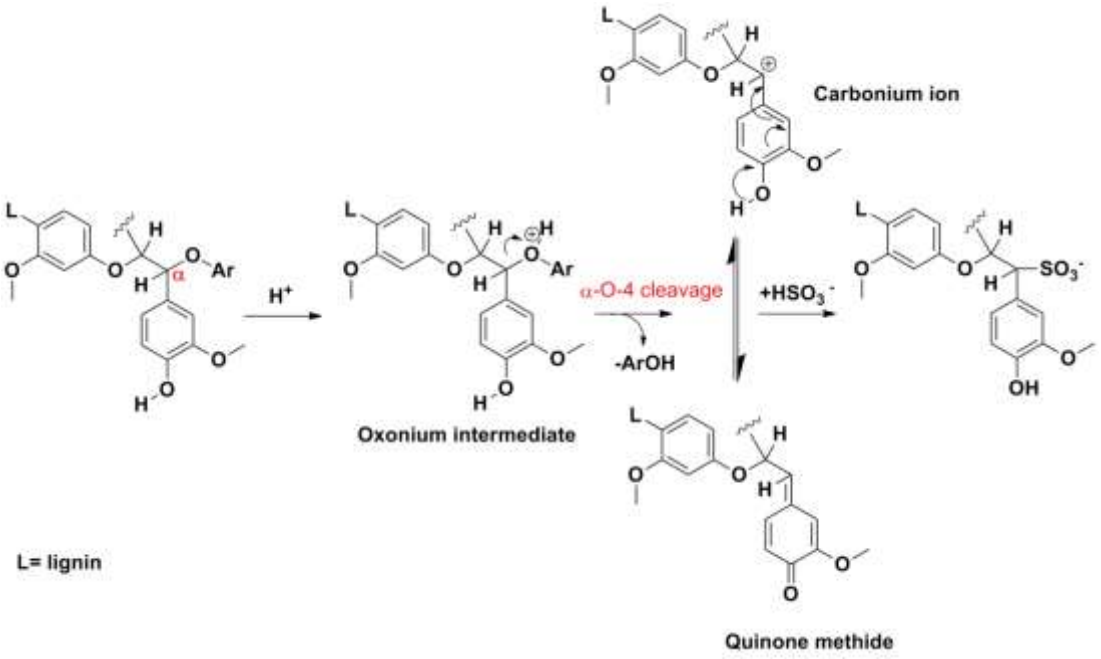

Figure 1.7 *Acidic sulfonation of lignin with cleavage of the α-aryl ether bond* [39]

1.5.1.2 Kraft process

The Kraft process is worldwide the most used delignification method in paper industry. It is an alkaline method, in which NaOH and sodium sulfide (NaS_2) both act as nucleophiles, breaking lignin-carbohydrate linkages and giving rise to a chemically-resistant isolated cellulose. The process proceeds in aqueous solution at a temperature of 170°C for 2 h, at the end of which a solid pulp and a brown liquid, the so called "dark liquor", are obtained. Cellulose isolation is achieved by purification of the pulp, while lignin is precipitated from the dark liquor by acidification. When compared with lignosulfonate, Kraft lignin (KL) contains fewer carbohydrate residues and inorganic impurities; the content of sulfur is also lower, presenting therefore a higher degree of purity. Unlike the sulfite process, in which the cleavage of α-aryl ether bond is favored, in alkaline conditions both α- and β-ether linkages can undergo cleavage. For this reason, KL has a lower Mw (up to 25.000 g mol^{-1}) and a narrower dispersity index (2.5-3.5) than lignosulfonate.[41] During the pretreatment two main reactions occur: degradation and condensation of lignin.[42] The formation of new C-C bonds under these conditions is due to the simultaneous addition of nucleophilic species (e.g. carbanions from phenolic structures) other than OH and SH (Fig. 1.8). As well as sulfite lignin, Kraft lignin is mostly used to power paper mills. In fact, the sulfur content in both the isolated lignins reduces the number of lignin applications. As mentioned above and later on,

lignin can undergo catalytic upgrade. For most of the employed catalysts, sulfur is a poison, preventing the use of lignin for further degradation steps.[32]

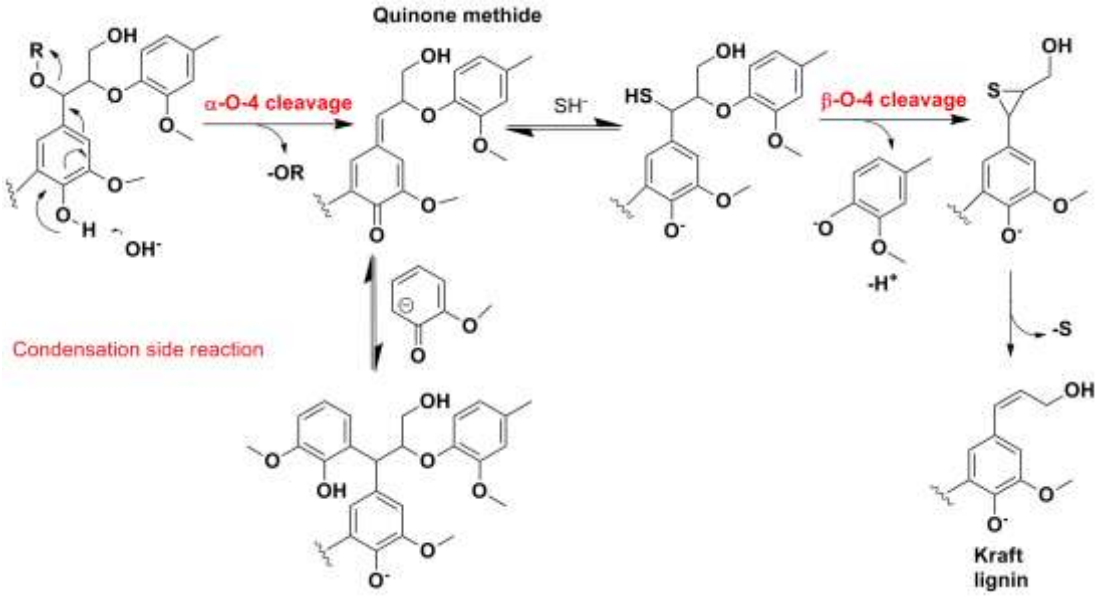

Figure 1.8 *Cleavage of α- and β-ether linkages during Kraft pulping and simultaneous formation of side condensation products.*[42]

1.5.1.3 Soda and Alkaline processes

The soda isolation process is industrialized since 1853 and generally applied to non-woody biomass (e.g. straw, sugarcane, bagasse).[38] In this method, lignocellulose is treated with highly concentrated (13-16 %) aqueous NaOH solution at around 140-170°C, yielding a low molecular weight lignin (Mw between 1000-3000 g mol^{-1}) with a dispersity comparable to that obtained by the Kraft pulping method (2.5-3.5). Delignification is a consequence of the saponification of ester bonds between lignin and hemicellulose, while partial lignin deconstruction is caused by the cleavage of the α- and β-ether linkages. (Fig. 1.9) Soda lignin, recovered as a precipitate after acidification of the dark liquor, is free of any additive such as sulfur. This feature offers distinct advantages for applications in the field of material chemistry (bioplastic and composites),[43] as well as in the area of catalytic deconstruction to obtain interesting aromatic building blocks. Besides the use of sodium hydroxide, alkaline hydrothermal processes with different bases have been explored. The treatment of corn cobs with $Ca(OH)_2$[44] and rye straw with $Ba(OH)_2$,[45, 46] allows the simultaneous generation of lactic acid and lignin. Respectively found in the dark liquor as metal lactate salts, and in the pulp as solid lignin. Hydrothermal-alkaline methods have been employed for the development of part of this work, and will be further discussed in the 2nd chapter.

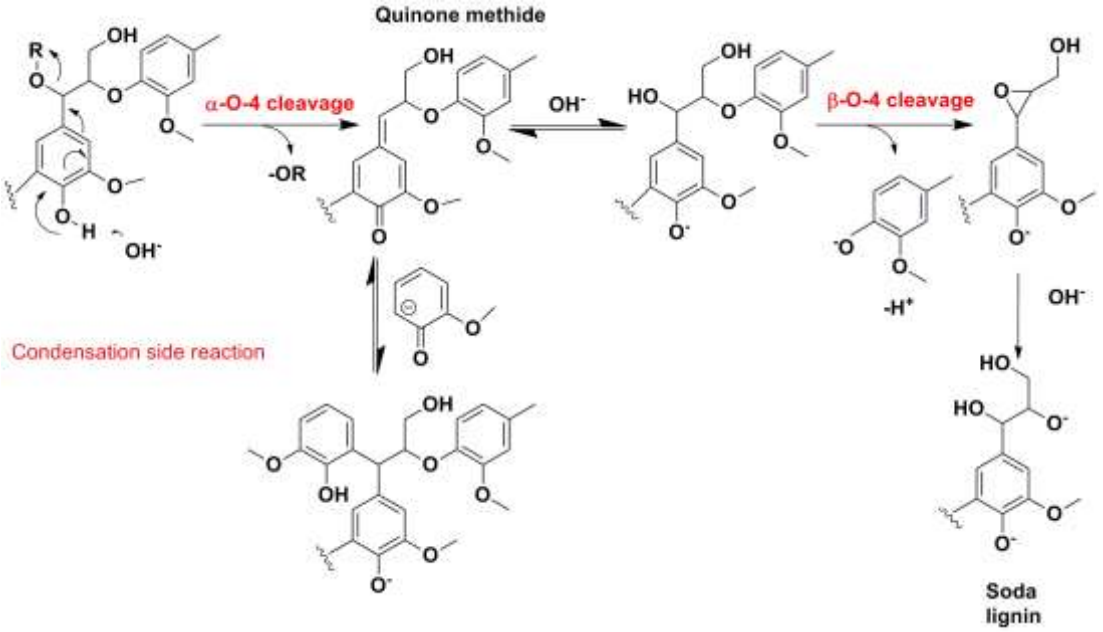

Figure 1.9 *Cleavage of α- and β-ether linkages during alkaline pulping and simultaneous formation of side condensation products.*[42]

1.5.2 Organosolv treatments (OS)

OS extraction methods are based on the hydrothermal treatment of biomass with a mixture of water, an organic solvent, and occasionally additional additives to give rise to a high-quality sulfur-free lignin. Most of the employed solvents have low boiling point and can be therefore easily removed and recycled. The resulting lignin features a low number of modifications compared to the native lignin. The OS treatment in fact cleaves preferentially the carbohydrate-lignin bonds leaving a high molecular weight and only partially modified lignin. For this reason, OS-lignin is a good candidate for the preparation of polymers, such as bio-based phenol-formaldehyde resins, polyurethanes and polyesters. Commonly used organic solvents are methanol, ethanol, acetone or a mixture thereof. Lignin is recovered at the end of the process as a precipitate, after addition of large amount of water.[47-49] The addition of an acid catalyst to the pulping media causes the cleavage of more ether-linkages, but also favors the occurrence of intramolecular condensation reactions, giving rise to a more complex lignin structure (Fig.1.10).[50, 51]

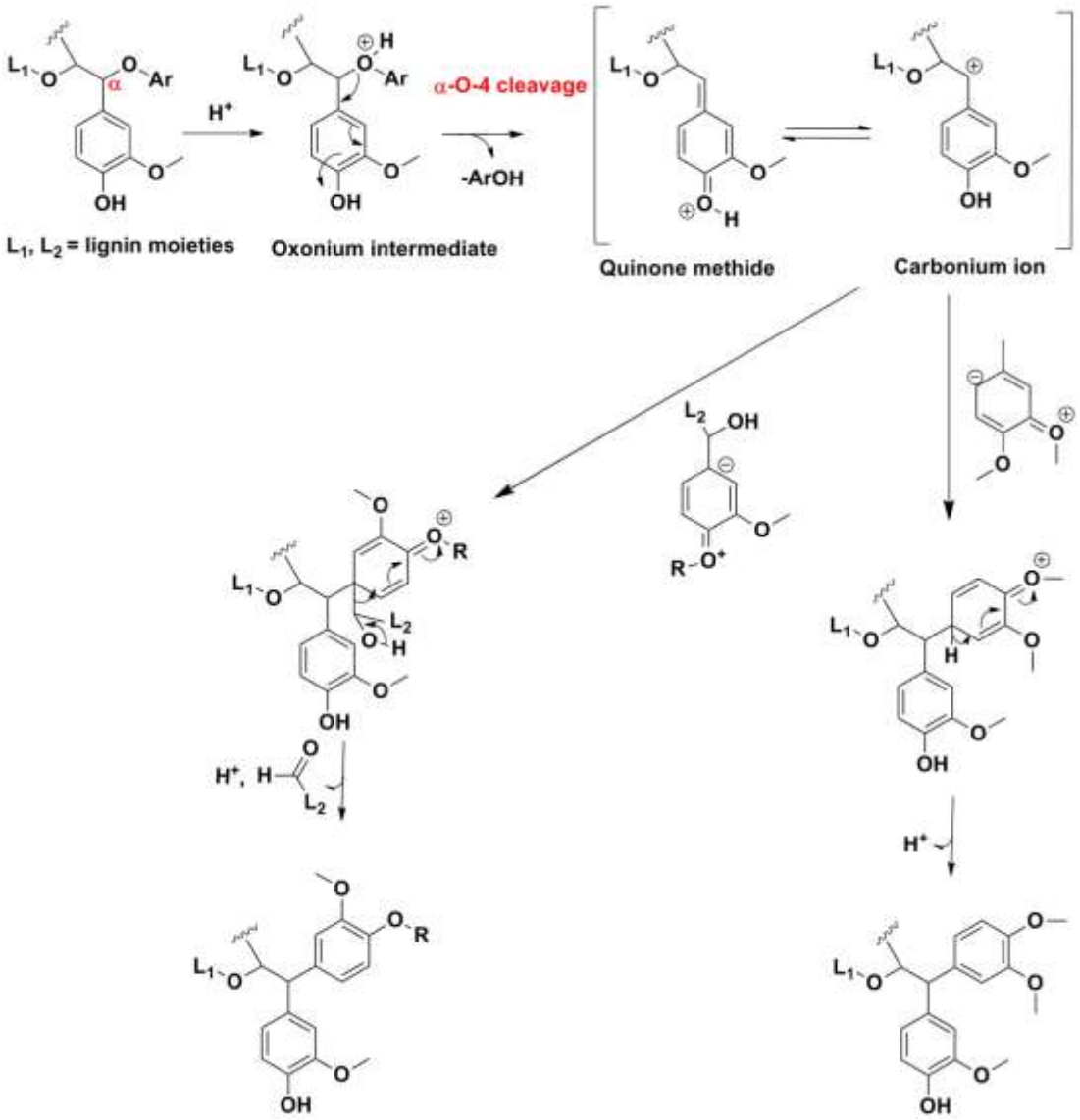

Figure 1.10 *Condensation reactions under acidic conditions*

Beyond the use of classical acid catalysts such as HCl, H_2SO_4, acetic and formic acid,[52] the influence of different Lewis acids (e.g. $FeCl_2$, $ZrOCl_2$) on the lignin structure was explored by the group of Quignard.[53] An interesting application of a heterogeneous-acid catalyzed OS process is the treatment of biomass with a mixture of 2-MeTHF (methyltetrahydrofuran) and a solution of oxalic acid in water. The main advantages of this method are the recovery of lignin by simple concentration of the organic phase and the use of a biomass-derived solvent (2-MeTHF).[54] Luterbacher et al.[55] offer a further example of biomass pretreatment with the biomass-derived solvent γ-valerolactone (GVL).

1.5.3 Other methods

The research of isolation methods which are more environmentally friendly, cheaper and which extract lignin in high yield and with a high purity, poses a continuous challenge. Among others, the use of ionic liquids (ILs) as extraction solvents (ionosolv process) is still at an exploratory stage.[56, 57] ILs show interesting characteristics, such as:

- liquid at room-temperature;
- low flash point;
- thermal stability;
- chemical and physical properties that can be tuned by changing the cation and anion;
- selectivity towards the dissolution of the different biomass components.[14]

Although not deeply discussed in this context, the use of ILs as biomass extraction-solvents has to be mentioned for their possible future development.
The use of water in supercritical conditions as a unique extraction solvent was performed by Smirnova [34] and Kostas. [58] Despite the total absence of additives that make this approach highly sustainable, it turned out that such hydrothermal treatments function as a good extraction method only for hemicellulose and can be thus regarded as valuable pre-pulping processes.[59]

1.6 Lignin applications

As mentioned above, isolated lignins possess structural features which depend on the applied extraction method and influence the application-field. In the following section, possible utilizations of lignin in its unmodified form or after further modifications will be described.

1.6.1 Applications of unmodified lignin

The use of lignin as a fuel is the oldest and most common application and is widely used by the paper industry, whereby black liquor is recovered from the wood pulping and directly combusted to power the paper mills. With the purpose of increasing the combustion heat, lignin is added to bio-fire logs made of cellulose and propane-1,3-diol. Considering its binding properties, it is often used as an additive in coal briquettes in which it increases the burning speed and additionally in packing paper material, where it enhances the strength of recycled paper. Despite the advancement of lignin combustion and gasification methods,[60, 61] the value of lignin for power and fuel production is low when compared with other aromatics, such as toluene or benzene.[62]

Its natural antibiotic and antioxidant properties make it a non-toxic binder in pelleted feeds. Moreover, it is suitable as a low cost and nonhazardous chelating agent, due to the presence of polar groups. Water soluble lignosulfonates can carry boron, iron or manganese ions, which are important nutrients for the plants, and release them slowly in the soil.[63] As a chelate, lignin can also be applied as a sequestrant of heavy metals (e.g. cadmium, nickel, zinc or mercury), often present in polluted water.[64]

1.6.1.1 Unmodified lignin in polymer chemistry

Unmodified lignin can be an excellent starting material for the preparation of polymer composites *via* formation of covalent bonds with other components. Moreover, unaltered lignin can be used as an additive to protect polymers from oxidation, light or high temperature.[63] The most important functionalities involved in the polymerization are the hydroxyl groups. Interestingly, although the relatively low amount of free active hydroxyls and the steric hindrance reduce the reactivity of lignin, the use of lignin in polymer materials has been already successfully reported in a number of cases. For instance, lignin can be employed as a reagent in the synthesis of phenol-formaldehyde adhesives for plywood, chipboards, etc. In this case, lignin is used as a substitute for phenol in the reaction between phenol and formaldehyde enhancing the sustainability of the binder.[65] In polyolefins (e.g. polypropylene, polyethylene), lignin can be blended, modifying the mechanical properties and enhancing the oxidative resistance.[63] The use of lignin in polyesters as a reaction monomer or filler has been reported. As an example, Kraft-lignin has been polymerized with sebacoyl chloride, enhancing the biodegradability of the resulting material.[66] The group of McDonald synthesized a hyperbranched poly(ester-amine) by esterification of a commercial lignin with a prepolymer made of adipic acid and triethanolamine (HBPEA).[67] They observed that the addition of an increasing amount of lignin strongly influenced the mechanical properties of the final polymer. For instance, the toughness of the material was enhanced when using up to 40 wt% of lignin. This approach was modified by our research group, employing different amount of lignin extracted from coconut, bamboo and beech wood. As will be described in detail in the 5th chapter, we introduced the use of the resulting poly(ester-amine) as adhesive for aluminum, with promising application in the field of the wood glues.

Furthermore, lignin is used as a macromonomer in the synthesis of polyurethanes (PUs). PUs are generally obtained by reaction of a diol with an isocyanate (Fig.1.11). Lignin can be reacted in the presence of other polyols, such as polyethylene glycol (PEG) and an isocyanate, such as methylene diphenyl isocyanate.[68] The addition of lignin grants rigidity to the system, while the polyol prevents brittleness of the PU.

Lignin-containing polyurethanes are also used to form biodegradable foams[69] and cheap composites for reinforcement within construction, drainage and soil stabilization.[70]

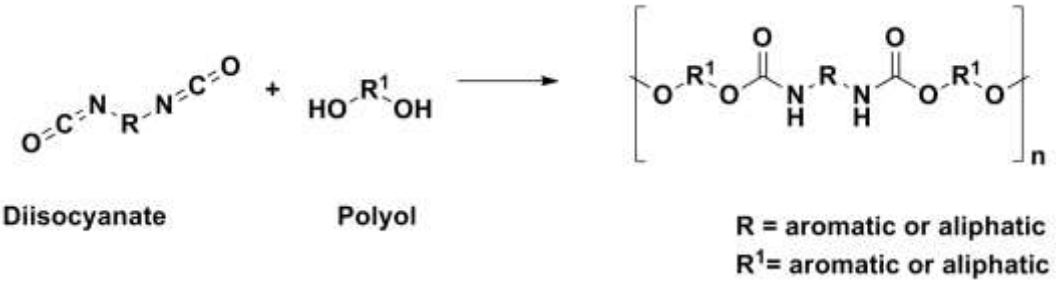

Figure 1.11 *General synthetic pathway for polyurethanes*

In addition, lignin can also be utilized in the field of bioplastic materials. For instance, in the case of Arboform,[71] the aromatic polymer is mixed together with cellulose fibers and natural additives to form a granulate plastic that can be molded and shaped. Furthermore, an example of a cellulose-lignin based hydrogel has been reported from Ciolacu et al. [72] Hydrogels are polymers able to absorb large amounts of water without dissolving in aqueous solution. They are used in several fields, such as personal hygiene products, medical devices or controlled drug release. In this case, the lignin-derived hydrogel could be used for the controlled release of polyphenols.

1.6.2 Lignin modifications and its applications

Lignin structure modification can be used to add new functionalities, and to increase the amount of already existing reactive sites, such as phenols and hydroxyls. A second approach of altering the lignin structure is deconstruction, which aims to produce low-molecular weight aromatics, which can be further employed as building blocks for fine chemicals.

1.6.2.1 Addition of new functionalities

Among the possible functionalizations of lignin's structure, several cases can be mentioned. For instance, lignin-amination *via* the Mannich reaction was reported to enhance the reactivity for further application as a surfactant and slow-release agent for fertilizers.[63] In the work of Fang et al.,[73] lignin was aminated using the Mannich reaction and successfully used to synthesize a lignin-based cationic flocculant, which was able to remove anionic dyes from water solutions. The study showed that the displacement of the dyes was mostly caused by a mechanism of charge neutralization. With the purpose of bioremediation applications, lignin was oxidized by molecular oxygen using polyoxometalate as catalyst, solely or in the presence of

laccase.[74] This approach minimized the oxidative-degradation of the polymer, increasing the amount of carbonyl and carboxyl groups. The resulting modified lignin showed an enhanced sorption capacity toward heavy metal and triazine pesticides. Furthermore, Katsumata and Meshitsuka[75] described the role of modified lignin as a removal agent of Al(III) from soil. The low pH favors the concentration of aluminum ions in the soil water which inhibits the growth of the plants. In the article, Kraft lignin was oxidized by O_2 under pressure and sulfonated by treatment with sodium sulfite. The increased number of carboxylic acids in the first case and the introduced sulfonic groups in the second case are able to complex aluminum ions, removing them from the soil. Moreover, activated lignin-derived carbon materials showed activity as adsorbents for water pollutants. In this regard, Kraft lignin was carbonized after impregnation with sulfuric acid at temperatures between 623 and 873 K.[76] The resulting activated carbons exhibited mesoporosity and high surface area. They were successfully tested for the removal of 2,4,5-trichlorophenol, Cr(VI) and phenol, as representative pollutants of industrial wastewater.

As will be described in detail in chapter 4, we introduced a new application for a nitrated-lignin. Isolated lignin from beech wood chips *via* the hydrothermal alkaline method was nitrated using nitric acid in acetic anhydride in the presence of a catalytic amount of sulfuric acid. The resulting nitro lignin was carbonized in the eutectic salt melt $KCl/ZnCl_2$, resulting in a nitrogen-doped carbon (NDC) with high surface area and mesoporosity. Moreover, the material was successfully tested for its electrocatalytic activity towards ORR (oxigen reduction reaction).[46]

1.6.2.2 Lignin modification for polymer applications

As described in paragraph 1.6.1.1, unmodified lignin can already be used in the synthesis of several polymers. In order to increase the number of reactive sites such as phenol and hydroxyl groups, different techniques have been developed. Among others, lignin-phenolation is the most used. Generally, it is conducted in acidic medium, using methanol or ethanol as solvent and at a temperature close to the solvent's boiling point. Phenolization reaction can occur both on the side chain and on the aromatic carbons of lignin, causing partial cleavage of the polymer. Phenolated lignin is mainly used in phenol-formaldehyde (PF) resins; however a 100 % phenol substitution with phenolated lignin is not possible.[63] In Kraft lignin, approximately 50 % of the hydroxyl groups are methylated, reducing the number of reactive sites for the synthesis of PF resins. As a result, demethylation is the second most common process employed with the purpose of increasing the amount of free hydroxyl groups in lignin. Among other chemical methods, sulfur-mediated demethylation was the cheapest and most efficient process.[77] Another way to

increase the reactivity of lignin for PF resin applications, is to use hydroxymethylation *via* the Lederer-Manasse reaction.[78] In this case, lignin is treated with formaldehyde in alkaline conditions, thereby introducing hydroxymethyl functionalities onto the aromatic ring. Although lignin modified by this method can substitute up to 40 % of phenol in the production of PF resins, the possible residues of free formaldehyde in the final lignin causes doubts towards the industrial scalability of this procedure.[63]

1.6.3 Catalytic lignin deconstruction

Lignin deconstruction occupies an important role in lignin refinery. In fact, it allows the achievement of a wide array of aromatic building blocks. These building blocks can be used as starting materials for the synthesis of polymers and pharmaceuticals, currently obtained mainly from oil-derived aromatics.[11]

Since C-O are the most abundant bonds and the easiest to break in the polymer structure, lignin degradation methods aim mainly to cleave ether linkages. Several acidic and alkaline methods have been explored,[79] but in general, they turned out lack selectivity, produce modest yields and require harsh reaction conditions.[80] Better results have been obtained using a catalytic deconstruction approach consisting of three main types of reaction: hydrogenolysis, oxidation and hydrodeoxygenation.

It is worth to mention that even enzymatic and biotechnological lignin deconstruction methods are currently used, but they will not be described in this work.[81]

1.6.3.1 Hydrogenolysis (HGL)

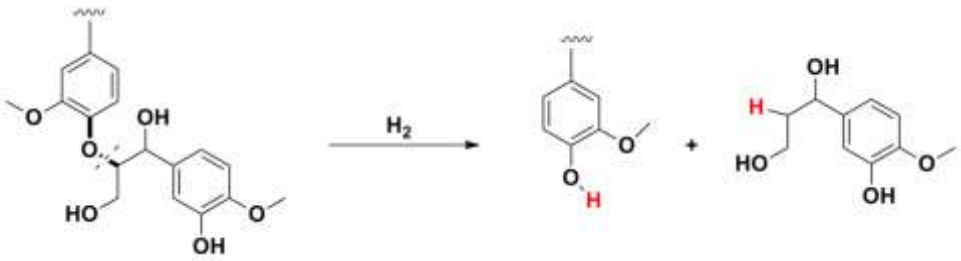

Figure 1.12 *Schematic representation of lignin Hydrogenolysis*

Hydrogenolysis results in the cleavage of ether bonds (Fig.1.12) by treating lignin in a hydrogen atmosphere at high temperature and pressure in the presence of a catalyst. The first HGL using Raney-Ni as a catalyst was performed in 1935.[32] Since this report, Raney-Ni was extensively utilized, and some of the obtained low-

molecular weight aromatics were identified as guaiacol, dihydroxysinapyl alcohol, dihydroconiferyl alcohol and 4-propylsyringol.[82]
Parameters such as the catalyst,[83-85] temperature[86] and the solvent[87] were taken into account recently in order to optimize the HGL conditions. Among several reports is that of Molinari et al. that showed the higher hydrogenolytic efficiency of TiN-Ni nanocomposite in comparison with Ni/C;[88] likewise the study of Yan et al. demonstrated the improved catalytic activity of a bimetallic Ni-based catalyst in water.[89]
While most of the works focused on the yields of the obtained HGL products, tuning the selectivity of the cleavage towards few molecules is still a big challenge in lignin degradation. Moreover, the nontrivial analysis of the complex mixture of aromatics makes the identification and the quantification of the components a challenging goal. In chapter 3, we will discuss our contribution to the analytical field of deconstructed lignin.

1.6.3.2 Oxidation

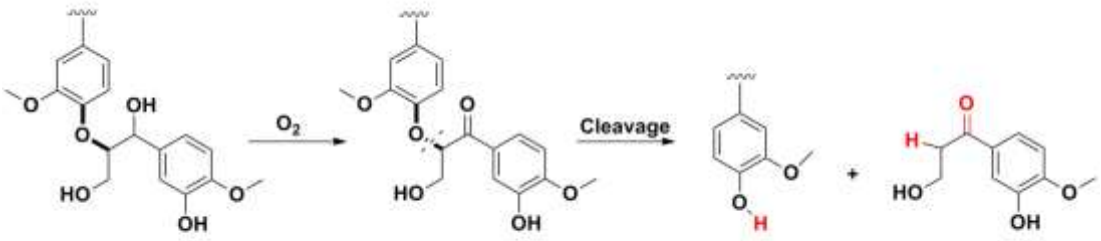

Figure 1.13 *Schematic representation of Lignin oxygenation*

During the lignin oxidation pathway (Fig.1.13) ether bonds are cleaved after an oxidation of the hydroxyl-benzyl group, giving rise to a mixture of aromatic aldehydes and ketones that are useful precursors to fine chemicals. Vanillin is the main commercial aromatic aldehyde obtained *via* lignin oxidation, which is performed under a high-pressure oxygen atmosphere and in an alkaline medium. In this regard, Fargues et al.[90] described the kinetics of vanillin production by treating Kraft lignin at different temperatures, relative oxygen pressures and varying the polymer concentration in the reaction solution. The general yield of the oxygenation reaction was greatly enhanced by the combination of oxygen with several catalysts. Classic examples of such catalysts are based on Mn or Cr, while other experimental procedures reported the use of Fe, V, Cu, or Au-based catalysts. For instance, Cui and Dolphin[91] tested the catalytic activity of iron and manganese complexes of the inexpensive and widely available phthalocyaninetetrasulfonic acid (TSPC) towards the oxygenation of lignin models, such as veratryl alcohol. The

reaction was performed in the presence of oxidising agents. The TSPC complexes were supposed to mimic the activity of lignin peroxidase, however, the complexes showed low catalytic activity towards the conversion of veratryl alcohol to the corresponding aldehyde. Moreover, both the metal complexes exhibited low stability in the reaction conditions. In a later report, the oxidation of lignin using Pd/Al_2O_3 as a catalyst yielded vanillin and syringaldehyde with relatively high selectivity. The test was conducted on alkaline lignin under batch conditions, and then the process was scaled up to a continuous flow reactor. The oxidation was performed at around 373-413 K, with O_2 as oxidant in basic environment.[92]

1.6.3.3 Hydrodeoxygenation (HDO)

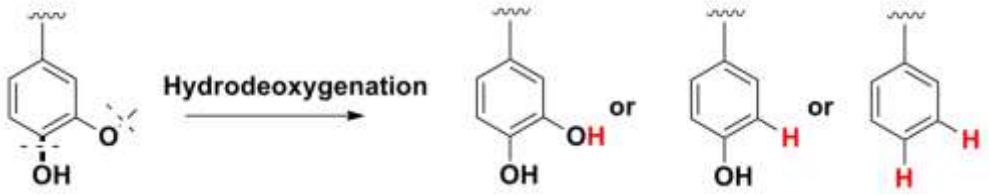

Figure 1.14 *Schematic representation of Lignin Hydrodeoxygenation.*[32]

Hydrodeoxygenation is a deconstruction process that affords aromatics with a low oxygen content (Fig.1.4). This method appears particularly useful for the synthesis of fuel from biomass. Indeed, if not performed under strict temperature and pressure control, lignin HDO induces a high loss of functionalities, favoring the formation of benzene and cycloalkanes.[32] However, when conducted under mild conditions, HDO can produce a narrow distribution of obtained products. Considering the complexity of the lignin structure, catalysts are generally tested on small molecules like guaiacol and catechol, before being applied for the treatment of crude lignin.[93] For instance, the use of Raney-Ni in combination with Nafion supported on acidic silica was tested for the conversion of lignin-derived compounds into hydrocarbons. The reaction was performed at temperatures between 473-573 K in presence of H_2 and gave rise mainly to cycloalkanes.[94] Mu et al.[95] screened the activity of metals such as Pd, Pt, Rh and Ru supported on active carbon, first towards the conversion of lignin models and then on lignin. The study showed that during the reaction, Pd, Pt and Rh catalysts were deactivated by coke formation, while Ru was the only metal not affected. The hydrodeoxygenation of Ru-catalyzed lignin led to a fully hydrogenated bio-oil. HDO will not be discussed in detail in this thesis, nevertheless other interesting examples of HDO systems applied on lignin have been reported in literature.[32, 96, 97]

1.7 Outline of the thesis

With this project we joined the scientific community in trying to develop new sustainable solutions to overcome the issue of fossil feedstock depletion. We challenged ourselves in the nontrivial field of lignin throughout all the aforementioned critical points, such as the complexity and variability of lignin structure and the difficulties in obtaining reliable and repeatable analytical data.
In the first part of this work, lignin is extracted from several biomasses by different isolation processes. A comparison of the resulting structures is performed by combination of the structural data obtained through different analytical techniques. The final purpose is to understand the influence of the selected lignocellulosic source and extraction processes on lignin structure. The second part of the thesis offers three different examples of lignin applications. As mentioned, one of the most interesting applications is the deconstruction of lignin to obtain aromatics, which could be used as starting building blocks for pharmaceuticals and polymers. In the 3rd chapter we try to deal with one of the problematic aspects of lignin-deconstruction, which is the analytical characterization of the reaction products.
Chapter 4 will report the use of lignin functionalized *via* aromatic nitration, as a precursor for nitrogen-doped carbons (NDCs). Moreover, a final electrocatalytic application of the lignin-based NDC towards the oxygen reduction reaction is reported. Finally, in chapter 5 we describe the synthesis of a highly branched amino-polymer by combination of lignin isolated from several sources with a prepolymer. The resulting material shows adhesive properties towards aluminum and promising application as a glue for the wood industry.

2. LIGNIN EXTRACTION AND CHARACTERIZATION

As mentioned in the introduction, there is a wide range of potential lignin applications and each requires the use of lignins with different structural characteristics. As an example, for the synthesis of lignin-based polymers the presence of free hydroxyl groups in the lignin structure is essential. Therefore, it is important to understand the influence of the isolation method and of the biomass source on lignin structural features. In this chapter we are going to discuss in details the analytical results obtained through the comparison of lignin structures, which were obtained by two different approaches. A first analytical comparison was performed between lignin structures isolated from the same source but employing different extraction processes. A second approach consisted in applying the same pretreatment method to different raw materials and investigating the diversities between the so obtained structures.

2.1 Analytic in lignin

Traditionally, several analytical methods have been employed for the characterization of the isolated lignin structure. The complexity of its structure requires the comparison and combination of results obtained from different analytical approaches. At the state of the art, no single method can be considered sufficient in order to define the complex aromatic structure since all of them present drawbacks. Therefore, data reported in literature are not always consistent and the deduced structure should be regarded just as a model.[98] The analytical techniques applied for lignin characterization can be classified in several categories:[99]

- wet chemical analysis, such as Klason process;
- chromatography, such as gel permeation chromatography (GPC) and gas chromatography (GC);
- thermo-chemistry, such as thermogravimetric analysis (TGA) and differential scanning calorimetry (DSC);
- spectroscopy, such as Fourier Transform Infrared Spectroscopy (FT-IR) and Nuclear Magnetic Resonance (NMR).

In this study, lignin structure was investigated using a combination of methods as described in table 2.1.

Table 2.1 *Analytical methods in lignin analysis*

Parameter characterized	Wet chemistry	Chromatography	Elemental analysis	Spectroscopy				Thermo-chemistry
	Klason test	GPC		FT-IR	^{1}H-NMR	^{31}P-NMR	2D HSQC-NMR	TGA
Lignin content/purity	√							
Molecular weight		√						√
Functional groups				√	√	√	√	
Atomic composition			√					
Monomer composition				√		√	√	√
Intramolecular linkages							√	√

As shown in Table 2.1, some features of lignin are described by employing a single analytical technique. For instance, exhaustive information about the lignin content in the biomass and the lignin purity are provided by the Klason test, whereas the elemental analysis gives a detailed characterization of lignin atomic composition. In contrast, other parameters such as the functional groups, the monomers composition and the intramolecular linkages of the structure are described by combination of the data obtained through the use of several analytical techniques. Based on these considerations, each of the following sections is dedicated to the description of one structural feature through the combination of different analytical information.

2.1.1 Biomass lignin content and lignin purity degree

The so called Klason test is the most used method to calculate the biomass lignin content and the purity of the isolated lignin. The process, applied for the first time at the beginning of the 20th century and optimized by Peter Klason in 1923,[100] is based on the hydrolysis of the lignocellulose carbohydrate fraction by sulfuric acid. Later on, several slight modifications of the Klason test were performed and the new obtained procedures were standardized. In general these modifications included the optimization of the reaction conditions, such as time, temperature or concentration. In this regard, we calculate the lignin content in beech wood and the purity of the isolated lignins by applications of the procedures standardized by the National Renewable Energy Laboratory (NREL).[101, 102] Before the test, ethanol soluble compounds such as waxes and chlorophyll (defined as extractives) were first removed from the dried beech wood. The free-extractive biomass was then treated with sulfuric acid to generate a solid acid insoluble lignin (AIL or Klason lignin), quantified by gravitation and an acid soluble lignin (ASL), determined by UV-

absorption of the acid solution at 240 nm. The same method was applied for isolated lignin to determine its purity.

2.1.2 Molecular weight, GPC

The parameters commonly used to express the polymer molecular weight are the number average molar mass (Mn), the mass average molar mass (Mw) and the molar mass ditribution (D). The last is related to the distribution of the molecular weight (Equation 2.1).[103]

Equation 2.1 *Calculation of Mw, Mn and D*

$$Mn = \frac{\sum_i N_i M_i}{\sum_i N_i} \qquad Mw = \frac{\sum_i N_i M_i^2}{\sum_i N_i M_i} \qquad D = Mw/Mn$$

N_i = number of molecules with molecular mass N_i

The most widely used technique to obtain Mw and Mn is GPC, a liquid-solid chromatography in which the separation is based on the different size of molecules.[104] The solid phase is a chemical-inert and cross-linked polydextran gel with pores of different size. Tetrahydrofuran (THF) is the common solvent for derivatized lignin (acetylated or methylated) whereas unmodified lignin is usually dissolved in N-Methyl-2-pyrrolidone (NMP), which serves also as the mobile phase. GPC data are obtained by comparison with calibrated standards, usually polystyrene in the case of lignin. Although some works in literature report the non-reproducibility of lignin GPC data,[105] this analytical method is widely used to compare the Mw of lignins extracted from different biomasses and by different processes.[103]

2.1.3 Elemental composition

Lignin composition is quite constant for carbon, oxygen and hydrogen, without significant changes due to the variation of biomass source or the isolation method. The content of carbon is generally in the range of 60-65 wt %, of hydrogen 5-7 wt % and of oxygen 28-35 wt % of the isolated lignin. In contrast, the extraction process has a remarkable influence on the amount of sulfur and nitrogen. In fact, lignin extracted by organosolv (OS) process, in which no additives are used, exhibits a high purity degree and a low amount of nitrogen (0.1-0.4 wt %) and sulfur (0.4-0.9 wt %). In contrast, as aforementioned, the content of sulfur in Kraft and sulfite lignin can increase up to 5 wt %. Therefore, the elemental analysis gives information about the isolated lignin purity.[103]

2.1.4 Monomer composition, functional groups and intramolecular linkages characterization

The complexity and reactivity of lignin structure is determined by the monomer composition, which is generally strongly dependent on the biomass source. Moreover, a key role is played by the functional groups and the linkages between the structural units, which are partially generated after the polymer cleavage. The pulping process influences these last two parameters through the preferential cleavage of certain lignin bonds. As shown in table 2.1, the characterization of monomer composition, functional groups and linkages in lignin structure, requires more than one analytical technique. Among the others, FT-IR is the most widely used method. It is based on the fact that molecules with different structure absorb energy with different frequencies. In general, chemical bonds vibration occurs after the energy absorption. The frequency required to induce this vibration depends on the atoms involved in the linkage, on the bond-nature and on the chemical environment.[103] Therefore, by detection of the absorbed energy FT-IR provides information about lignin functional groups and linkages. Moreover, FT-IR is fast, has high signal-to-noise ratio, is a non-destructive analysis, it is simple and does not require the dissolution of the analyte.[106] The TGA analysis measures the loss of mass of the material at different temperatures and provides information about the sample thermal stability and decomposition. It can be performed in the presence of oxygen or in nitrogen atmosphere and requires a few milligrams of sample. Lignin decomposition in nitrogen atmosphere occurs in a broader temperature range (200-500 °C), if compared to cellulose and hemicellulose and it is dependent on the intramolecular linkages, functional groups, and the monomers ratio of the analyzed lignin.[107]

NMR spectroscopy is based on the difference in the magnetic properties of several nuclei. The variation is due to the nature of the nucleus as well as to its chemical environment. Therefore, by measuring the magnetic properties of a nucleus, it is possible to understand its chemical surrounding. Common NMR techniques applied on lignin are ^{1}H-NMR, ^{13}C-NMR, 2D HSQC-NMR and ^{31}P-NMR.

The first application of ^{1}H-NMR spectroscopy on lignin characterization was published by Ludwig at al. in 1964.[108] Lignin was acetylated to increase its solubility and deuterated chloroform was used as solvent. From that moment on, the progress of technology achieved higher signal/noise ratio and more accurate data. The study of ^{1}H-NMR lignin-spectra provided the identification of functional groups and the quantification of hydroxy and methoxy functionalities.[103, 109, 99, 110, 111] Although ^{1}H-NMR represents an efficient instrument to compare lignins, it suffers of signals overlapping and proton-coupling effects. Thanks to the absence of the latter

effects, ^{13}C-NMR allows a better resolution than ^{1}H-NMR but with a lack of sensitivity. This lack is caused by the lower natural abundance of the ^{13}C isotope (1.1 %) when compared to the 100 % abundance of ^{1}H isotope and makes the analytical time long and the amount of required specimen high. Therefore, the two spectroscopy methods are often combined to obtain a more complete characterization. The ^{13}C chemical shift of the different carbons detected in acetylated and non-acetylated lignins can be found in literature.[103, 112] Nowadays, Two -Dimensional Heteronuclear Single Quantum Coherence (2D-HSQC) spectroscopy is widely used as complementary analysis to identify functional groups, monomers and intramolecular linkages in lignin structure.[113-115] 2D-HSQC correlates the ^{1}H nucleus with the ^{13}C, displaying therefore less signal overlapping.
As already mentioned lignin reactivity is mainly due to the hydroxyl groups (OH) hence, the reliable determination of their nature (phenolic, aliphatic or carboxylic) and their quantification is highly desired. ^{1}H-NMR allows the acquisition of such information but it requires the previous acetylation of lignin. Lignin acetylation generally consists in the treatment of lignin with acetic anhydride with or without the addition of pyridine as catalyst and it results in the esterification of the polymer hydroxyl functionalities. The different reactivity and steric hindrance of hydroxyls functions is not a guarantee for a total acetylation. Therefore, OH quantification by ^{1}H-NMR can cause the underestimation of the reactive sites. Although more expensive ^{31}P-NMR spectroscopy applied on lignin, which is first derivatized by phosphitylation, represents a more reliable and faster method for the OH quantification. In fact, the 100 % natural abundant ^{31}P nucleus makes ^{31}P-NMR analysis faster and more sensitive than ^{13}C-NMR spectroscopy. Moreover, ^{31}P-NMR generates spectra with higher resolution and better peaks separation than ^{1}H-NMR, due to the larger range of chemical shifts of the former (1000 ppm for ^{31}P-NMR and 13 ppm for ^{1}H-NMR). ^{31}P-NMR enables the determination of the different types of OH such as aliphatic, phenolic and carboxylic. In addition, lignin monomer composition can be described through the ^{31}P-NMR distinction of guaiacyl, syringyl and p-hydroxyphenyl hydroxyls.[116] During the phosphitylation (Fig. 2.1), OH groups are derivatized by an organophosphorous compound and in order to accelerate the relaxation time of the ^{31}P nucleus, a relaxation agent based on Chromium, Cr(III) is added to the sample.[103, 113]

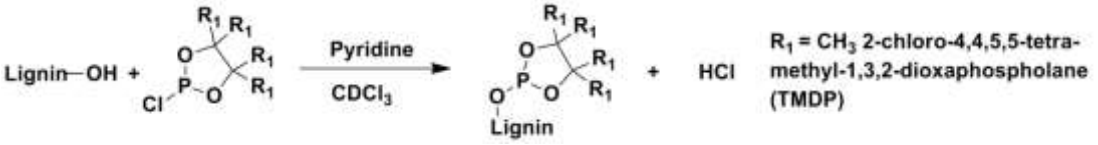

Figure 2.1 *Phosphitylation of OH groups in lignin.*

2.2 Influence of the isolation method on lignin structure

Beech (*Fagus sylvatica*) is one of the most diffused hardwood trees in Europe, therefore was chosen as starting material for our experiments. As mentioned, before the biomass characterization and the lignin extraction it is necessary to remove the ethanol soluble materials (extractives) from the beech wood chips. In fact, extractives such as waxes or other components could interfere with the analytical procedures. Therefore, beech wood chips purchased by GOLDSPAN® were dried at 45 °C for 48 h and the extractives were removed by refluxing the chips with ethanol for 24h.[102, 117] The measurement of the wood moisture, which is caused by its exposure to air, is called "Determination of Total Solid" and was performed by drying the chips at 105 °C overnight.[118] Moreover, the determination of the ash was carried out by calcination of the wood at 575 °C.[119] As above mentioned, the biomass content of acid soluble and insoluble lignin (ASL and AIL, respectively) was calculated by acid hydrolysis of the wood (see 2.1.1).[101] All these procedures are explained in detail in the experimental part of this work (B2, B3, B4), whereas the results of the characterization are reported in Table 2.2.

Table 2.2 *Characterization of beech wood chips*

Raw material	Total Solids (wt %)	Extractives (wt %)	Ash (wt %)	AIL_{wood} (wt %)	ASL_{wood} (wt %)	Total Lignin in beech wood (wt %)
Beech wood chips	95.9	0.4	0.03	6.6	15.0	21.6

Extractive-free beech wood chips were subjected to three different pretreatments: a classic soda pulping, a hydrothermal alkali method based on the use of $Ba(OH)_2$ as base and an organosolv acid-catalyzed process. The isolated lignins were named soda lignin (SL), alkali lignin (AL) and organosolv lignin (OL), respectively. All the extraction processes were performed under endogenous pressure in a sealed autoclave equipped with a mechanical stirrer (Fig. 2.2).

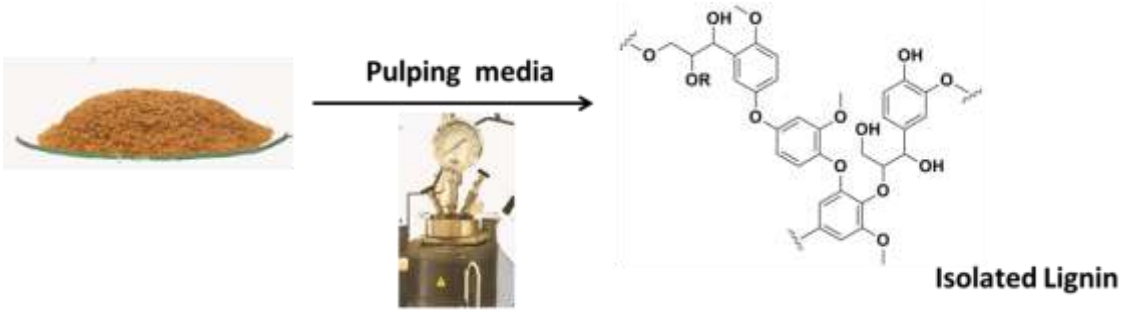

Figure 2.2 *General scheme of lignin extraction processes in autoclave*

During the soda process, the chips were treated by a NaOH aqueous solution at 175 °C for 12 hours. The mixture was filtrated to separate the pulp from the liquid part (dark liquor) and lignin (SL) was precipitated by acidification of the liquid fraction.
A second hydrothermal alkaline process was performed employing $Ba(OH)_2$ as base. Although $Ba(OH)_2$ is more expensive and toxic than NaOH, a previous work about the treatment of rye straw with $Ba(OH)_2$ showed the advantage of the simultaneous generation of lactic acid and lignin. This alkaline hydrothermal method was initially developed by Esposito et Al.[45] for the generation of lactic acid from rye straw. We optimized the extraction conditions, such as time and temperature, with the purpose of lignin isolation from beech wood. Thus, a mixture of beech wood chips and a $Ba(OH)_2$ aqueous solution, was heated in the sealed autoclave at 220 °C for 15 hours. After filtration of the mixture, lignin (AL) was isolated from the solid pulp. The latter was washed by acid to remove the excess of barium and a tetrahydrofuran (THF) soluble lignin was recovered.
As reported in paragraph 1.5.2, organosolv methods lead to the isolation of a high pure and less modified lignin structure. Therefore, an organosolv lignin (OSL) was extracted by treatment of beech wood chips with ethanol in water (65 V/V %) and in the presence of sulfuric acid as catalyst.[120] The process was carried out in autoclave, at 195 °C for 80 minutes and lignin was precipitated from the liquid phase by addition of water. The details of all the pulping methods are reported in the experimental part.
The collected SL, AL and OSL, were dried and characterized by the analytical methods mentioned in paragraph 2.1. The results of molecular weight, dispersity (D), yield, lignin purity (acid insoluble and soluble lignin, AIL and ASL respectively) and the elemental composition are reported in Table 2.3. The lignin yield of the extraction processes, was calculated considering the lignin purity degree (AIL+ASL) and employing the equation 2.2.

Equation 2.2 *Calculation of lignin-yields reported in Table 2.3*

$$\text{Yield} = \frac{\text{PL (g)} * 100 * (\text{AIL}+\text{ASL})}{B_w(g) * 21.6}$$

PL: precipitated lignin (g)

B_w: biomass weight (g)

21.6: absolute lignin content in beech wood chips (wt %)

AIL: acid isoluble lignin (wt %)

ASL: acid soluble lignin (wt %)

Table 2.3. *Characterization of soda, alkaline and organosolv lignin (SL, AL and OSL, respectively).*

Extraction process	Yield (wt %)	M_w (g mol^{-1})	M_n (g mol^{-1})	D (Mw/Mn)	ASL (wt %)	AIL (wt %)	Elemental analysis (wt %)		
							N	C	H
SL	42.6	1542	826	1.9	25.1	62.7	0.2	60.9	5.7
AL	42.1	1341	868	1.6	25.4	65.7	0.2	64.5	6.2
OSL	41.6	2905	1596	1.8	1.5	95.6	0.2	67.3	5.3

Mw, mass average molar mass; Mn, number average molar mass; D, dispersity (molar mass distribution); AIL, acid insoluble lignin; ASL, acid soluble lignin. Yields are calculated by equation 2.2.

Table 2.3 shows that the yields of the three processes are similar as well as most of the parameters of the two lignins obtained by alkaline treatments (SL and AL). As mentioned in the introduction, the extraction of lignin in an acid environment favors a lower degradation degree and a higher probability of condensation reactions when compared to the alkaline methods. Therefore, the resulting OSL structure is more complex and richer in C-C bonds, which are more difficult to break down than C-O bonds (see Fig.1.10 for the mechanism of acidic deconstruction). This explains the higher Mw of OSL, its lower amount of acid soluble lignin (ASL) and the higher carbon content, when compared with the alkaline lignins. All the isolated polymers showed Mw and D values aligned with the data reported in literature.[53,32, 121, 122]

2.2.1 Qualitative solubility

SL, AL and OSL were dissolved in a concentration of 1 mg/mL in the most common solvent and stirred at room temperature overnight. The solubility was determined by visual observation[14] and the results are reported in Table 2.4. It can be observed that all lignins are soluble in alkaline solvents, such as pyridine, due to the presence

of acid phenols and the consequent formation of phenolates. The solubility in $CHCl_3$ is increasing with the decreasing of the hydroxyls amount (see following section), while no lignin is soluble in extremely protic (H_2O) or hydrophobic (hexane) solvent.

Table 2.4 *Solubility of 1 mg mL^{-1} SL, AL and OSL in the most common solvents.*

Extraction process	THF	MeOH	EtOH	H_2O	$CHCl_3$	Hexane	Pyridine	DMSO	DMF
SL	S	S	S	I	Ps	I	S	S	S
AL	S	S	S	I	I	I	S	S	S
OSL	S	S	S	I	S	I	S	S	S

S, soluble; I, insoluble; Ps, partially soluble; THF, tetrahydrofuran; MeOH, methanol; EtOH, ethanol; H_2O, water; $CHCl_3$, chloroform; DMSO, dimethylsulfoxid; DMF, dimethylformamide.

2.2.2 ^{1}H and ^{31}P-NMR quantification of hydroxyl and methoxyl groups

For the ^{1}H-NMR analysis, the three different lignins were acetylated by treatment with acetic anhydride at 100 °C. Thus, the acetylated lignins were analyzed by ^{1}H-NMR using deuterated chloroform ($CDCl_3$) as solvent. DMF was added in the NMR tube as internal standard (IST). In the ^{1}H-NMR spectrum the proton signal of lignin-hydroxyl and methoxyl groups, which fall in the range of 2.0-2.3 ppm and 3.2-4.0 ppm respectively (Fig. 2.3A), was integrated and referred to the integrated peak of the DMF amide proton (peak at 7.8-7.7 ppm). The reliability of the analytical method was first tested for the quantification of hydroxyl and methoxyl functionalities of acetylated homovanillyl alcohol, which was used as lignin model. The quantification results of lignin hydroxyl and methoxyl groups are reported in Table 2.5.

In order to have a further analytical comparison, hydroxyl groups were quantified as well by ^{31}P-NMR (Fig. 2.3B). As already mentioned, phosphorous spectroscopy requires the use of both a phosphitylation and relaxation agent. Following the procedure reported from Pu et al.,[116] DMF was used to dissolve dried-lignin in a mixture of anhydrous pyridine/DMF (1:1 v/v). Thus, chromium(III) acetylacetonate and cyclohexanol as relaxation agent and internal standard respectively, were added. The TMDP derivatization reagent is then incorporated and the final solution is analyzed.

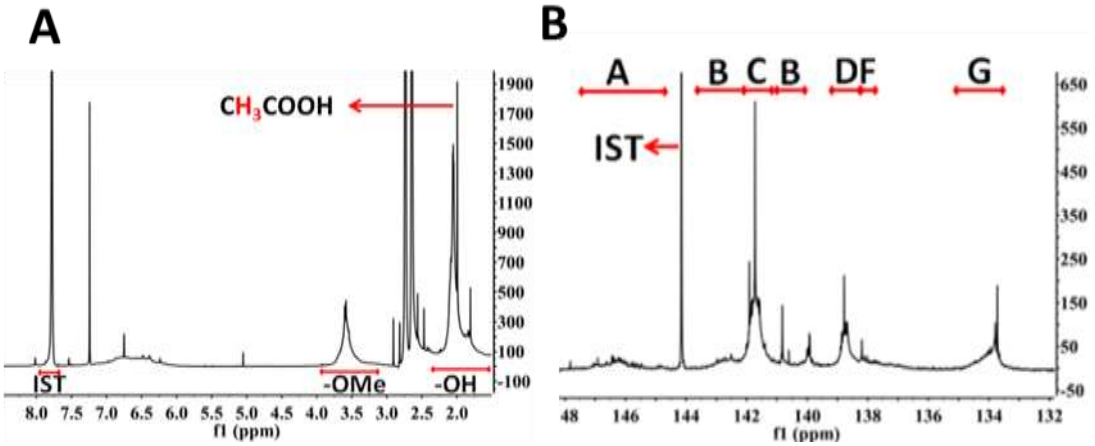

Figure 2.3 A- *^{1}H-NMR spectrum of acetylated AL with DMF as internal standard (IST).* **2.3 B-** *^{31}P-NMR spectrum of AL with cyclohexanol as IST. A: aliphatic-O-P-groups; B: condensed phenolic-O-P-groups; C: syringyl-O-P groups, D: guaiacyl-O-P-groups; F: p-hydroxyl-O-P-groups; G: carboxyl-O-P-groups.*[116]

As shown in Fig. 2.3B the resolution of the different peaks allows the identification and quantification of aliphatic (A), syringyl (C), guaicyl (D), p-hydroxyphenyl (F) and carboxyl moieties (G).

Table 2.5 *^{1}H-NMR and ^{31}P-NMR quantification of hydroxyl and methoxyl groups*

Extraction process	^{1}H-NMR quantification (mmol/ g)		^{31}P-NMR quantification (mmol/ g)							
	Total -OH	Total -OMe	G -OH	S -OH	H -OH	Condensed ph -OH	COOH	Aliph -OH	Total ph -OH	Total -OH
SL	5.0	6.0	0.7	1.7	0.1	0.9	0.6	0.4	3.4	4.4
AL	5.6	2.3	0.6	1.8	2	0.9	0.8	0.1	5.3	6.2
OSL	2.4	4.3	0.6	0.7	0.3	1.7	0.03	0.3	3.6	3.6

The amount of OH and OMe is expressed as mmol g^{-1} (mmol of OH or OMe functionalities per gram of lignin) in beech wood lignin obtained from soda (SL), alkali (AL) and organosolv extraction (OSL). Ph, phenolic; aliph, aliphatic; S, syringyl-OH-groups G, guaiacyl-OH-groups, p, p-hydroxyphenyl-OH-group.

Table 2.5 shows differences in the total amount of hydroxyl gropus quantified by the two spectroscopy methods. In the case of AL and OSL, the total amount of OH groups found by ^{1}H-NMR is respectively 11 and 50 % lower than the one calculated by ^{31}P-NMR. These remarkable differences, especially in the case of OSL, are probably due to a not complete lignin-acetylation. In fact, hydroxyl moieties display

different reactivity and steric hindrance. In contrast, in case of SL about 12 % more hydroxyl functionalities are measured by ^{1}H-NMR compared to the phosphorous spectroscopy. The inhomogeneity of the results can be explained considering also the partial overlapping of the peak related to the residual acetic acid (peak at 2.0 ppm in Fig. 2.3A) and the peaks related to lignin hydroxyl groups. The complete removal of acetic acid formed during acetylation was not possible even after drying the sample under vacuum for a long time. For these reasons, results calculated by ^{31}P-NMR were considered more reliable. Interestingly and despite the discrepancies according to both NMR approaches, the OH content of the three lignins is increasing inversely to Mw (Table 2.3). The high condensation degree of OSL structure is confirmed by its highest content of condensed phenolic functionalities (47 % referred to the total phenolic hydroxyls, Table 2.5). The calculated ratio of S/G/H (syringyl/ guaiacyl/ p-hydroxylphenyl units respectively) in SL and OSL are 68/28/4 and 44/28/19 respectively and are in line with the data reported in literature.[6, 23, 99, 103] Moreover, although it is reported that the amount of methoxy functions is just slightly influenced by the lignin isolation process,[103] the results in table 2.5 show a considerable difference between the methoxy content of the lignins. In detail, the lower amount of methoxy groups in OSL could be caused by the acid-catalyzed hydrolysis of methoxyls. As well, the huge difference in the methoxy group content in AL (6.0 mmol g^{-1}) and SL (2.3 mmol g^{-1}) can be explained with a greater alkaline hydrolysis of the methoxy functionalities in the first sample, increasing the number of free phenolic hydroxyls. In fact, the $Ba(OH)_2$ hydrothermal treatment is performed at higher temperature, for longer time and with a higher amount of base than the soda process. This is a further reason for the higher amount of phenolic hydroxyls in the AL structure than in SL (Table 2.5).[123, 124]

2.2.3 FT-IR analytical comparison of AL, SL and OSL

AL, SL and OSL were characterized by FT-IR spectroscopy (Fig 2.4). They show characteristic absorbance bands of lignin, such as the C=O stretching band in the range of 1715-1710 cm^{-1}, the bands related to the aromatic ring vibrations (1515-1505 cm^{-1}) and the C-H and C-O deformations bands in the range of 1085-1030 cm^{-1}. Although the spectra of the three samples are quite similar, it is possible to notice some indicative differences. For instance, the bands related to the methoxy groups (1425-1460 cm^{-1}) are more intense in SL, whereas the absorbance of the phenolic hydroxyl groups (1375-1325 cm^{-1}) is higher in AL than in SL.[125] The data confirm the quantitative results reported in table 2.5.
A complete list of lignin IR-adsorption bands is reported in Table S2.1 in the supplementary information.

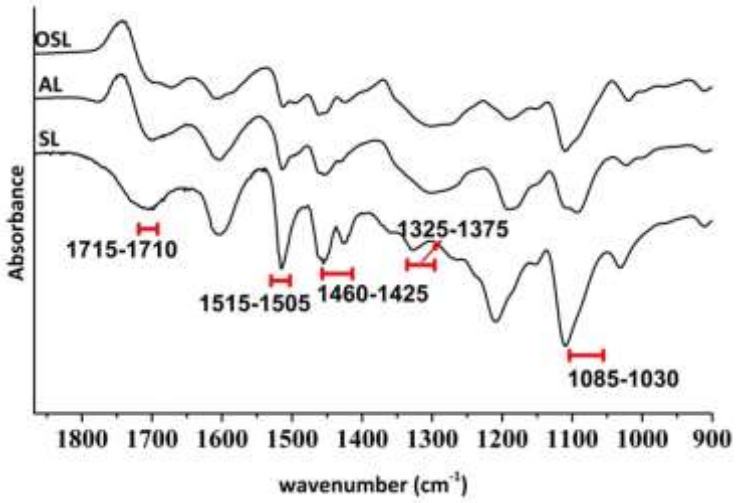

Figure 2.4 *FT-IR spectra of OSL, AL and SL in the range of 1860-900 cm^{-1}*

2.2.4 2D HSQC-NMR: monomer composition and linkages

2D HSQC-NMR was used to collect more data about the monomer composition and the main intramolecular linkages of lignins structure. The spectra were obtained by dissolution of 100-110 mg of acetylated-lignin in deuterated chloroform. Although the comparison of the 2D HSQC-NMR spectra is just qualitative, some important information can be extrapolated. The region of the spectra included in the range of 100-130 ppm for the carbon chemical shift (y axis) and 6.3-7.3 ppm for the proton chemical shift (x axis) provides information about the substitution of the aromatic rings (column A in Fig. 2.5) and therefore about the monomer composition. For instance, the presence of all the three main units, syringyl (S), guaiacyl (G) and p-hydroxyphenil units (H) in AL, SL and OSL is confirmed. As well, the spectra comparison displays a lower amount of syringyl units in OSL and a higher amount of guaiacyl units in AL. Moreover, the 2D spectroscopy highlights the further existence of γ-p-hydroxybenzoates (Pb) and of oxidized syringyl units (S´), although the signal related to the former is overlapping with the signal of p-hydroxyphenyls.[52, 103, 126] The last consideration confirms the partial oxidation of lignin structure during all the three extraction processes. The region included in the range of 50-65 ppm in the carbon chemical shifts and 3.3-4.0 ppm for the proton chemical shifts, provides information about the alkyl side chains and the linkages between the units (column B in in Fig. 2.5). The spectra comparison shows a remarkable difference between the intensity of the signal related to the β-O-4 linkages in OSL and the same signal in AL and SL. In fact, the signal corresponding to the ether bond is more evident in OSL, suggesting a lower degradation degree in comparison with AL and SL.[126]

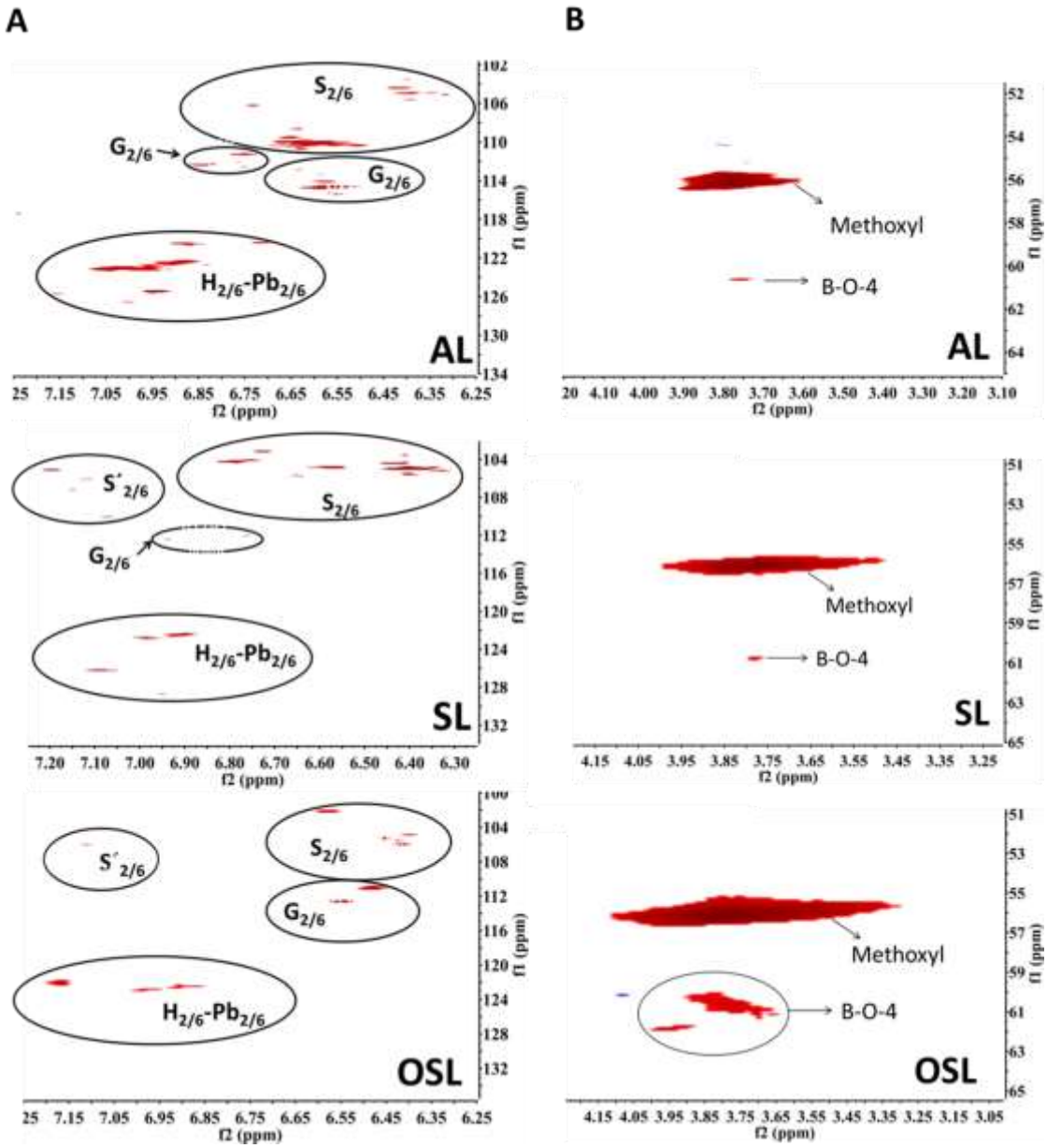

Figure 2.5 *2D HSQC-NMR of AL, SL, OSL* **Column A-** *Aromatic region* **Column B-** *Side chains region. S, syringyl units; G, guaiacyl units; H, p-hydroxyphenyl units; S´, oxidized syringyl units; Pb, γ-p-hydroxybenzoates. 2/6 indicates the position of the considered C-H on the aromatic ring.*

2.2.5 Thermal data: TGA and DSC of AL, SL and OSL

Although lignin thermal decomposition starts approximately at 200 °C, the TGA analysis (Fig.2.6) displays three main regions, described by temperature intervals. The first region A, between 100-120 °C is not due to the lignin decomposition but is attributed to the loss of humidity. In the range of 200-450 °C, the intramolecular lignin linkages break and the released monomers start to evaporate. Above 400 °C (corresponding region C), the aromatic rings degradate.[47]

By comparison of the TGA curves of AL, SL and OSL, it can be observed that the degradation of AL occurs at lower temperatures than in the other two lignins. Indeed, a mass loss of 5 % occurs at 144 °C for AL, 204 °C for SL and 229 °C for OSL. These results correlate with an increasing Mw of the three lignins. The higher temperature of maximum decomposition (T_{md}) of OSL (390 °C) in comparison with the T_{md} of SL (324 °C) and AL (333 °C), can be attributed to a higher amount of resistant C-C linkages present in the OSL condensed structure. Furthermore, the lower amount of OSL residual mass at 998 °C (1 wt %) and a higher one of AL and SL (16 and 30.wt % respectively), could be explained by the residual presence of cations such as Na^+ and Ba^+ in the alkaline lignins (AL and SL).[107] In fact, it is reported that the presence of cations, such as Na^+ in lignin structure, favors the formation of char.[127] For this reason, an alkaline hydrothermal method should be considered for further lignin application involving carbonization processes. For instance, it could have an important role in the application of lignin as precursor of carbon materials (4th paragraph). Moreover, the results obtained by differential scanning calorimetry (DSC) and reported in Table 2.6, show a higher glass temperature (Tg) in the case of OSL, pointing out its more rigid and condensed structure.

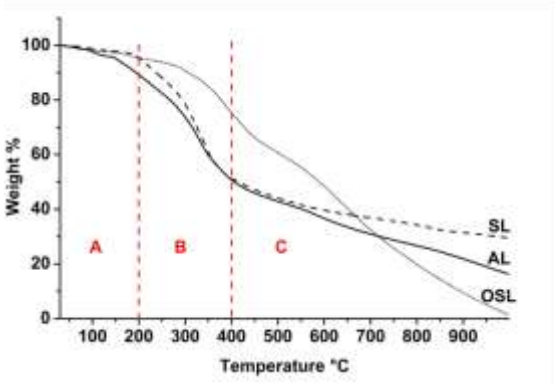

	TGA		DSC
Lignin sample	T_{md}	Residual Mass (wt %) at 1000°C	Tg °C
SL	324.2	29.5	84.5
AL	333.4	16.2	62.1
OSL	389.5	1.3	160.5

Figure 2.6 *Thermal gravimetric analysis (TGA) of AL, SL and OSL. The analysis is conducted in nitrogen atmosphere. The temperature is increased from 30 to 1000 °C with a rate of 10 °C/min.* **Table 2.6** *TGA and DSC results. Tg, glass temperature; SL, soda lignin; AL, alkaline lignin; OSL, organosolv lignin.*

2.3 Structural differences of lignin from different biomass sources

In order to compare the lignin structures obtained by isolation of the aromatic polymer from different biomass sources, we applied a soda treatment both to woody bamboo (*Phyllostachys pubescens*) and coconut (*Coconut nucifera*). We compared the characterization data of the resulting lignins to the results obtained by soda treatment of beech wood lignin (SL) reported in the previous paragraph.

Bamboo was chosen because it is a woody grass plant widely distributed in Asiatic countries, fast-growing and already used as alternative source for paper and textiles production.[115, 128, 129] Coconut belongs to the group of drupes, which are fruits consisting of a seed enclosed by a hard endocarp, which is enveloped by a thin outer part (exocarp). In particular, coconut is one of the most used drupe endocarp[130] with high lignin content (up to 33 wt %) in the fibrous husk, which is usually regarded as a waste.[131] Coconut is a very hard material, whereas bamboo has a more fibrous nature. Considering the physical characteristic of both the biomasses, their fine grinding requires the use of specific mills. Due to a lack of these instrumentations, the two materials could not be grinded. Therefore the characterization of coconut and bamboo lignin content was not possible. The two biomasses were subjected to the soda pulping method in order isolate lignin, applying the procedure described in paragraph 2.2. Hence, bamboo sticks and coconut shells were roughly cut in about 2 cm long and 2 cm long and 2 cm wide pieces. The biomasses were treated in autoclave with a NaOH aqueous solution at 175 °C for 12 hours. After filtration of the mixture, lignin was precipitated by acidification of the dark liquor. Such obtained coconut and bamboo lignins (CL and BL, respectively), were dried and characterized, comparing their structural features to the previously isolated beech wood lignin (SL). The extraction method is schematized in Fig.2.7.

Figure 2.7 *Scheme of soda isolation process of bamboo and coconut lignin (BL and CL respectively).*

The purity of both coconut and bamboo lignin, was measured through the calculation of acid soluble and insoluble lignin (ASL and AIL respectively, paragraph 2.1.1), Mw, Mn and D, were determined by GPC employing NMP as solvent and elemental composition was studied by elemental analysis. As mentioned, since the fine grinding of coconut and bamboo was not possible, their characterization before the alkaline treatment could not be performed. Therefore, lignin yields are calculated in relation to the initial mass of raw material and not to in relation to the lignin content of the biomass. As described by equation 2.3, the yields are calculated considering the lignin purity (AIL + ASL) and the results are reported in Table 2.7.

Equation 2.3 *Calculation of bamboo, coconut and beech wood lignin extraction yield by soda isolation process.*

$$\text{Yield} = \frac{\text{PL (g)} * 100 * (\text{AIL}+\text{ASL})}{B_w(g)}$$

PL: precipitated lignin (g)

B_w: biomass weight (g)

AIL: acid insoluble lignin (wt %)

ASL: acid insoluble lignin (wt %)

Table 2.7 *Characterization of SL, BL and CL*

Biomass source	Yield (wt %)	M_w (g mol^{-1})	M_n (g mol^{-1})	D (Mw/Mn)	ASL (wt %)	AIL (wt %)	Total L ASL+AIL	Elemental analysis (wt %)		
								N	C	H
SL	9.2	1542	826	1.9	25.1	62.7	87.8	0.2	60.9	5.7
BL	9.8	1761	932	1.9	17.5	72.1	89.6	0.2	63.6	6.1
CL	14.7	3799	1535	2.5	2.5	93.6	96.1	0.4	60.2	5.3

Mw, mass average molar mass; D, dispersity; AIL, acid insoluble lignin; ASL, acid soluble lignin. The yields are calculated by equation 2.3.

As expected from literature coconut has the highest yield of extracted lignin, while the one of SL and BL is similar. CL displays the highest Mw and dispersity (D) degree and the lowest amount of acid soluble lignin (ASL). Probably this is due to a high amount of C-C bonds, which are more resistant to the alkaline treatment than C-O linkages. The elemental composition of the three lignins is similar and aligned to the general lignin composition.[103, 132]

2.3.1 Qualitative solubility

The qualitative solubility test was performed as described in paragraph 2.2.1 on SL, BL, and CL. Table 2.8 summarizes the observed results. In contrast with the other two lignins, CL was difficult to dissolve in most of the solvents. This can be attributed to its high average molar mass and to the complexity of the structure, which will be discussed in the following chapters.

Table 2.8 *Solubility of 1 mg mL^{-1} SL, BL and CL in the most common solvents.*

Biomass source	THF	MeOH	EtOH	H_2O	$CHCl_3$	Hexane	Pyridine	DMSO	DMF
SL	S	S	S	I	Ps	I	S	S	S
BL	S	S	S	I	I	I	S	S	S
CL	Ps	Ps	Ps	I	I	I	S	S	S

S, soluble; I, insoluble; Ps, partially soluble; THF, tetrahydrofuran; MeOH, methanol; EtOH ethanol; H_2O, water; $CHCl_3$, chloroform; DMSO, dimethylsulfoxide; DMF, dimethylformamide.

2.3.2 ^{1}H and ^{31}P-NMR quantification of hydroxy and methoxy groups

Acetylated SL, BL and CL were subjected to ^{1}H-NMR spectroscopy in order to quantify the methoxyl and hydroxyl functionalities. Both samples were phosphitylated (see paragraph 2.1.4 for the method) and analyzed by ^{1}P-NMR. The results are reported in Table 2.9.

Table 2.9 *^{1}H-NMR and ^{31}P-NMR quantification of hydroxy and methoxy functionalities in SL, BL and CL.*

Biomass source	^{1}H-NMR quantification (mmol/ g)		^{31}P-NMR quantification (mmol/ g)							
	Total -OH	Total -OMe	G -OH	S -OH	H -OH	Condensed ph -OH	COOH	Aliph -OH	Total ph-OH	Total -OH
SL	5.0	6.0	0.7	1.7	0.1	0.9	0.6	0.4	3.4	4.4
BL	3.4	3.3	1.0	1.0	0.8	1.0	0.7	0.4	3.8	4.9
CL	2.9	3.1	0.8	1.1	0.8	0.8	0.6	0.5	3.5	4.6

The amount of functional groups is expressed as mmol g^{-1}. Ph, phenolic; aliph, aliphatic; S, syringyl-OH-groups; G, guaiacyl-OH-groups; ph, p-hydroxyphenyl-OH-groups.

A remarkable disparity between the data obtained by the two spectroscopic methods can be observed. For both BL and CL, the OH amount calculated by ^{1}H-NMR is lower than the one measured by ^{31}P-NMR confirming the possibility of a not complete acetylation of lignin structure. The total amount of phenols and hydroxyls is similar in the three samples. In this case, the highest amount of methoxy functions in SL, calculated by ^{1}H-NMR, can be justified by its highest amount of

syringyl (S) units, quantified by ^{31}P-NMR (Table 2.9). In fact, the syringyl unit contains two methoxy functionalities for each aromatic ring, while only one OMe group can be found in the guaiacyl monomer (Fig. 1.3 in the introduction). Based on the data obtained by ^{31}P-NMR, the monomer composition of the three lignins is described by a G/S/H (guaicyl/syringyl/p-hydroxyphenil) ratio of 28/68/4 for SL, 35/36/29 for BL and 30/40/30 for CL. As observed, BL and CL show an equal distribution of the three units, whereas SL monomer composition is shifted towards syringyl units. The ^{1}H-NMR and ^{31}P-NMR spectra of BL and CL are reported in the supplementary information (S2.3-S2.4 respectively).

2.3.3 FT-IR analytical comparison between SL,BL and CL

A comparison between the FT-IR spectra of SL, BL and CL is reported in Fig.2.8. As observed, the similar amount of hydroxyl functionalities is reflected in the similarity between the spectra. Typical lignin absorbance bands can be observed. The hydroxyl stretch band falls in the range of 3450-3400 cm^{-1}, the C=O stretch band is found between 1715-1710 cm^{-1}and in the range of 1515-1505 cm^{-1} there are the aromatic ring-vibration bands. The absorbance between 1270-1275 cm^{-1} corresponds to the guaiacyl and siryngyl ring vibration, respectively. Furthermore, a band at 1122 cm^{-1} can be related to a guaicyl-syringyl (GS) lignin type.[132]

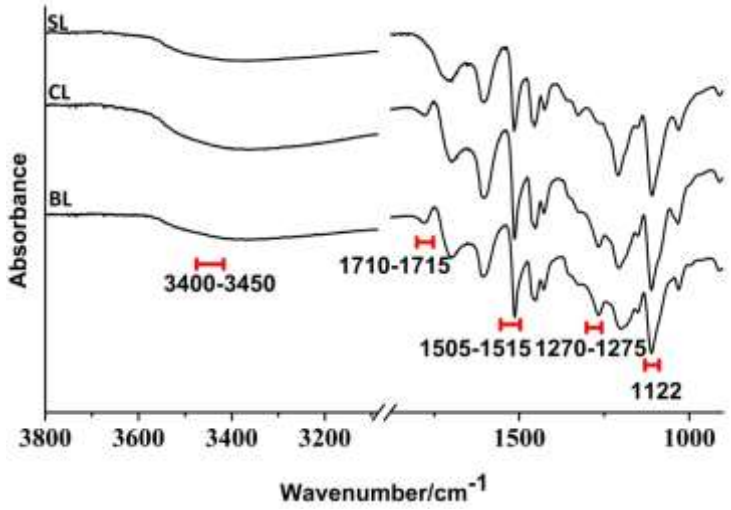

Figure 2.8 *FT-IR spectra of beech wood lignin (SL), bamboo lignin (BL) and coconut lignin (CL)*

2.3.4 2D HSQC-NMR: monomer composition and linkages

Lignin structure composition was further investigated by qualitative comparison of the 2D HSQC-NMR spectra of acetylated SL, BL and CL. The aromatic region of the spectra (Fig. 2.9) shows the monomer composition of the structures. As displayed, SL has abundant signals related to the syringyl and oxidized syringyl units (S and S´ respectively), whereas the intensity of the signal corresponding to the guaiacyl units is weaker. Therefore, SL is considered a syringyl-lignin type. In contrast, the spectrum of bamboo lignin (BL) shows a more equal ratio of syringyl and guaiagyl monomers, as confirmed by the hydroxyl quantification (Table 2.9). Interestingly, both SL and CL spectra show a weak signal related to the guaiacyl -CH, which confirm the lower G content of SL and CL when compared to BL.

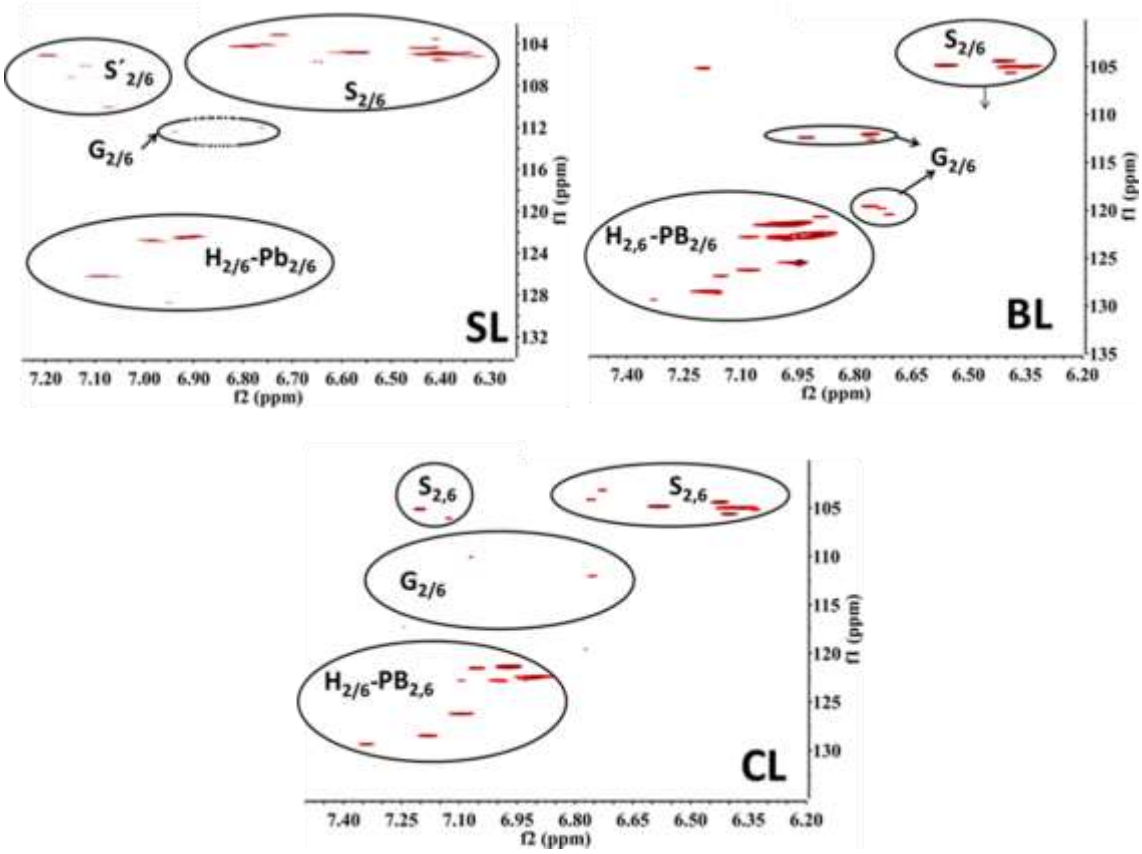

Figure 2.9 *2D HSQC-NMR spectra of acetylated beech wood lignin (SL), bamboo lignin (BL) and coconut lignin (CL), aromatic region*

2.3.5 Thermal data: comparison between SL, BL and CL

The TGA analyses of the three lignins are in agreement with the typical decomposition trend of lignin (paragraph 2.2.5). However, the curves show the different thermal behavior for SL, BL and CL. (Fig. 2.10). The trend of the curves

between 100-170 °C is similar, while increasing the temperature, the decomposition of SL takes place at the lowest temperature, followed by BL and CL decomposition at 205 °C and at 240 °C respectively. While SL curve has a clear T_{md} (temperature of maximum decomposition) at 324 °C, in both BL and CL the presence of two wide decomposition bands make the determination of the T_{md} point not trivial. Therefore, a range of temperature between 338-388 °C for BL and 352-397 °C for CL was considered, instead of a single decomposition point. The different temperature-range of decomposition between BL and CL, can be explained by their different degradation and condensation degree. The residual mass of SL and CL is around 30 wt %, while in the case of BL it is 16 wt %. A further confirmation of the more complex and rigid structure of CL is its higher glass temperature calculated by DSC and reported in Table 2.10. Considering the TGA results, lignins extracted from coconut and from beech wood by a soda isolation method, could be valid candidates as carbon precursors (chapter 4).

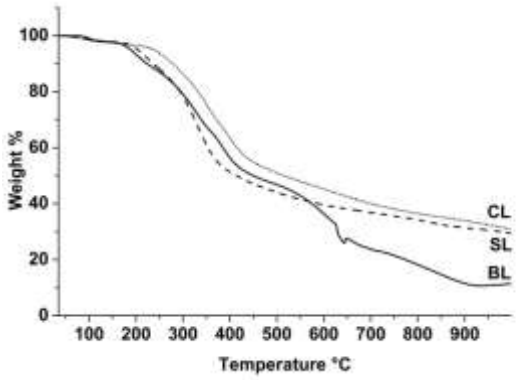

	TGA		DSC
Lignin sample	T_{md}	Residual Mass (wt %) at 1000°C	Tg °C
SL	324.2	29.5	84.5
BL	337.5-387.5	16.2	72.2
CL	351.9-396.8	31.0	117

Figure 2.10 *TGA of SL, BL and CL.* **Table 2.10** *TGA and DSC results. SL, beech wood lignin; BL, bamboo lignin; CL, coconut lignin; Tg, glass temperature; T_{md}, temperature of maximum decomposition. The TGA analysis is conducted in nitrogen atmosphere. The temperature is increased from 30 to 1000 °C with a rate of 10 °C/min.*

2.4 Final considerations

This work emphasizes the contribution of the isolation method and of the biomass source on isolated lignin structure. Several extraction processes were applied on beech wood, common hardwood tree in Europe. The different lignin extraction methods were chosen considering the cost and the toxicity of the utilized reagents, the ease of lignin recover from the obtained mixture and the possibility of a simultaneous recover of other interesting biomass products. This study shows that the isolation method affects lignin elemental composition while the atomic composition depends more on the lignin source. The isolation processes exhibited

only a slight influence on the lignin extraction yield. However, due to different cleavage mechanism, they strongly affect the mass average molar mass of the isolated lignin. In detail, we confirmed that alkaline processes afford a more degraded structure, whereas the organosolv treatment of the aromatic polymer in acidic environment leads to a less deconstructed and more condensed lignin structure. In fact, the acidity favors the nucleophilic addition of electronrich species, which are generated during the pulping to electrophilic species (Fig.1.10). The results were confirmed by ^{1}H-NMR and ^{31}P-NMR hydroxyls quantification. Indeed, the OH content which is related to the cleavage of aryl ether bonds, is higher for alkaline lignins In particular, the extraction method affects more the content of phenolic OH and less the amount of aliphatics. Moreover, lignin isolated by hydrothermal $Ba(OH)_2$ alkaline method, showed the highest amounts of free hydroxy groups and the lowest Mw.

The thermal analysis of the three samples showed a higher thermal stability of organosolv lignin than the others. Nevertheless, above 700 °C OSL decomposition-rate is accelerating, to a final residual mass of 1.3 wt % , low when compared to the residual mass of the alkaline lignins (30 and 16 wt % for SL and AL respectively).

These considerations are extremely important to design a lignin application. Since hydroxyl functionalities have a key role in lignin reactivity for a further condensation reaction, i.e. in the synthesis of bio-based polymer, the use of alkaline lignins (with higher OH amount than orgasosolv lignins) should be favored. In addition, the Mw plays an essential role in lignin solubility and in the consequent possibility to process it. Lignin obtained by $Ba(OH)_2$ (AL) hydrothermal process, which showed the lowest Mw and the consequent highest solubility, resulted therefore the easiest to be processed. For this reason and considering the high residual mass of AL after carbonization, AL was chosen from our group for a nitrogen functionalization followed by the synthesis of a nitrogen doped carbon material (chapter 4).

On the other side, OSL seems a good candidate as a blending material for composites or bioplastics, in which the mechanical advantages induced by its addition, such as thermal stability and rigidity, overcome the problem of its low reactivity. On the base of these considerations, lignin obtained by $Ba(OH)_2$ was chosen In the second part of the chapter, an analytical comparison between lignin extracted from coconut (CL), bamboo (BL) and beech wood (SL) by soda method was performed. As expected, the highest amount of extracted lignin has been found for coconut. CL displayed the highest Mw, structural complexity and the less solubility, with consequent difficulties to be processed. However, the three lignins showed a similar amount of hydroxyl functionalities, which could lead to a consequent similar reactivity, i.e. towards esterification reaction. In chapter 5, we report the synthesis and the application of an amino-ester polymer based on the

use of CL, SL and BL as macromonomers. Such materials, containing the same ratio of lignin but coming from different sources, showed similar gluing properties.
One of the main obstacles to lignin-refinery is supposed to be the heterogeneity of lignin structure due to the biomass source. With our work, we will show an example of lignin application, in which the structural heterogeneity does not represent a complication.

3. CHARACTERIZATION OF AROMATIC PRODUCTS FROM LIGNIN AND LIGNIN-LIKE MOLECULES HYDROGENOLYSIS

3.1 Introduction

In 1983 Busche reported that around 170 platform chemicals were produced in the United States via petroleum and natural gas refinery. Modification of these primary building blocks allows for the preparation of thousands of different materials including polymers, dies, medicinal chemicals, pesticides and so on.[133] Among the primary building blocks, benzene, phenol, styrene and toluene play a special role and through their further derivatization an array of different compounds can be produced.[32] Keeping in mind that the goal of our work is the substitution of fossil feedstock with alternative sources, lignin is the best candidate as sustainable resource of aromatics. In order to obtain small arenes and derived compounds, lignin structure is deconstructed. Among others deconstruction methods, such as enzymatic and biotechnological processes, widely used are the catalytic processes such as hydrogenolysis, oxidation and hydrodeoxygenation (paragraph 1.6.3). Beside the optimization of the catalytic processes, the development of reliable analytical methods to identify and quantify the resulting mixture of products is a not trivial aim. This is mainly due to the fact that the largest number of the extracted compounds is not commercial therefore, a direct comparison with the standard is not possible. In this chapter we focus on the characterization of the complex mixture of aromatic molecules obtained by heterogeneous catalytic hydrogenolysis (HGL) of lignin. A method for the identification and quantification of such generated small aromatics will be described.

Moreover, the versatility of the analytical method will be showed by the use of the same for the quantification of polyphenolic compounds extracted from olive leaves.[134]

We decided to investigate lignin hydrogenolysis because, unlike oxygenation and hydrodeoxygenation, HGL allows the deconstruction of the polymer with the retention of most of the lignin functionalities (e.g. the hydroxyl functions).

Hence, a study of the influence of different HGL parameters such as catalysts, temperature, reactor system and starting material, both on the yield and on the distribution of the produced mono-aromatics was performed.

3.1.1 Nickel-based heterogeneous catalysts for lignin hydrogenolysis

As explained in paragraph 1.3.1, ether linkages are the most abundant bonds in lignin-structure. Their relative abundance follows the order: β-O-4 > α-O-4 > 4-O-5 and the corresponding bond dissociation enthalpies (BDE) are 290-305 kJ mol^{-1}, 215 kJ mol^{-1} and 330 kJ mol^{-1} respectively.[135] Therefore, the largest number of recently published deconstruction methods aim to the hydrogenolysis of β-O-4 and α-O-4 bonds, due to their predominance and relative ease of cleavage. During lignin HGL, C-O bond are cleaved by hydrogen (H_2) to form phenols and arenes-derived molecules.[136] In the attempt to increase the yield of the obtained monomers and to easily recover the employed catalyst, a heterogeneous process based on the use of transition metal-catalyst is generally used.[137] The most used transition metals are palladium (Pd), Cobalt (Co), Ruthenium (Ru), Platinum (Pt) and Nickel (Ni).[21] For all of them there are several examples in literature, which investigate the effect of metal loading, reaction temperature and solvent, on the yield and on the selectivity of products.[32, 87, 138] Ni was chosen from our group because of its advantageous properties. In fact it is cheap, widely available and it showed selective cleavage activity towards benzyl, alkyl and diaryl-ether linkages, both in homogeneous and heterogeneous conditions,[135, 136, 139] without significantly affecting the aromaticity or the arenes. Furthermore, the use of metal nanoparticles supported on carbon, alumina or silica, was reported to increase the hydrogenolytic activity.[140, 141] Based on these considerations, Molinari et al.[88] recently synthesized a Titanium Nitride-Nickel (TiN-Ni) catalyst, in which Ni-nanoparticles are supported on Titanium nitride (TiN). The catalyst was initially used for the hydrogenolysis of diphenyl-ether, used as a model for the cleavage of 4-O-5 ether-bond. The reaction was performed in a continuous flow reactor, at mild conditions (150°C, 12 bar), in presence of H_2 and with a flow of 0.3 mL min^{-1}, showing the full conversion of the model.
The catalytic process was then optimized by our group for the hydrogenolysis of the commercial Kraft lignin, comparing the catalytic activity of TiN-Ni with the activity of Pd/C and TiO_2-Ni.[142] This work will be reported in the following paragraphs focusing on the analytical studies of the so generated aromatic products.

3.1.2 Analysis of lignin-hydrogenolysis products

The complexity of lignin structure requires a preliminary study of hydrogenolysis reactions on simple models, such as diphenyl ether or benzyl phenyl ether. The qualitative characterization of the obtained products is generally performed by the use of gas chromatography (GC) equipped with electrospray ionization mass (EI-MS). The quantification, in turn, is obtained by the use of GC coupled with a flame ionization detector (FID). Transferring a method that has been developed on model

molecules on lignin is always problematic. Among the reasons, there are the analytical difficulties in characterizing the mixture of obtained lignin-HGL products. Lignin degradation generates a wide range of mono-, di- and polyaromatic molecules, which are currently difficult to separate, identify and quantify. In fact and as aforementioned, most of the generated molecules are not commercial and therefore, their identification and quantification relies on the analytic comparison with similar available compounds.[143]

Although the characterization of aromatic molecules can be performed by the use of several analytical techniques, such as liquid chromatography coupled with mass spectrometry (LC-MS)[144] and high pressure liquid chromatography (HPLC),[145] capillary gas chromatography (GC) represents the main employed tool.

Gas chromatography is an analytical technique applied on volatile and thermostable molecules, which are separated on the base of their boiling point as well as for their chemical affinity to the chromatographic stationary phase. During GC analysis the compounds are vaporized, pushed through the column by an inert gas and finally detected. The FID is the most used GC-detector for the quantification of organic molecules. In fact, FID has proportional response to the concentration of the sample, which means that it allows the detection of both traces and high amount of compound. Moreover, the FID generates chromatograms with high signal/noise ratio, in which separated compounds appear as peaks with different retention times (RT). The identification of organic molecules by GC-FID is possible only by direct comparison with the corresponding reference standard. The combination of gas chromatography with mass spectrometry (GC-MS), favors the identification of compounds in complex mixtures. Indeed, the molecules previously separated by GC are collected, ionized and identified on the basis of their fragmentation patterns by the mass spectrometry. Despite of that, the sensitivity (defined as the signal output *per* concentration of a substance) of the mass detector is remarkably lower than FID sensitivity. On the base of these considerations, the identification of aromatic molecules generated by lignin hydrogenolysis is generally performed by GC-MS, whereas the more sensitive GC-FID is preferred for the quantification.

The use of GC to analyze lignin deconstruction-products goes back to the 1961, when Coscia et al. isolated and identified a series of C1-C3 alkyl substituted guaiacols and syringols obtained by hydrogenation of birch and oak lignin. The reaction was catalyzed by copper chromite and the products were compared with the corresponding standards.[146] In this work, the isolation of the compounds was performed by a rudimentary version of the current gas chromatography, called vapor phase chromatography, while the identification by Fourier Transform Infrared Spectroscopy (FT-IR). Few years later, Pepper et al.[147-149] performed a comparison of the yield and the selectivity for the hydrogenolysis of spruce lignin, employing different catalysts. They isolated several molecules, such as vanillin and

syringaldehyde, which were quantified by GC-FID and with the use of an internal standard (IST).

Currently, the quantification of lignin hydrogenolysis-products is performed mainly by three different approaches. In a first approach, the amount of the aromatic compounds is expressed as percentage ratio between the peak area of the considered molecule and the total area of the peaks in the chromatogram.[150,137] A second approach is the comparison of the compounds peaks area with the peak area of a reference standard (RS), which displays similar structural features to the analyzed molecules and is used to prepare the calibration curve.[86, 135, 151] The group of Galkin[138] and the group of Pecina[152] reported a third analytical method. In both the works lignin hydrogenolysis mixture was previously derivatized by N,O-Bis(trimethylsilyl)trifluoroacetamide) (BSTFA) and then the aromatic molecules were characterized by GC-MS/FID.

The pretreatment of the sample with a trimethylsilyl agent, such as BSTFA, is performed in order to enhance the volatility and thermostability of polar organic molecules. In fact, compounds generated by lignin hydrogenolysis, are mainly substituted phenols, which are polar molecules characterized by low volatility and often low thermostability. The hydroxyl groups cause the formation of strong intermolecular-hydrogen bonds and consequently, the decrease of the molecule volatility. Furthermore, the presence of OH ionizable groups is responsible for the interaction of the polar functionalities with the stationary phase of the GC-column. This phenomenon causes the not reproducibility of peak area and shape in the GC-chromatogram. The disadvantages of these molecules towards GC analysis can be overcome by derivatization of the hydroxyl functions by silylation agents. Among them, we used BSTFA, which is commonly utilized for the analysis of alcohols, phenols and carboxylic acids. The chemical reaction between BSTFA and the polar compound consists in the nucleophilic attack of the OH group upon the silica atom of the silyl reagent (Fig. 3.1).

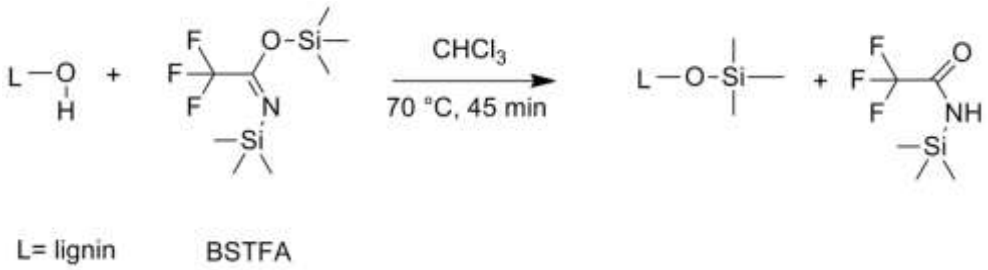

Figure 3.1 *Derivatization of lignin hydroxyl groups by BSTFA*

Based on these considerations, the mixture of compounds, obtained by lignin hydrogenolysis (following paragraph) are derivatized by BSTFA before the GC-MS/FID characterization. The procedure consists in the dissolution of the samples in

$CHCl_3$ followed by the addition of BSTFA. The solution is heated at 75 °C for 45 minutes.[152]

3.2 Characterization of products generated by Kraft lignin hydrogenolysis TiN-Ni catalyzed in flow and batch conditions

The work described in this chapter is the result of a collaboration with Valerio Molinari et al. [142] The purpose of the chapter is the analytical characterization of the lignin-hydrogenolysis products. Therefore, more details about the synthesis of the utilized catalysts are reported in the corresponding literature.
Commercial Kraft lignin (KL) purchased by Sigma-Aldrich was chosen as substrate of the HGL process. As mentioned in paragraph 1.5.1.2, Kraft process uses Na_2S therefore, KL-structure contains sulfur (~1.5%) which is a known poison agent towards most of the metal catalysts. Nevertheless, KL is the most abundant lignin on the market since it is the main byproduct of the paper industry.[42]
Kraft lignin was characterized by elemental analysis for its composition and by GPC for the calculation of the mass average molar mass (Mw), number average molar mass (Mn) and dispersity (D). The lignin purity is expressed as acid insoluble lignin (AIL) percentage of lignin (the method is explained in the experimental part, B4). Such obtained analytical data are reported in Table 3.1. FT-IR and solubility test were also performed and the corresponding spectrum and table are reported in Fig. S3.1 and in Table S3.1 (SI), respectively.

Table 3.1 *Characterization of commercial Kraft lignin*

Sample	M_w (g mol^{-1})	M_n (g mol^{-1})	D (Mw/Mn)	AIL (wt %)	Elemental analysis (wt %)			
					N	C	H	S
Kraft lignin	4565	1930	2.4	91.8	0.8	62.3	5.7	1.5

AIL, acid insoluble lignin; Mw, mass average molar mass; Mn number average molar mass; D, dispersity.

Kraft lignin resulted insoluble in most of the common organic solvents, with an exception for methanol (MeOH) and tetrahydrofuran THF. Therefore, MeOH was chosen as solvent for the reaction.
TiN-Ni catalyst was obtained by Molinari by a first synthesis of the TiN support *via* urea route and a second addition of 50 mol % of Ni. For a catalytic comparison TiO_2-Ni (Ni/TiO2 = 50 %) was synthesized in the same fashion but performing the carbothermal reduction of the Ti-urea gel in air atmosphere. The two catalysts

presented similar surface area and particle size. Furthermore the catalytic activity of Ni-based catalyst was compared with the activity of the commercial Pd/C. The hydrogenolysis was performed by the use of a continuous flow reactor equipped with a stainless steel column packed with the catalyst and an internal hydrogen source. KL was dissolved in MeOH with a final concentration of 1.4 mg mL^{-1}, filtered, pumped into the system and mixed with gaseous hydrogen before reaching the catalytic bed. Temperature and flow rate where optimized at 150 °C and 0.3 mL min^{-1} respectively. The reacted solution was collected at the end of the system, dried and fractionated by silica gel chromatography using solvents of increasing polarity. In this way three main fractions with an increasing Mw, were isolated in different yields for each of the tested catalysts (Fig. 3.2 and Table 3.2). Due to its high Mw the third fraction was considered unreacted lignin.

Table 3.2 *Yield of the fraction obtained by Kraft lignin HGL*

Catalyst	Fraction yield (wt %)			Mw (g mol^{-1})	
	1st fraction	2nd fraction	Total fractions	1st fraction	2nd fraction
TiN-Ni (50 %)	21.6	40.0	61.6	682	1745
TiO_2-Ni (50 %)	18.0	25.5	43.5	602	1480
Pd/C (10 %)	12.2	20.3	32.5	630	1224

*Reaction condition: H_2, 25 bar, 150 °C, 1.4 mg mL^{-1} Kraft lignin in MeOH, flow rate 0.3 mL min^{-1}. Yield= mg dried fraction / mg dried reacted lignin *100. Fractions are obtained by chromatographic column separation.*

The results point out the highest deconstruction degree obtained by TiN-Ni catalyzed hydrogenolysis (Table 3.2). In fact, after the chromatographic separation of the reaction mixtures, the amount of molecules with the lowest Mw (1st fraction) is higher when TiN-Ni is used as catalyst, compared to the experiments employing TiO_2-Ni and Pd/C.

The identification of the compounds was performed by GC-MS, which can detect molecules with a maximum Mw of 1000 g mol^{-1}. Therefore, only the 1st fractions, which show average molar masses in the range of 602-682 g mol^{-1}, were considered for the gas chromatographic characterization. As aforementioned, the preparation of the sample for the GC analysis includes a silylation step, during which the BSTFA derivatization agent is added to the chloroform solution of the analyte. For this reason, the three first-fractions obtained by chromatographic separation, were

further fractionated by dissolution of the dried samples in $CHCl_3$ (Fig. 3.2). Only the $CHCl_3$-soluble part was derivatized by BFTFA and fully characterized.

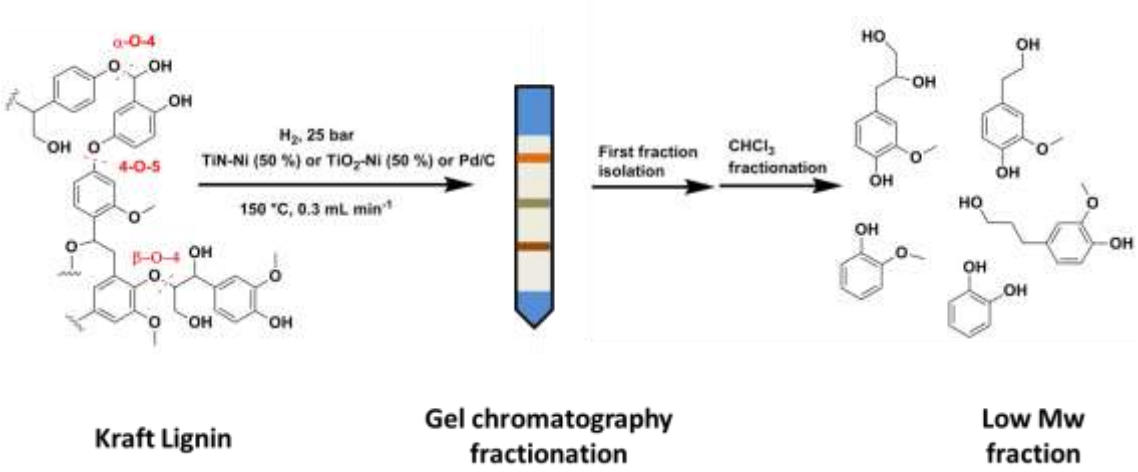

Figure 3.2 *Reaction scheme of Kraft lignin-HGL in a continuous flow reactor followed by chromatographic separation of the products with isolation of the first fraction and a final $CHCl_3$ separation to obtain the lowest Mw molecules.*

A preliminary identification of the main molecules obtained by TiN-NI catalyzed lignin hydrogenolysis was performed by GC-MS on the derivatized chloroform soluble fraction. Six different molecules were first identified by comparison with the NIST.5-MS library (National Institute of Standards and Technology). The identification was then confirmed by a comparison of their retention time with the corresponding commercial standards (Fig. 3.3). Unlike the others (cathecol, guaiacol, vanillin, homovanillyl alcohol and oleic acid), hydrogenated coniferyl alcohol is not commercial. Therefore, it was synthesized by Pd/C catalyzed reduction of the commercial coniferyl alcohol (B13 in the SI).

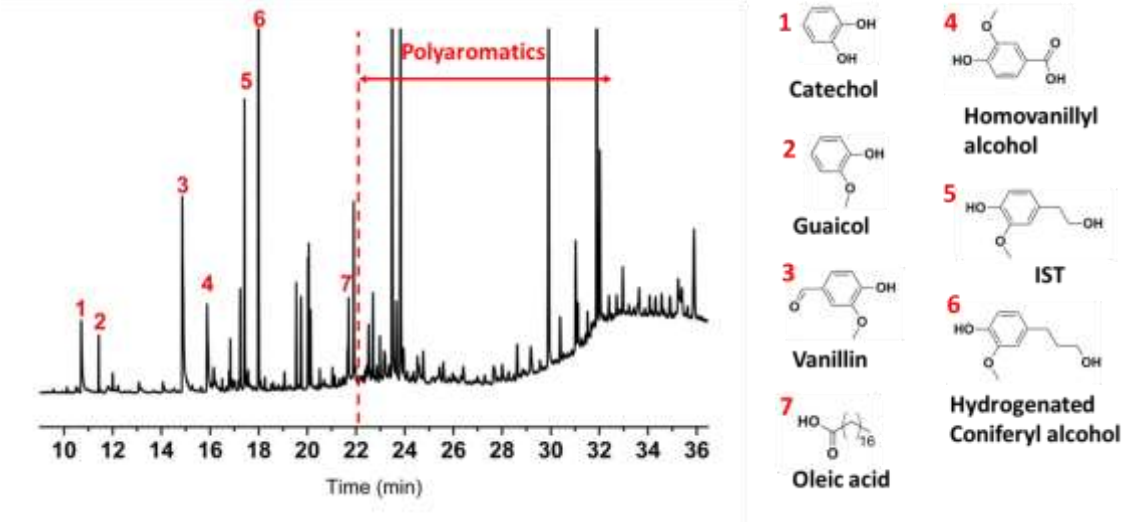

Figure 3.3 *GC-MS chromatogram of the $CHCl_3$ soluble portion of the first fraction obtained by HGL TiN-Ni catalyzed. On the right, the standards used for the identification. IST, internal standard.*

As observed from Fig. 3.3, lignin hydrogenolysis generates a huge number of compounds and most of them cannot be identified with 100 % certainly. A comparison with the NIST.5-MS library confirms the assumption that the molecules with a retention time after 22 minutes contain more than one aromatic ring. The GC-FID quantification of these fractions is described in the next section of this chapter.

In order to study the influence of the reaction system and temperature on the lignin hydrogenolysis, the catalytic activity of TiN-Ni was further explored in batch condition and at two different temperatures. The reactor consisted in a steel autoclave equipped with a mechanical stirrer and a temperature and pressure control. In this situation the critical solubility of Kraft lignin has a lower influence, since there is no risk of a system blockage due to undissolved sample. The hydrogenolysis was performed by heating a mixture of KL in MeOH in the presence of TiN-Ni at 150 and 175 °C, under an initial H_2 pressure of 5 bar for 24 h. After reaction, the mixture was cooled down and filtered to remove the catalyst and the undissolved lignin. The dried mixture of products, called reacted lignin, was subjected to gravimetric fractionation by solvents addition. Firstly the dried mixture was suspended in hexane to eliminate the highest-Mw fraction, which was collected as hexane-precipitate. The hexane-soluble fraction was dried and further suspended in $CHCl_3$ to separate a soluble and insoluble chloroform fraction (Fig. 3.4).

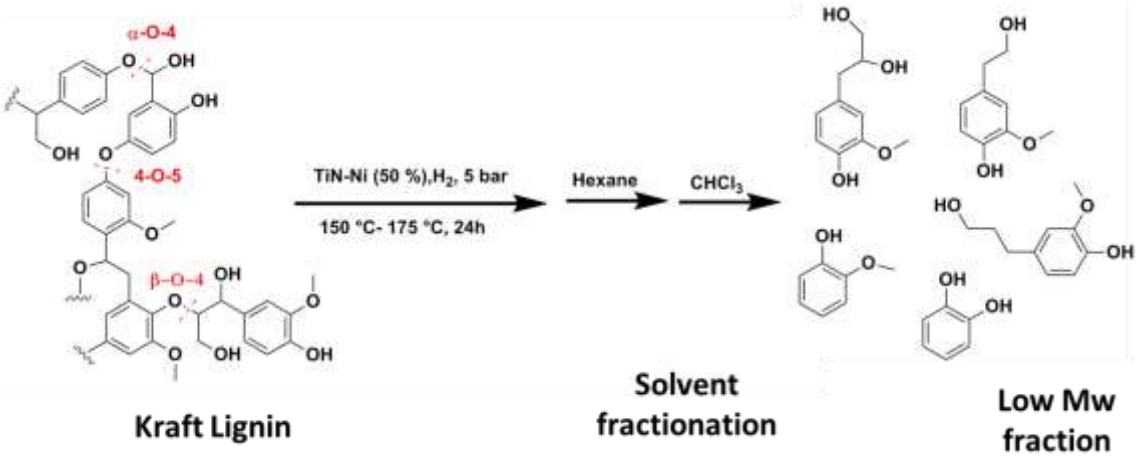

Figure 3.4 *Reaction scheme of Kraft lignin-HGL in batch reactor, followed by gravimetric fractionation of the products to a final isolation of low Mw molecules.*

The amount of the different fractions is expressed as mass percentage of the starting Kraft lignin. The mass average molar mass (Mw) and the dispersity (D) of each isolated fraction were calculated by gel permeation chromatography (GPC) analysis. The collected results (Table 3.3) show that the reaction temperature does not significantly influence the amount of reacted lignin, however it strongly affects the selectivity of the fractionation. In fact, the reaction performed at 175 °C afforded the generation of a higher amount of low Mw molecules, which are soluble in $CHCl_3$ (23 wt % for the reaction conducted at 175 °C and 8.9 wt % for 150 °C) than at 150 °C.

The dried $CHCl_3$ soluble fraction was silylated by BSTFA and subjected to GC-FID quantification, described in the next section.

Table 3.3 *Yield and Mw of the isolated fractions*

Reaction temperature	Fraction yield (wt %)			GPC data (g mol^{-1})					
	Reacted lignin	Hexane insoluble	$CHCl_3$ soluble	Reacted lignin		Hexane insoluble		$CHCl_3$ soluble	
				Mw	D	Mw	D	Mw	D
150 °C	58	16	8.9	1880	1.7	4680	1.5	947	1.5
175 °C	60	10	23	1914	1.7	5920	1.6	1424	1.6

*Reaction condition: 10 g L^{-1} of Kraft lignin in MeOH, H_2 5 bar, 24h. Fraction yield= (g) recovered fraction/ (g) loaded lignin*100. Mw, mass average molar mass; D, dispersity. Reacted lignin: dried mass recovered after filtration of the reaction mixture.*

3.2.1 GC-FID quantification: procedure and calculations

The quantification of the aromatic molecules obtained by lignin hydrogenolysis, both in flow and batch condition, was performed using the GC-FID and by the use of an internal standard and calibration curves. As mentioned, the previous isolated chloroform-soluble fractions were first silylated by BSTFA and then injected in the GC-FID. Fig. 3.5 reports the comparison of the GC-FID chromatograms of the $CHCl_3$ soluble portions obtained by HGL using TiN-Ni, TiO_2-Ni and Pd/C as catalysts.
With the purpose of the quantification, the molecules of the mixture were classified in three categories, based on the retention time (RT) of their corresponding GC-FID peaks (Fig. 3.5). We assumed that the molecules included in each category have structural features similar to the identified compound with a GC-FID peak in the same RT range. Hence, the first group of peaks (region A) with a RT between 12-21 minutes was attributed to monoaromatic compounds because the guaiacol GC-FID peak has a RT of 13.3 min. A second group of peaks (region B, RT 21-24 minutes) was related to monoaromatic molecules with a short aliphatic side chain (C3-C4), since the retention time of hydrogenated coniferyl alcohol peak is 21.4 min. A final group (region C), with a RT in the range of 24-30 minutes was assumed to include molecules with high Mw and more than one aromatic ring.

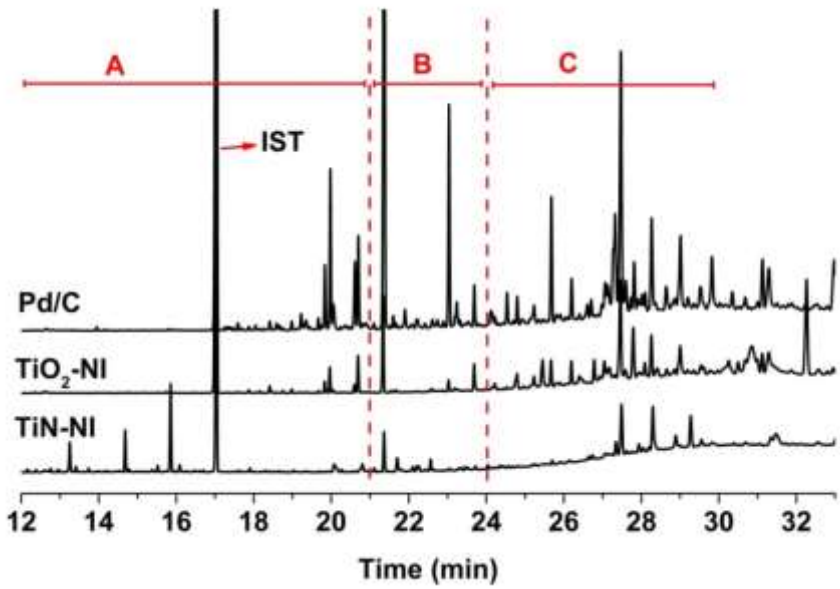

Figure 3.5 *FID-GC chromatograms of $CHCl_3$ soluble fractions obtained from the hydrogenolysis of Kraft lignin by TiN-Ni (50 mol %), TiO_2-Ni (50 mol %) and Pd/C (10 %) in flow reactor.*

With the purpose of quantifying the peaks included in the three regions, three calibration curves were created using different reference standards. The reference

standards for the region A and B calibration curves were chosen on the base of the retention time of their GC-FID peak. Hence, guaiacol and hydrogenated coniferyl alcohol were used as reference standards for the quantification of region A and B peaks, respectively. For the quantification of region C compounds, 3-phenoxyphenol was chosen as calibration curve reference standard because it is a two aromatic rings compound. 2-methoxy-4-propylphenol (compound 5 in Fig. 3.3) was used as internal standard (IST) at a constant concentration of 1 mg mL^{-1}. The area of each GC-FID peak was integrated and quantified in relation to the calibration curve of the corresponding reference standard. The amount of each compound is calculated as mass percentage of $CHCl_3$-soluble fraction (wt %). The total amount of aromatic molecules (called TOT aromatics in Table 3.4) is calculated by the sum of all the chromatogram peaks and it is expressed as the mass rate of aromatics *per* 100 mg of dried $CHCl_3$ fraction. The amount of each group of molecules (region A, B and C) is calculated as percentage sum of the region-peaks of the total amount of aromatics.

As showed from the quantification results (Tab. 3.4), the hydrogenolysis catalyzed by TiN-Ni and Pd/C led to a similar yield of total aromatic molecules (3.2 and 3.9 wt % respectively). Despite of that, the hydrogenolysis catalyzed by TiN-Ni exhibits a remarkable higher selectivity towards the generation of small monoaromatics (region A) than in the case of TiO_2-Ni and Pd/C. In fact, the amount of region A-molecules is 32.4 wt % for TiN-Ni and 5.1 and 10.4 wt % for the reaction catalyzed by TiO_2-Ni and Pd/C respectively.

The $CHCl_3$ soluble fractions obtained by lignin batch HGL at 150 and 175 °C, were also derivatized by BSTFA and quantified by GC-FID. Fig. 3.6 reports the comparison of their chromatograms (B-150 and B-175, respectively).

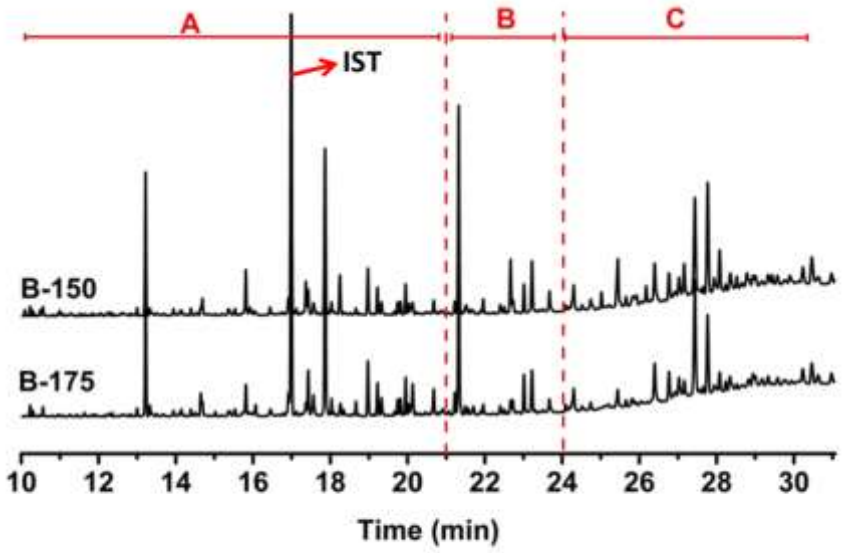

Figure 3.6 *FID-GC chromatograms of $CHCl_3$ soluble fractions obtained from the KL hydrogenolysis catalyzed by TiN-Ni (50 %) in batch at 150 °C (B-150) and 175 °C (B-175).*

The comparison shows that the different reaction temperature does not affect significantly the yield of the obtained molecules. In contrast, increasing the temperature considerably influences the selectivity of the deconstruction reaction towards small monoaromatic molecules. In fact, when the reaction is performed at 175 °C, the amount of region-A compounds increases by *circa* 9 % (Table 3.4)

A significant comparison between the hydrogenolysis performed in batch and flow reactors cannot be realized because of the multiple differences between the systems (e.g. reaction pressure, time and lignin/catalyst ratio). However, we can observe that the reaction performed at the same temperature but in batch condition led to a higher deconstruction degree.

Indeed the total amount of aromatics in the batch case is in the range of 15-17.5 wt % of the starting material, while in the case of a flow condition (F-150) the yield was 3.2 wt %. Therefore, it could be assumed that longer reaction time lead to greater cleavage of lignin linkages.

On the other side, it should be considered that the flow reactor shows several advantages, such as the possibility of using the same catalyst several time without the need of its recover from the reaction solution, the automation of the reaction, etc. However, the focus of this project is the analytical characterization of the lignin HGL products. Therefore, a discussion about catalyst stability and the engineering comparison between the two reaction systems will not be performed here.

Table 3.4 *Total yield and selectivity of the HGL reactions performed by different catalysts and in different reaction conditions.*

Catalyst	TOT aromatics (wt %)	Selectivity		
		Region A (wt %)	Region B (wt %)	Region C (wt %)
[a] FL-TiN-Ni (50 %)	3.2	32.4	23.2	44.5
[a] FL-TiO_2-Ni (50 %)	2.0	5.1	13.9	81.0
[a] FL-Pd/C (10 %)	3.9	10.4	35.5	54.1
[b] B-TiN-Ni (50 %)-150 °C	17.4	30.5	21.7	47.8
[c] B-TiN-Ni (50 %)-175 °C	15.4	39.2	22.3	38.2

a: *H_2, 25 bar, 150 °C, 1.4 mg mL^{-1} Kraft lignin in MeOH, flow 0.3 mL min^{-1}.* ***b:*** *10 g L^{-1} of lignin in MeOH, H_2 5 bar, 150 °C, 24 h.* ***c:*** *10 g L^{-1} of lignin in MeOH, H_2 5 bar, 175 °C, 24 h. FL: flow reactor. B: batch reactor (autoclave).*

3.2.2 Final considerations

In this project an accurate GC-MS/ FID method was developed with the purpose to quantify mixture of aromatic molecules obtained by lignin deconstruction. The analytical procedure consists of the identification of three main groups of aromatic molecules on the basis of their volatility and therefore of their GC-FID retention time (RT). Each group of molecules was quantified by the use of different calibration curves, which were prepared using a reference standard. Guaiacol, hydrogenated coniferyl alcohol and 3-phenoxyphenol were used as reference standards for the quantification of monoaromatics, monoaromatics with a side chain (C3-C4) and polyaromatics, respectively. The protocol requires the preliminary silylation of the samples, for the purpose of the analysis.

The analytical method was applied to the lowest Mw-fraction generated by Kraft lignin hydrogenolysis. The quantification of the molecules was used to describe the influence of the catalyst, the reaction system (batch and flow) and the temperature on the distribution of the aromatic molecules of the mixture. The performed experiments showed the better performance of TiN-Ni both for yield and selectivity in comparison with TiO_2-Ni. TiN-Ni showed a higher selectivity towards the generation of small aromatics when compared to Pd/C. The lignin HGL TiN-Ni catalyzed was performed even in batch condition at two different temperatures,

150 and 175 °C. The reaction temperature affected mainly the HGL selectivity towards the generation of smaller molecules.

In future studies will be interesting to test the catalytic efficiency of TiN-Ni in a flow reactor with the possibility of longer reaction time and of working at temperatures higher than 150 °C.

As will be confirmed in the following paragraph, the analytical method used for the quantification of lignin HGL products has the advantage that it can be applied for the general quantification of aromatic molecules in complex mixtures.

3.3 Extraction and characterization of lignans like molecules from olive leaves

As mentioned, lignin is the most abundant natural source of aromatic molecules but not the unique. Aromatic compounds, with structural features similar to the molecules obtained by lignin hydrogenolysis, can be extracted from several natural sources. In this regard, this paragraph will focus on the extraction of α-hydroxytyrosol and other polyphenolic compounds from olive plant leaves and on their characterization by application of the above described analytical method.
The well-known antioxidant activity of polyphenols is due to the high reactivity of phenolic groups towards radicals.[153] Among the polyphenols-rich species of plant, such as *Vitis Vinifera, Camellin Sinensis* and hundreds of others,[154] there is *Olea Europea*, a widely diffused tree in Mediterranean countries like Spain, Greece and Italy. Olive oil is the main product obtained by squeezing the fruits of this plant, while the leaves are often burned, composted or used as animal feed. Interestingly, it has been estimated that every 100 kg of olives about 3-5 Kg of leaves are discarded. For this reason, olive leaves represent a very attractive waste biomass from the agricultural sector in Spain.[155, 156] As well as olive fruits, the leaves are rich in polyphenols that showed activity against cancer, hypertensions, diabetes and arteriosclerosis.[157,158] Among others, hydroxytyrosol is a hydroxyaromatic compound with antimicrobial and antioxidant activity presents in low percentage in olive leaves.[159-162] This interesting compound has high value for phytotherapic, cosmetic and healthy food industry. Generally, hydroxytyrosol is not isolated in a free form but mostly as a component of Oleuropein, a secoiridoid compound abundant in several plants.[163] Hydroxytyrosol can be generated by enzymatic hydrolysis or alternatively via acid hydrolysis of Oleuropein (Fig. 3.7).

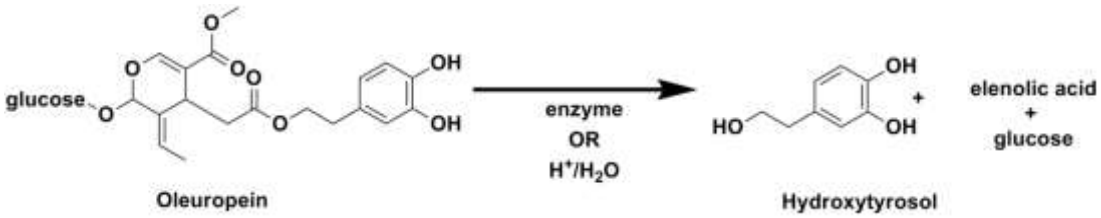

Figure 3.7 *Hydroxytyrosol release via enzymatic or acid hydrolysis of Oleuropein*

Currently several groups work on the extraction of phenols from olive leaves. Among them, Sajady et al.[158] extracted hydroxytyrosol from the leaves by an acid catalyzed hydrolysis (HCl 2M) followed by a solvent extraction with ethyl acetate. The analytic was performed by the use of high performance liquid chromatography (HPLC) and the isolated hydroxytyrosol was studied for its activity against breast

cancer. In 2012 Rigane et al.[164] performed a detailed study on the effect of pH, temperature and time on hydroxytyrosol yield from olive pomace in batch condition. They concluded that the optimal reaction conditions for the extraction of the highest hydroxytyrosol amount were the use of H_2SO_4 as catalyst at 120 °C in water and for 20 min. Of interest is also the extraction of polyphenolic compounds and hydroxytyrosol from olive leaves by acid steam with a further isolation by ethyl acetate.[155] Considering the similarity between hydroxyrosol and depolymerized lignin-molecules, we suggest the extraction of polyphenols and hydroxyrosol from olive leaves by a process originally developed for lignin isolation. The quantification of the generated molecules was performed by application of the above mentioned analytical method, showing the versatility of the analytical protocol.

3.3.1 Phenol extraction from olive leaves: procedure and discussion

We took in consideration the interesting lignocellulose fractionation method developed by Grande et al.[54] The process applied to beech wood consists in the recovery of the three lignocellulosic components, cellulose, hemicellulose and lignin, in one step. In detail, the biomass is treated by a biphasic mixture of solvents made of an aqueous solution of oxalic acid and methyltetrahydrofuran (2-MeTHF) in acidic condition. Lignin is recovered directly from the organic phase by 2-MeTHF distillation. The advantage of a fast process, of the easy recovery of the aromatic polymer and of the use of reagents such as oxalic acid and 2-MeTHF, which can be derived from biomass,[165, 166] attracted our attention. Therefore, we adjusted the method with the purpose to extract the polyphenolic components from olive leaves. The extraction was performed by suspension of the olive leaves in a 1:1 (V/V) mixture of 2-MeTHF and an aqueous oxalic acid solution. The reaction was carried out in autoclave, for 1 h at two different temperatures, 100 °C and 140 °C. After filtration, the phenolic compounds are directly recovered by concentration of the organic phase. The amount of the dried 2-MeTHF residues, obtained from the reaction at the two different temperatures, were calculated respect to the starting amount of leaves (Table 3.6). With the increasing of the temperature, the amount of the extract raised from 14.4 to 17.1 wt % of the olive leaves. The 2-MeTHF extract obtained at 100 °C was silylated by BSTFA and analyzed by GC-MS (Fig 3.8).

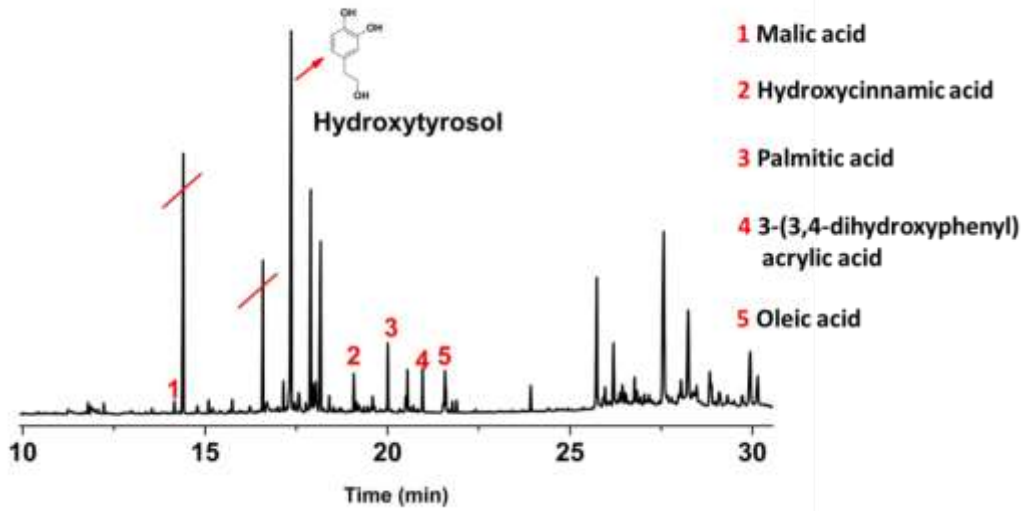

Figure 3.8 *GC-MS chromatogram of phenols extracted from olive leaves by treatment at 100 °C, 1 h, in a mixture 1:1 V/V of 0.1 M oxalic in water and MeTHF. The two barred peaks are related to the 2-MeTHF solvent stabilizer.*

The GC-MS chromatogram highlights the high amount of molecules present in the extracted mixture. The peaks identification was performed by a comparison with the NIST.5-MS library. As can be observed hydroxytyrosol is the main peak. Quantification was performed by GC-FID using 2-methoxy-4-propylphenol as IST for both the mixtures extracted at 100 and 140 °C, in order to compare the effect of the extraction temperature on the distribution of the obtained molecules. Applying the analytical method developed for the quantification of lignin hydrogenolysis products (paragraph 3.2.1), the GC-FID chromatogram was divided in three main regions, A, B and C, based on the different retention time of the compounds (Fig. 3.9). The Mw of the molecules included in each region is assumed to increase in the order C >B > A.

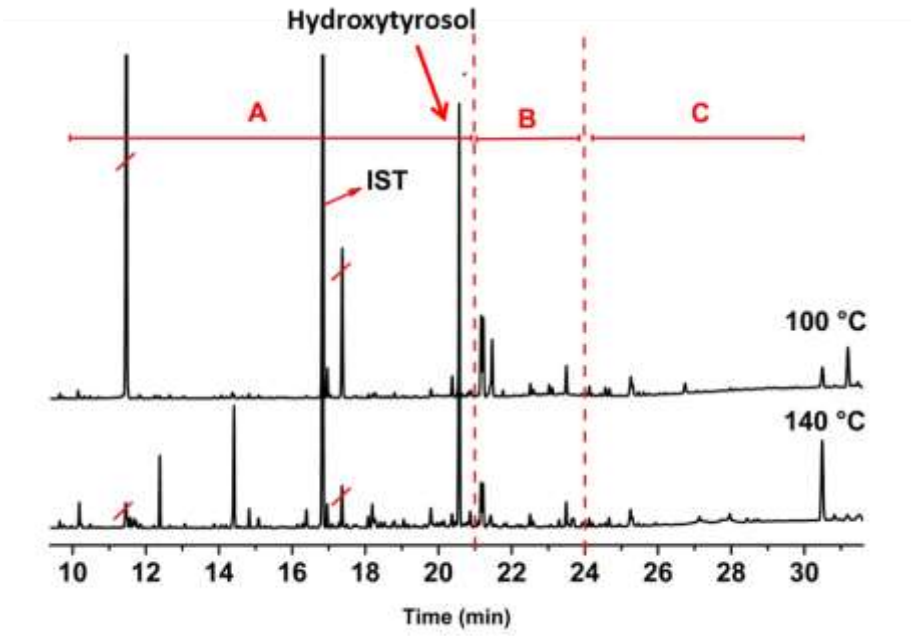

Figure 3.9 *GC-FID quantitative chromatograms of the mixture of product extracted after treating olive leaves at 100 and 140°C in autoclave with a mixture 1:1 V/V of 0.1 M oxalic acid in water and MeTHF for 1 h. The bared peaks are relative to the solvent.*

The amount of hydroxytyrosol is expressed as mass percentage of olive leaves, while the selectivity consists in the ratio between the sum of peaks included in the considered region and the total amount of peaks in the chromatogram (Table 3.5)
The visual comparison of the two GC-FID chromatograms (Fig. 3.9) shows the increase fragmentation when the extraction is conducted at 140 °C. Nevertheless, the quantification data show that a higher extraction temperature leads to the generation of high Mw molecules (region C). In contrast, the amount of extracted hydroxytyrosol at both the temperatures has a constant value of 0.1 wt % of the olive leaves, lower value than the content of hydroxytyrosol generally extracted by other methods reported in literature.[134, 155, 167]

Table 3.5 *Extraction yields and distribution of the molecules extracted*

Extraction temperature	Yield (wt %)			Selectivity		
	MeTHF extract	Total aromatics	hydroxytyrosol	% Region A	% Region B	% Region C
100 °C	14.4	1.0	0.1	76.4	15.7	7.9
140 °C	17.1	3.2	0.1	71.6	10.6	17.8

*Reaction conditions: solid/ liquid 50 g L^{-1}, 1:1 V/V 0.1 M oxalic acid in water and MeTHF, 1 h. The yields are calculated as dried mass over the starting material mass. Selectivity: ∑ peaks of the region / ∑ GC-FID chromatogram peaks*100.*

3.3.1 Phenol extraction from olive leaves: conclusion

We adjusted a heterogeneous extraction method, which was originally developed to fractionate in one step the lignocellulosic components, on olive leaves. The advantages showed by the applied process are the sustainability of the employed reagents and the fast recovery of the aromatic molecules. In fact, both the employed 2-MeTHF and oxalic acid can be derived from biomass and the isolation of the aromatics is achieved by a simple concentration of the organic phase after reaction. The quantification of polyphenols was performed by application of the analytical method developed for the quantitative characterization of lignin deconstruction products (previous paragraph). In this way, we showed the versatility of the analytical protocol towards the general category of small aromatic molecules. The extraction was performed at two different temperatures, 100 and 140 °C. The increasing of the reaction temperature led to a higher yield of aromatic molecules among which hydroxytyrosol is the most intense of many compounds. A future optimization of the reaction conditions and a further purification step could lead to a more selective polyphenolic fractionation.

4. NITRATED LIGNIN AS NITROGEN-DOPED CARBON PRECURSOR FOR OXYGEN REDUCTION REACTION CATALYSTS

Another purpose of this project was the use of lignin as a carbon precursor for a nitrogen-doped carbon (NDC). In this work lignin was extracted from beech wood chips by hydrothermal-alkaline treatment of the biomass using $Ba(OH)_2$ as base.[45] The isolation process was chosen because it allows the simultaneous generation of the bioplastic-precursor lactic acid and of lignin, thus representing a biorefinery scheme. Therefore, isolated lignin was characterized and successively functionalized with nitro-groups *via* straightforward aromatic nitration to overcome the lack of nitrogen. In collaboration with J. Pampel and T.P. Fellinger of the "carbon and energy" group, the samples were carbonized by ionothermal approach with a eutectic $KCl/ZnCl_2$ mixture, resulting in mesoporous nitrogen-doped carbons (NDCs). The influence of the precursor-nitrogen functionality on the morphology of the so obtained carbonaceous materials was investigated. Moreover, the NDCs were tested in alkaline media for their electrocatalytic activity towards the oxygen reduction reaction (ORR). The latter takes place at the cathodic site of a fuel cell, and the lignin-derived NDCs showed efficiency comparable to the more recent non-noble metal based catalysts.[46] Fig. 4.1 is a schematic representation of the synthesis of lignin derived NDCs.

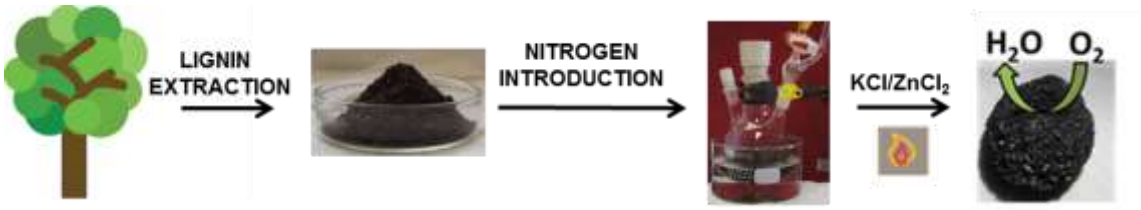

Figure 4.1 *Schematic process for the synthesis of mesoporous nitrogen-doped carbon from beech wood lignin.**

4.1 Mesoporous carbon (MC)

Porous carbons are described as light materials with high surface area and porosity. They show unique properties such as chemical, physical and thermal stability and electric conductivity.[168] The various application fields of these materials include adsorbents for water and air purification, hydrogen storage, catalyst supports (fuel cells) and supercapacitor electrodes.[169-173] MC properties and consequent

*Reprinted with the permission from Graglia, M., Pampel, J., Hantke, T., Fellinger, T.-P., Esposito, D., Nitro Lignin-Derived Nitrogen-Doped Carbon as an Efficient and Sustainable Electrocatalyst for Oxygen Reduction. ACS Nano **2016,** 10, 4364-4371. Copyright (2016) American Chemical Society.

applications depend on the size and shape of the pores as well as on the connections between them.[174] Regarding the pore-size, the IUPAC defines as "micropores" pores with diameter (d) smaller than 2 nm, "mesopores" if 2< d< 50 nm and "macropores" if d > 50 nm.[175] At the state of the art, materials utilized as carbon sources are mainly fossil-based hydrocarbons, biomass or polymers. In order to introduce porosity in these raw materials "activation" steps are generally employed. Among the possible processes utilized to generate porosity, the most used are physical and chemical activation and hard and soft templating. Although physical and chemical activation result in high surface area carbons, both methods are time and energy consuming. They are characterized by low yields and afford the formation of mainly microporous structures with relatively low total pore-volume. For these reasons, activated carbons are limited in their application, especially when the mass transport through the carbonaceous structure plays a key-role, such as for supercapacitors electrodes and catalyst supports.[176, 177] Templating methods generally employ a porogen agent that directs the structure formation and is removed at the end of the process. Both techniques, hard and soft templating, afford the introduction of pores with different size and shape and the achievement of a final material with various possible morphologies. Nevertheless, the utilization of hazardous chemicals to remove the templates reduces the possibility of an industrial scale-up and increases the need for more environmentally friendly processes.[178] Fechler et al.[179] introduced the "salt templating" approach, in which the carbon precursor is pyrolized in presence of an inorganic and non-carbonizable eutectic salt mixture. The porogen and solvent acting salt can be easily removed at the end of the process by washing the MC with water. The final material exhibits high surface area, while the pore size distribution depends on the secondary salt combined with $ZnCl_2$ in the eutectic mixture. In this single-step process, ionic liquids as carbon source were carbonized using a mixture of salts as porogen-solvent agent. The possibility of tuning the morphology of the final material by varying the composition of the porogen agent was showed. Ma et al.[171] utilized the same approach carbonizing several biomasses in the presence of the eutectic salt melt $KCl/ZnCl_2$. They investigated the influence of the weight ratio of carbon-precursor/porogen and of the pyrolysis temperature on the pore-size of the final material. Later, Pampel et al.[180] studied the impact of the molar composition of the employed $KCl/ZnCl_2$ mixture during the synthesis of glucose derived carbons. The authors concluded that a higher amount of KCl in the eutectic mixture promotes the formation of mesopores on costs of micropores.

4.1.1 Nitrogen-doped mesoporous carbon biomass-derived

The introduction of heteroatoms such as nitrogen and boron (N and B, respectively) is known to increase the electrical conductivity of the carbon material.[174] Above all, the insertion of electron-rich N-functionalities was reported to increase the catalytic activity of MC towards the oxygen reduction reaction (ORR).[181] When the employed carbon precursor is originally nitrogen-free, the carbon obtained by a first precursor carbonization has to be modified. Such additional modification step consists for instance, in the treatment of the carbonized material with urea or ammonia in order to add nitrogen-functionalities.[182, 183] The overall process is therefore characterized by several steps, which lead to low yield of the final material and to an inhomogeneous N-distribution. Therefore, increasing attention was paid to the production of NDCs using cheaper and more sustainable biomass based N-containing precursors. As an example, NDCs were obtained by hydrothermal treatment of carbohydrate-derived chitosan and glucosamine[184] and from chitin.[185] The latter was first pyrolyzed, then mixed with $ZnCl_2$ and subjected to a second carbonization, finally leading to an active ORR-catalyst. Moreover, the work of Gao et al. should be mentioned.[186] They synthesized a NDC by hydrothermal treatment of the fermented natural-nitrogen rich rice. Such obtained NDC was applied at the working electrode for the catalysis of ORR. The utilization of lignin as raw material for the production of carbon materials has also been reported and in comparison with cellulose lignin resulted a better carbon precursor.[187-190] For its high content of carbon lignin is considered a good candidate as carbon material precursor. Furthermore, lignin displays high redox activity due to the presence of aromatic and phenolic functionalities. Although these advantageous structural features, the generation of lignin-derived carbon materials with a potential electrochemical application, requires an additional nitrogen functionalization of lignin.[176, 191] At the state of the art, only few attempts to introduce nitrogen in lignin structure have been reported in literature generally, resulting in a low amount of incorporated nitrogen, such as the lignin pretreatment by ammonia percolation.[192]

4.2 Lignin extraction and functionalization

4.2.1 Extraction and characterization of alkali lignin

Lignin was extracted from beech wood chips using the aforementioned hydrothermal alkaline treatment. The absolute amount of lignin in beech wood is 21.6 wt % and was calculated in chapter 2 by the determination of the acid soluble and insoluble lignin (ASL and AIL, respectively). Such characterized biomass was heated at 220 °C for 15 h in the presence of $Ba(OH)_2$ in water. Unlike the procedure

*Reprinted with the permission from Graglia, M., Pampel, J., Hantke, T., Fellinger, T.-P., Esposito, D., Nitro Lignin-Derived Nitrogen-Doped Carbon as an Efficient and Sustainable Electrocatalyst for Oxygen Reduction. ACS Nano **2016,** 10, 4364-4371. Copyright (2016) American Chemical Society.

described in paragraph 2.2.1.2, lignin isolation was performed here in small autoclaves without the possibility of a continuous stirring of the mixture and using a normal oven as heating system. After the process the solid pulp was isolated from a dark liquid rich in barium lactate. The pulp was subjected to acidic washing and a THF-lignin fraction was recovered by the suspension of the pulp in THF. Lignin was obtained in a 10 wt % of the starting biomass. Extracted lignin (L) was characterized by GPC, elemental analysis, FT-IR, ^{1}H-NMR and 2D HSQC-NMR. Lignin exhibited elemental composition and Mw in agreement with other alkaline-lignins, as already mentioned in the previous sections (Table 4.1). Respect to the methods used for the preparation of alkali lignin (AL), which is discussed in chapter 2, in this case the lignin isolation process occurs with the absence of stirring and in a broader temperature gradient. This slightly modified procedure resulted in a higher value of Mw and dispersity index (D).

FT-IR spectrum of isolated lignin (Fig. 4.2A) shows the presence of hydroxyl and phenolic groups (3660-3020 cm^{-1}) linked to aromatics (1605-1270 cm^{-1}) and aliphatic units (1085-1030 cm^{-1}). 2D HSQC-NMR spectrum of lignin acetylated for the analytic purpose (Fig. 4.2B), displayed the signals of characteristic methoxyl groups of syringyl and guaicyl units and confirmed the presence of β-O-4 linkages, which are the most abundant linkages in lignin structure.

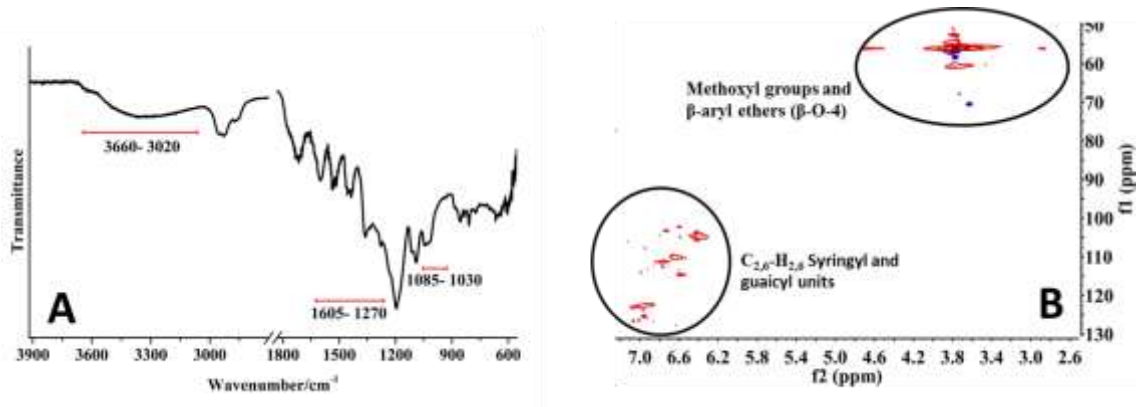

Figure 4.2 A- *FT-IR spectra of isolated lignin.* **B-** *2D HSQC-NMR of acetylated-lignin.**

A further characterization of lignin main functionalities was obtained by ^{1}H-NMR (Fig. S4.1 in the SI). The spectrum highlights the presence of aromatic, aliphatic and methoxy protons. Moreover, it shows the signal with characteristic chemical shift of phenol protons.

4.2.2 Lignin nitrogen-functionalization

Aromatic nitration of lignin was performed using nitric acid and acetic anhydride in presence of a catalytic amount of sulfuric acid (Fig. 4.3). Compared to different approaches for the aromatic nitration reported in literature, such as the use of

*Reprinted with the permission from Graglia, M., Pampel, J., Hantke, T., Fellinger, T.-P., Esposito, D., Nitro Lignin-Derived Nitrogen-Doped Carbon as an Efficient and Sustainable Electrocatalyst for Oxygen Reduction. ACS Nano **2016,** 10, 4364-4371. Copyright (2016) American Chemical Society.

$AgNO_2$ catalyzed by $Pd(OAc)_2$[193] or $Cu(NO_3)_2$ supported on zeolite,[194] we considered the present method the simplest process in order to covalently link nitrogen containing-functionalities to lignin-structure.

Figure 4.3 *Schematic pathway of lignin conversion. From alkali lignin (L) to nitro lignin (NL) via aromatic nitration, followed by reduction of NL to aminated lignin (AmL).**

The reaction conditions were first optimized by nitration of 2-methoxy-4-propylphenol, which is considered a good model of the complex structure of lignin. Indeed, its backbone includes phenylpropanoic, methoxy and phenolic functionalities. The electrophilic addition of the nitro-groups on the model was monitored by ^{1}H-NMR and showed the preferential substitution of the protons in ortho-position to the propylphenolic chain (Fig. S4.2 in the SI). The reaction afforded the desired compound in 55 mol % yield and as expected, it led to the simultaneous acetylation of hydroxyl functionalities. Thus, the nitration was optimized for lignin in order to introduce the maximum amount of nitrogen. In detail, the reaction time was extended from 1 to 3 hours, leading to a lignin conversion of 75 wt % and to the introduction of 6.5 wt % of nitrogen, according to the elemental analysis (Table 4.1). The covalent introduction of nitro and acetyl groups in lignin-structure was accompanied by the hydrolysis of more labile ether-bonds, thus justifying the decrease of the average molecular weight in nitrolignin (NL, Table 4.1). In the FT-IR spectrum of NL (Fig. 4.4) the presence of characteristic N-O (1365 and 1537 cm^{-1}) and C-N (1643-1632 cm^{-1}, 1273-1196 cm^{-1} and 1045 cm^{-1}) stretching bands, confirmed the occurrence of the nitration.[40]

*Reprinted with the permission from Graglia, M., Pampel, J., Hantke, T., Fellinger, T.-P., Esposito, D., Nitro Lignin-Derived Nitrogen-Doped Carbon as an Efficient and Sustainable Electrocatalyst for Oxygen Reduction. ACS Nano **2016,** 10, 4364-4371. Copyright (2016) American Chemical Society.

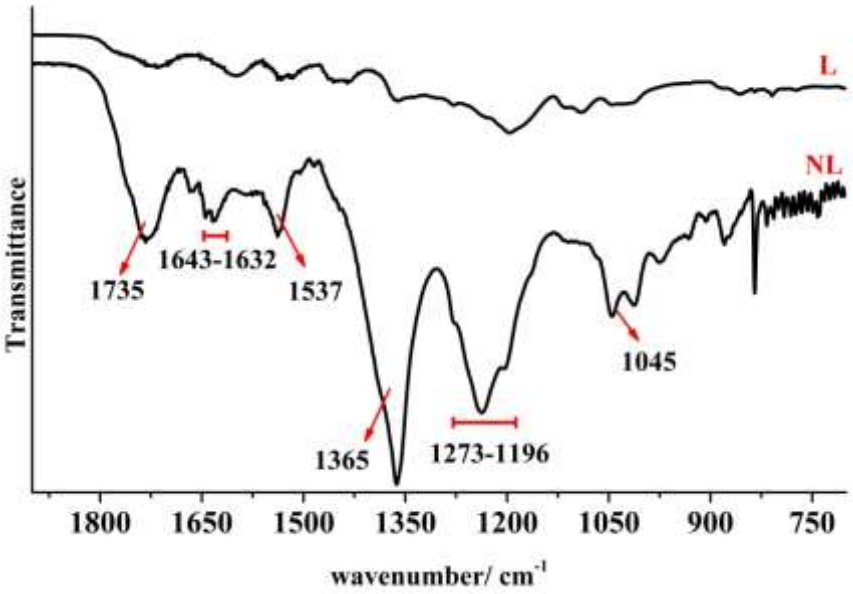

Figure 4.4 *FT-IR spectra of nitro lignin (NL) versus the starting isolated lignin (L)*

Moreover, the lower amount of aromatic C-H exhibited from NL in the qualitative 2D HSQC-NMR spectrum (Fig.4.5 A) in comparison with isolated lignin (Fig.4.5 B), represents a further confirmation of the occurred nitration.

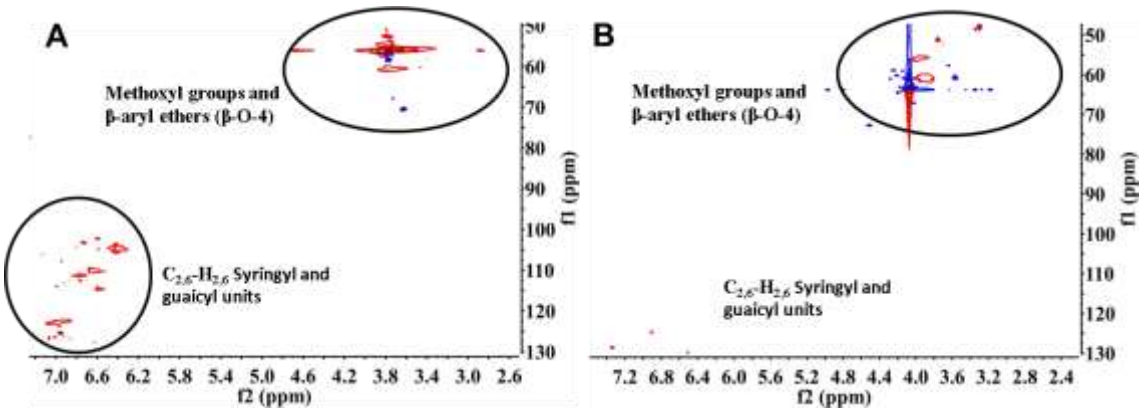

Figure 4.5 A- *2D HSQC-NMR of isolated acetylated lignin.* ***B-*** *2D HSQC-NMR of acetylated nitrolignin (NL). The chromatograms are obtained by dissolution of 100-110 mg of acetylated lignin in* $CDCl_3$.

As detailed below, lignin nitration is followed by a deacetylation step, which leads to the formation of a nitro-deacetylated lignin (NDL). The comparison of the ^{1}H-NMR spectra of L, NL and NDL reported in Fig. 4.6, can be used to visualize the simultaneous acetylation of phenolic and aliphatic hydroxyl functions during lignin-nitration. Indeed, the peak 2.0 ppm , which is related to the methyl ester protons, appears after the nitration step and disappears after the successive deacetylation reaction.

*Reprinted with the permission from Graglia, M., Pampel, J., Hantke, T., Fellinger, T.-P., Esposito, D., Nitro Lignin-Derived Nitrogen-Doped Carbon as an Efficient and Sustainable Electrocatalyst for Oxygen Reduction. ACS Nano **2016,** 10, 4364-4371. Copyright (2016) American Chemical Society.

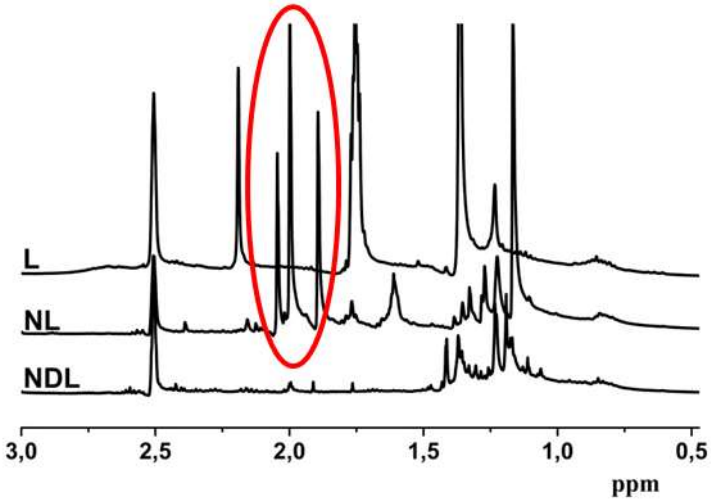

Figure 4.6 *^{1}H-NMR of L,lignin; NL, nitrolignin and nitro-deacetylated lignin (NDL).**

Although nitro-lignin already fulfills the requirements for a promising nitrogen-doped carbon (NDC) precursor, it was reduced to the corresponding amino-form (AmL). In this way, we prepared the reference material to investigate the influence of different nitrogen containing functional groups on the properties of the final NDC. The reduction step was preceded by the deacetylation of NL in order to avoid the formation of acetamide functionalities. Otherwise, the transfer of acyl functions could minimize the amount of free amino groups. Deacetylation of NL was performed in a methanolic KOH solution yielding nitro-deacetylated lignin (NDL) in 60 wt %. As for the other synthetic steps, the reaction parameters for the reduction were first optimized for the lignin-model. For this purpose, a solution of nitro-2-methoxy-4-propylphenol in methanol was flowed over Pd/C (10 wt %) at 130 °C in the presence of hydrogen, employing the continuous flow reactor H-Cube Pro™. The reaction led to a quantitative conversion of the starting molecule to the corresponding aniline. Hence, the reduction was applied to the methanolic solution of NDL resulting in the formation of AmL in a yield of 72 wt %. The reduction of NDL was monitored *via* colorimetric ninhydrin test (Fig. 4.7).

Figure 4.7 *Colorimetric ninhydrin test performed on L, NL, NDL and AmL. The latter (first vial at the right) shows a dark blue coloration due to the formation of Ruhemann´s purple-like compounds.*

During the test the samples are treated with ninhydrin, which leads to the formation of a blue coloration only after reaction with free amino groups, due to the generation of Ruhemann´s purple-like compounds. As shown from Fig 4.7, after ninhydrin reaction all the lignins display the classical brown color of lignin solution, whereas AmL solution is dark-blue.
Moreover, it is worth to mention that the amount of nitrogen introduced with the nitration step exhibited just a slightly decrease after deacetylation and remained constant after reduction of NDL to AmL. The drop of the polymer average molar mass from NL to AmL is consistent with the variation of structural functions during the reaction (Table 4.1).

Table 4.1 *Mw, dispersity (D) and elemental composition of lignin and its nitrogen derivatives.*

sample	GPC analysis		Elemental analysis			
	M_w (g mol^{-1})	D (Mw/Mn)	N wt %	C wt %	H wt %	C/N
L	3416	3.1	0.2	64.5	6.2	318
NL	1275	1.5	6.7	52.5	5.6	7.7
NDL	1082	1.4	6.2	53.5	5.6	8.9
AmL	786	1.5	6.2	54.4	6.4	9.1

L, alkaline lignin; NL, nitro lignin; NDL, nitro-deacetylated lignin; AmL, amino lignin.

4.3 Ionothermal carbonization of lignin-derivatives

4.3.1 Procedure for the synthesis of mesoporous carbons.

The thermal behavior of NL, NDL, AmL and L was investigated by thermogravimetric analysis (TGA) in nitrogen atmosphere up to a final temperature of 1000 °C. NL and

*Reprinted with the permission from Graglia, M., Pampel, J., Hantke, T., Fellinger, T.-P., Esposito, D., Nitro Lignin-Derived Nitrogen-Doped Carbon as an Efficient and Sustainable Electrocatalyst for Oxygen Reduction. ACS Nano **2016,** 10, 4364-4371. Copyright (2016) American Chemical Society.

AmL showed residual masses of 20 and 30 wt %, respectively (S4.2 in the SI). Thus, the nitrogen-containing samples and the starting lignin as reference were carbonized in the eutectic $KCl/ZnCl_2$ salt melt. The lignin derivatives were grinded under argon atmosphere with a mixture of $KCl/ZnCl_2$ (molar ratio 51:49) in a sample/salt weight ratio of 1:5, thus pyrolized to a final temperature of 850 °C. The residual salt was removed after the process by twice washing the carbonized samples with deionized water.

4.3.2 Characterization of mesoporous carbons

The ionothermal carbonization yielded 21.1, 18.7 and 27.9 wt % for NL, NDL and AmL respectively, calculated on the dry weight of the precursor (Table 4.2). The eutectic $KCl/ZnCl_2$ mixture was chosen after a comparison of the yields obtained by the ionothermal carbonization of lignin-derivatives performed in the same fashion but using $NaCl/ZnCl_2$ as alternative porogen-solvent agent. Table S4.1 in the SI shows the lower total yields achieved by carbonization of the samples with the latter salt melt, probably due to the low miscibility degree of $NaCl/ZnCl_2$ with lignin derivatives. Carbonized samples are indicated by the addition of C following their corresponding name (indicating the carbonization).

Table 4.2 *Total yield and elemental composition of the carbonized derivatives.*

		Elemental composition					
		N (wt %)		C (wt %)		H (wt %)	C/N
sample	Total Yield (wt %)	Elemental analysis	XPS	Elemental analysis	XPS	Elemental analysis	
L-C	-	0.4	-	79.1	-	1.7	204.2
NL-C	21.1	6.1	6.7	78.5	81.8	1.7	13.2
NDL-C	18.7	5.3	4.8	80.2	83.1	1.7	15.3
AmL-C	27.9	5.6	3.5	80.7	82.5	1.7	14.2

Carbonization was performed in the presence of $KCl/ZnCl_2$ at 850 °C. L-C, carbonized lignin; NL-C, carbonized nitro-lignin; NDL-C, carbonized nitro-deacetylated lignin; AmL-C, carbonized amino-lignin. The yield is calculated on the dry starting lignin derivative

As showed in Table 4.2, the amount of incorporated heteroatom calculated by elemental analysis just slightly decreased after carbonization, confirming the strong incorporation of nitrogen upon the lignin backbone in the precursor. X-ray photoelectron spectroscopy (XPS) was performed in order to understand the nature of the nitrogen-sites in the carbonized specimens. The content of nitrogen

calculated by XPS was generally lower of the one obtained by elemental analysis. Nevertheless, the nitrogen amount calculated by both the analytical techniques confirms the highest N-content in nitrolignin and the lowest content in aminolignin. The abundance of different nitrogen sites is represented in Fig. 4.8 and reported in Table 4.3. XPS data revealed the highest amount of pyridinic and graphitic nitrogen in the case of the nitrogen-derivatives, with a maximum for NL, which could suggest its higher electrocatalytic activity towards ORR.

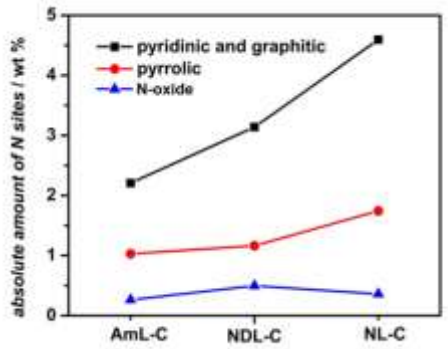

sample	pyridinic –N (wt %)	pyrrolic-N (wt %)	graphitic-N (wt %)	N-oxide (wt %)
AmL-C	1.1	1.0	1.1	0.3
NDL-C	1.1	1.2	2.0	0.5
NL-C	2.2	1.7	2.4	0.4

Figure 4.8 (Left) *Absolute abundance of nitrogen sites calculated by XPS for carbonized aminolignin (AmL-C), carbonized nitro-deacetylated lignin (NDL-C) and carbonized nitrolignin (NL-C).* **Table 4.3 (Right)** *Absolute amount of N sites present in the carbonized samples according to XPS analysis.**

The material porosity was analyzed by nitrogen physisorption. Brunauer-Emmett-Teller (BET) method was used for the calculation of the specific surface areas (Table 4.4).The latters showed values typical for carbons activated by $ZnCl_2$, such as 258 m^2 g^{-1} for L-C increasing to 1589, 1381 and 1564 m^2 g^{-1} for NL-C, NDL-C and AmL-C, respectively.

*Reprinted with the permission from Graglia, M., Pampel, J., Hantke, T., Fellinger, T.-P., Esposito, D., Nitro Lignin-Derived Nitrogen-Doped Carbon as an Efficient and Sustainable Electrocatalyst for Oxygen Reduction. ACS Nano **2016,** 10, 4364-4371. Copyright (2016) American Chemical Society.

Table 4.4 *Pores properties in L-C, NL-C, NDL-C and AmL-C*

Sample	S_{bet} (m^2 g^{-1})	Pore volume (cm^3 g_{-1})				C yield (wt %)
		V_{tot}	S_{ext}	V_{micro}	V_{meso}	
L-C	258	0.152	64	0.084	0.068	61.1
NL-C	1589	0.826	122	0.643	0.183	38.3
NDL-C	1381	0.704	135	0.524	0.180	28.2
AmL-C	1564	0.744	102	0.595	0.149	41.8

Conditions: the samples mixed with KCl/ $ZnCl_2$ were carbonized in nitrogen atmosphere at 850 °C. S_{bet}, specific surface area; V_{tot}, total pore volume; S_{ext}, external pore volume; V_{micro}, micropores volume; V_{meso}, mesopores volume.

The isotherms of the four samples show a general type IV behavior ascribed to the presence of mesopores (Fig.4.9A) The high uptake of the gas at low relative pressure indicates the existence of micropores, while the high nitrogen uptake at high relative pressure is due to macropores. Fig. 4.9A shows the lower gas uptake of L-C compared to the nitrogen-containing samples, which is due to the low total pore-volume and surface area of L-C. This phenomenon could be ascribed to the lower ability of non-functionalized lignin to undergo dissolution in the salt melt, probably due to the higher average Mw of L-C. Moreover, a significant role for the dissolution of the sample in the salt could be played by the different chemical reactivity of the nitrogen functionalities towards the salt.
For these reasons nitrogen-derivatives and especially NL-C, allow for a more efficient pores generation.

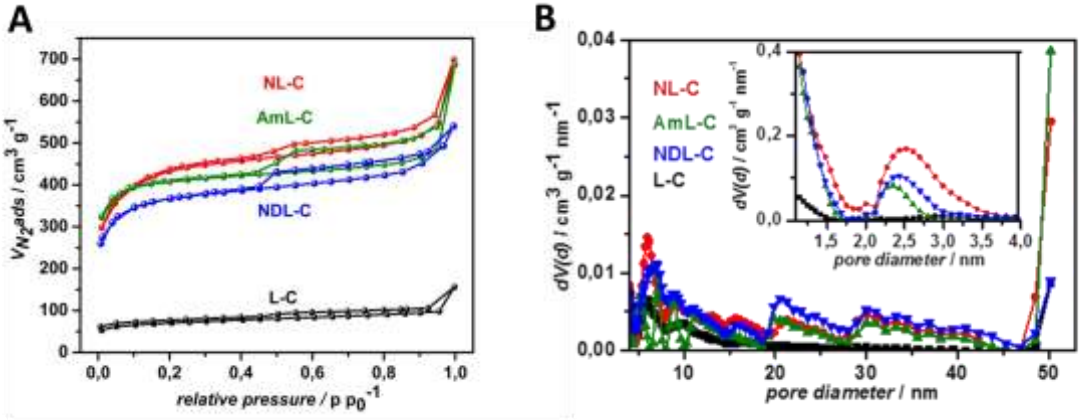

Figure 4.9 A- *Isotherms* **B-** *Pore Size Distribution (PSD) of carbonized lignin L-C, NL-C, carbonized nitrolignin carbonized; NDL-C, nitro-deacetylated lignin; AmL-C, carbonized aminolignin calculated by nitrogen adsorption.**

The pore size distribution curves (Fig. 4.9B) point out the predominant presence of micropores in all the samples. Nevertheless the NDCs displayed a small peak in the range of 2 and 3.5 nm, indicating the performed formation of mesopores and the abundance of macropores, totally absent in carbonized lignin. Since the generation of meso and macropores plays a key role in mass transport, the performed porosity in NDCs is indicative of their potential electrocatalytic application.

The morphology of the samples was investigated by scanning electron microscopy (SEM, Fig. 4.10). Comparing the pictures of the starting materials (A for lignin, C for nitro lignin, E for amino lignin) and the pictures of the corresponding carbonized samples (B for carbonized lignin, D for carbonized- nitro lignin, F for carbonized amino lignin and G for carbonized nitro deacetylated lignin), the development of porosity is evident in the second series. Indeed, the smooth and dense surfaces, characteristic of thermoplastic materials, are converted in rough surfaces as a consequence of the pores generation during the ionothermal carbonization. However, all the samples exhibit a rather non-homogeneous surface, typical for biomass-derived carbons. In detail, SEM pictures highlight better than the nitrogen adsorption results, the differences between the porosity developed from NL-C and the other two NDCs. NL-C (Fig. 4.10D) reveals the presence of small particles among larger interstitial pores, in the meso to macropore range. In contrast, AmL-C and NDL-C (Fig.4.10 F and G respectively), show bulky aggregates containing micro- and macropores which are less connected than in NL-C, suggesting a low mass transport through the carbon material. We suggested that the various morphologies of the surfaces reflect the different interaction between the precursor and the salt melt. In this regard, AmL-C and especially NDL-C, were thought to develop pores as a consequence of the swelling in the eutectic salt melt.

*Reprinted with the permission from Graglia, M., Pampel, J., Hantke, T., Fellinger, T.-P., Esposito, D., Nitro Lignin-Derived Nitrogen-Doped Carbon as an Efficient and Sustainable Electrocatalyst for Oxygen Reduction. ACS Nano **2016,** 10, 4364-4371. Copyright (2016) American Chemical Society.

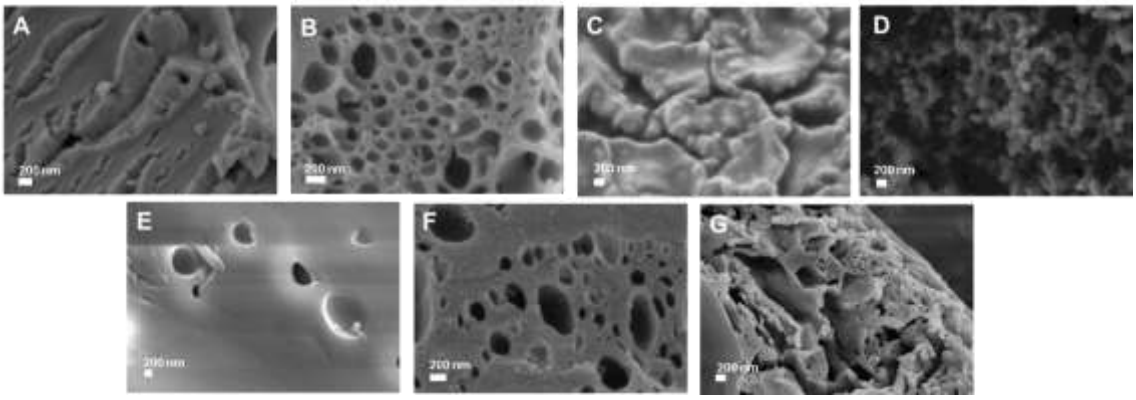

Figure 4.10 *SEM pictures of L, (A); L-C (B); NL (C); NL-C (D); AmL (E); AmL-C (F); NDL-C (G).**

Finally, the X-ray diffraction (XRD) analysis (Fig.S4.3 in the SI), showed disordered carbon structures and the absence of residual salt, confirming that the water-washing was able to remove the entire porogen agent.

4.4 Mesoporous nitrogen doped carbons as catalyst for the ORR

4.4.1 Oxygen reduction reaction (ORR)

Oxygen reduction reaction (ORR) plays a key-role among the reactions taking place in fuel cells. It occurs at the cathode, whereas the hydrogen oxidation takes place at the anode. The latter has in general a higher reaction rate than the ORR, which therefore represents the limiting factor for the efficiency of the fuel cell. At the state of the art, the main ORR catalysts are based on expansive noble metals, such as platinum.[195] Therefore, the need of more environment-friendly catalytic systems, is shifting the attention to the use of biomass derived materials. NDCs have been investigated for their activity towards ORR, and the type of nitrogen site seems to play an important role. Although the results in literature report contradicting data, carbon containing graphitic and pyridinic species of nitrogen showed a higher activity.[196]

NL-C, NDL-C and AmL-C satisfied the requirements as good sustainable candidates for the catalysis of the ORR. In fact, they are biomass-derived and present strongly and homogeneously included nitrogen in the carbon backbone. Furthermore, nitrogen is contained in both the pyridinic and graphitic form, and their synthesis is relatively cheap. Therefore, as discussed in the next paragraph, the obtained NDCs were tested for the catalytic activity towards the ORR. The experiments were performed in collaboration with J. Pampel and T.P. Fellinger

*Reprinted with the permission from Graglia, M., Pampel, J., Hantke, T., Fellinger, T.-P., Esposito, D., Nitro Lignin-Derived Nitrogen-Doped Carbon as an Efficient and Sustainable Electrocatalyst for Oxygen Reduction. ACS Nano **2016,** 10, 4364-4371. Copyright (2016) American Chemical Society.

4.4.2 ORR catalytic activity of lignin derived-NDCs

All the samples were tested at the working electrode (cathode) of a Gamry three electrodes setup in a 0.1 M KOH aqueous solution. The efficiency of the catalyst is expressed by the half-wave potential ($E_{1/2}$) in the polarization curves showed in Fig. 4.11A.

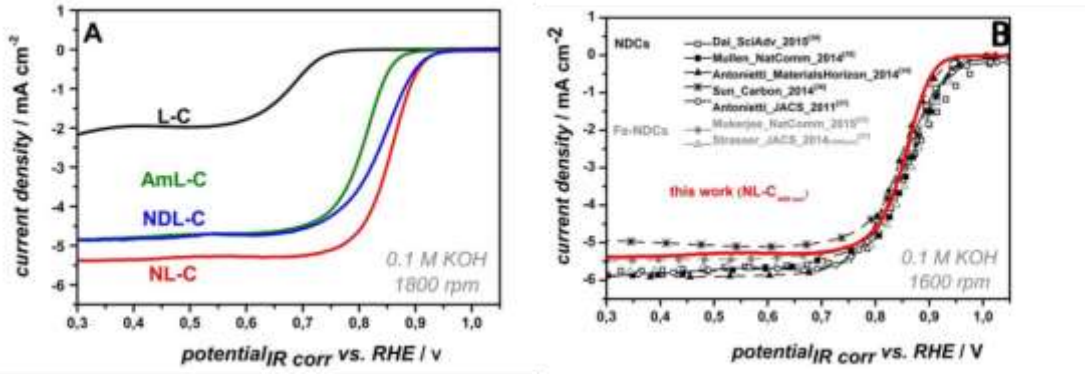

Figure 4.11 A- *RDE polarization curves in O_2-saturated 0.1 M KOH with a sweep rate of 5 mV s-1, 1800 rpm.* **B-** *Comparison of NL-C curves with recent works in literature (in alkaline conditions)**

As shown in the Fig. 4.11 A, the lignin-derived carbon displays a lower half-wave potential of 0.67 V when compared to the $E_{1/2}$ values of the NDCs. In detail, the $E_{1/2}$ of AmL-C results 140 mV shifted towards positive values if compare to L-C. Although NL-C and AmL-C showed similar surface area and nitrogen-content based on elemental analysis (Tab. 4.4 and 4.2), the higher amount of pyridinic and graphitic nitrogen of the former promotes the formation of more ORR-active sites, reflected in a higher $E_{1/2}$. In addition, the lower kinetic of NDL-C compared to NL-C, is due to the lower S_{bet} with a consequent lower availability of electrochemical active surface area. The morphology of NL-C seemed to facilitate the O_2 accessibility to the active sites, confirming the important role of the connection between the pores. The results obtained for the electrocatalytic activity of the lignin-derived NDCs towards ORR were compared to the ones of non-noble metal catalysts generally mentioned in literature (Fig. 4.11B). More details about electrochemical results are reported in the work of Graglia, Pampel et al. [46]

4.4 Conclusion

In this project NDCs were synthesized using cheap and widely available lignin as carbon precursor. Lignin was extracted from beech wood chips by hydrothermal alkaline method with the simultaneous isolation of the bioplastic-precursor lactic acid. Nitrogen functionalities were added to lignin *via* straightforward aromatic

*Reprinted with the permission from Graglia, M., Pampel, J., Hantke, T., Fellinger, T.-P., Esposito, D., Nitro Lignin-Derived Nitrogen-Doped Carbon as an Efficient and Sustainable Electrocatalyst for Oxygen Reduction. ACS Nano **2016,** 10, 4364-4371. Copyright (2016) American Chemical Society.

nitration using nitric acid in acetic anhydride, achieving the introduction of about 6 wt % covalently bonded nitrogen. A reduction reaction was performed in order to obtain NDCs with different functionalities of nitrogen and with the consequent opportunity to study their influence on the properties of the final carbon. The NDCs were prepared by ionothermal carbonization of the lignin-derived samples in the presence of the eutectic salt melt $KCl/ZnCl_2$. The so obtained NDCs presented high surface area, mesoporosity and high retention of nitrogen. Moreover, the final materials and above all, NL-C showed the presence of pyridinic and quaternary nitrogen, which are considered active electrochemical-sites for the reduction of oxygen in the ORR. Hence, the NDCs were tested for their electrocatalytic activity towards ORR and showed activity higher than L-C and even comparable to the one of non-noble metals catalysts reported in literature. The key-role of morphology, porosity and pore-connectivity of the NDCs for the electrochemical applications was confirmed. More detailed investigations on the possibility to functionalize lignin with different heteroatoms, such as sulfur, to obtain N-X doped carbons will be performed in work to follow.

5. SYNTHESIS OF LIGNIN BASED ADHESIVES

5.1 Lignin based polyesters

The employment of lignin for the synthesis of novel bio-based polymers is noteworthy. In this regard, lignin can be used as a macromonomer for the synthesis of polyesters without the necessity of a previous modification. Generally, polyesters are synthesized by reaction of carboxylic acids or their corresponding chlorides with polyalcohols, with the simultaneous release of water or hydrochloride acid, respectively.[197] In both condensation reactions, lignin can act as polyalcohol increasing stiffness, thermal stability and mechanical strength of the final material. Nevertheless, the reproducibility of these lignin-based class of polymers, remains a big challenge due to the variability of the lignin-structure.[49] The mechanical and thermal properties of the lignin-based polymer can be tuned either by changing the ratio of the components[198] or by addition of co-monomers in the reaction system. As an example, Gandini et al.[199] cross-linked lignin with sebacoyl and terephtaloyl chloride by condensation in N-dimethylacetamide (DMAc) or N-methyl-2-pyrrolidone (NMP) as solvents. The reaction mechanism was first investigated for model molecules, such as hydroquinone and 1,4-butanediol and the involvement of both lignin-aliphatic and phenolic hydroxyl functions in the crosslinking was confirmed. Later, the same group performed the aforementioned reaction employing polyethylene glycol (PEG) both as solvent and co-monomer.[200] The inclusion of PEG in the polyester resulted in an increasing flexibility, yielding an elastomeric material, in contrast to the previous, more rigid material. Maintaining the approach of using a reagent with a double role in the reaction, the group of McDonald[201] synthesized a hyperbranched polyester with a tertiary amine-center and amide groups (HBPEAA). In this case, a one-pot condensation was performed between a dicarboxylic acid (such as adipic acid, AA and succinic acid, SA), triethanolamine (TEA) and tris(hydroxymethyl)aminomethane (THAM). THAM acts both as a monomer and solvent. The thermal properties of the resulting polyester were strongly affected by the length of the aliphatic side chain carried by the carboxylic acid. For instance, the increase of the chain-length up to seven atoms of carbon gave rise to a more flexible polymer. The further condensation of HBPEA with the unmodified lignin resulted in enhanced stiffness of the material. A more detailed study on the role of lignin in the hyper-branched poly(ester-amine) HBPEA, was performed from the same group.[67] L-HBPEA was synthesized in a two-steps condensation process, at mild temperature (100-120 °C), in bulk and under vacuum. Thus, the thermal and mechanical properties of the purified polymer were studied while varying the employed amount of lignin. This last work presented several

advantages, such as the simplicity of the synthesis and the utilization of not toxic TEA and of adipic acid, which can be obtained from biomass. Several applications have been suggested for general lignin-based esters such as in blends, coatings and resins.[202, 203] In the last mentioned work a detailed study on the influence of the lignin ratio in the polymer on the mechanical properties of the final material was performed. However, a correlation between the mechanical and thermal properties of the final material and the structural features of the employed lignin is missing.
In the 2nd chapter of this work, a detailed structural characterization of lignins from different source was performed. As mentioned, lignin extracted from coconut (CL), bamboo (BL) and beech wood (SL) by soda isolation method showed different mass average molar mass (Mw), dispersity (D), structural condensation degree and solubility. In contrast, the total amount of hydroxyl groups in the three lignin structures is similar (4.4 wt % for SL, 4.9 wt % for BL and 4.6 wt % for CL). The OH functionalities are the lignin reactive sites in the condensation reaction. In order to study the contribution of parameters other than the amount of hydroxyl groups, we decided to use SL, BL and CL as starting material for the synthesis of lignin-based polymers. In this way, we assumed to minimize the differences between the final materials caused by a different amount of hydroxyl functions. Our last goal was to find an application for the obtained materials considering their chemical and mechanical properties. Therefore, several L-HBPEA materials were obtained employing BL, SL and CL. Interestingly, we observed the sticky nature of L-HBPEA towards metals and its resilient adhesion upon them after solidification. Hence, the gluing properties of the different polyesters were tested through the measurement of their shear stress when applied at the interface of two aluminum layers. In this section we describe the influence of the lignin source and of the lignin content on the gluing properties of the final lignin-based adhesive towards aluminum, with the future prospective of testing it as wood-adhesive.
The project reported in this section is the result of a collaboration with Dr. Michaela Eder and Nils Horbelt of the Max Planck biomaterial department.

5.2 Lignin in the synthesis of bio-based adhesives

At the state of the art adhesives for wood materials are mainly based on the combination of formaldehyde with urea,[204] resorcinol[205] or phenol,[206] on epoxy resins and on polyurethanes.[207] Despite their high tensile strength, all these polymers exhibit disadvantages, such as the release of the carcinogen formaldehyde, flammability and the need of additional additives, which are usually toxic. Hence, there is the necessity to develop more eco-friendly, less toxic and cheaper adhesives for wood application. As already mentioned in the introduction, lignin satisfies the requirements of a raw material for the synthesis of bio-

compatible adhesives, but its complex and variable structure increases the difficulties of the task. Fiberboard production is the main application of lignin in the wood-adhesives field.[208] In this regard, Mancera et al.[209] showed that the addition of Kraft lignin powder in *vitis vinifera* fiberboards improves their mechanical properties and enhances the stiffness of the material. The addition of the 20 wt % of lignin, leaded to internal bond (IB) strength up to 1 MPa with the 20 wt % content of lignin. There are also several attempts to integrate lignin in phenol-formaldehyde glues as a partial substitute of phenol. For instance, Mansouri at al.[210] studied the IB strength of adhesives containing 4,4´-diphenyl methane diisocynate (pMDI), different ratios of methyolahed lignin and glyoxal as substitute of formaldehyde in particleboard. The optimal IB strength was found to be for a 60 wt % of lignin content. Noteworthy, are also the attempts to prepare lignin-epoxy resins.[211, 212] Phenolated Kraft lignins with different purity degrees, were prepared and tested as adhesives for plywood. The glues were obtained by acid and basic catalyzed phenolation of Kraft lignin. The strength and waterproofness of the final resin were higher when the phenolation was acid catalyzed. Furthermore, lignin purity did not influence the gluing properties of the material.[213]

5.3 Synthesis of L-HBPEA

Lignins extracted from coconut (CL), beech wood (SL) and bamboo (BL) by soda process were utilized as monomers in the synthesis of different L-HBPEAs. Their isolation and characterization is described in the 2nd chapter, while Table 5.1 summarizes the parameters relevant for the purpose of this application.

Table 5.1 *Main parameters of SL, BL and CL.*

Lignin	Mw ($g\ mol^{-1}$)	Aliphatic -OH ($mmol\ g^{-1}$)	aromatic -OH($mmol\ g^{-1}$)	Total -OH ($mmol\ g^{-1}$)	Tg, °C (DSC)
SL	1542	0.4	3.4	4.4	84.5
BL	1761	0.4	3.8	4.9	72.2
CL	3799	0.5	3.5	4.6	117

SL, beech wood lignin; BL, bamboo lignin; CL, coconut lignin. Quantification of hydroxyl functionalities is performed by ^{31}P-NMR and the results are expressed as mmol of OH/ g of lignin.

The highly branched poly(ester-amine) was prepared by bulk condensation of triethanolamine (TEA) and adipic acid (AA) in a molar ratio of 1:1.7, at 100 °C in vacuum for four hours. The so obtained HBPEA resulted in a viscous pale-yellow fluid. As can be observed from the synthetic scheme in Fig. 5.1, HBPA is formed by

esterification of the carboxylates hydroxyls in AA with the alcohol functionalities of TEA. The excess of the formers guarantees the presence of free carboxylic groups for the successive condensation with lignin. A THF-lignin solution was added to HBPEA at 100 °C and the mixture stirred for few minutes to ensure the obtainment of a homogeneous system. After removal of the organic solvent, the sticky mixture was polymerized in a glass petri dish at 120 °C in vacuum for 20 h.

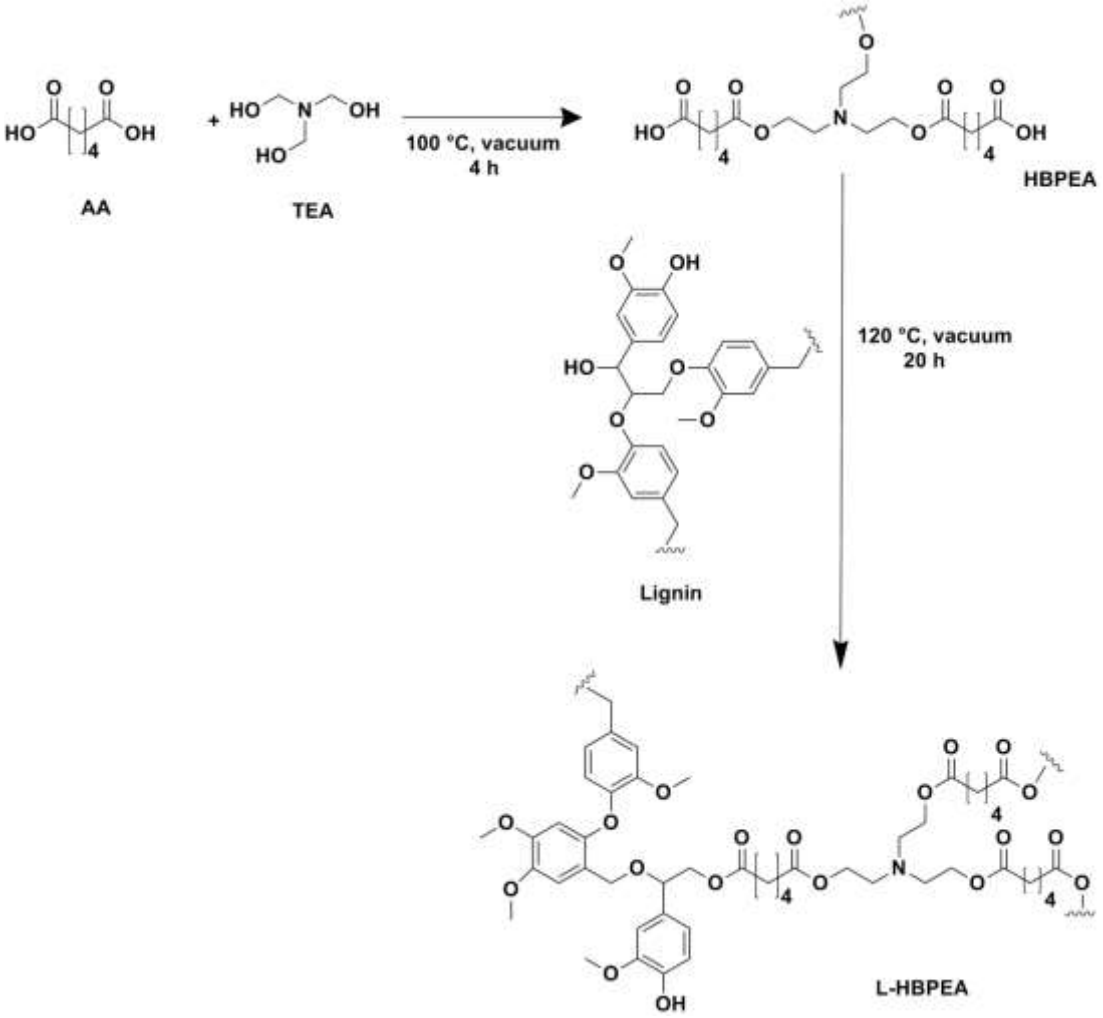

Figure 5.1 *Synthetic pathway of L-HBPEA*

SL, BL and CL were added in order to reach a final L/HBPEA mass ratio of 20:80. Moreover, to study the influence of the lignin-content on the chemical and mechanical properties of the final material, a SL-HBPEA was prepared with a beech-lignin content of 50 wt %. The so obtained polymers featured a dark-brown color, glossy surface and were insoluble in most of common organic solvents. 20 wt % CL-HBPEA (coconut lignin- HBPEA) presented higher rigidity to the touch than SL- and BL- HBPEA (beech and bamboo lignin- HBPEA respectively) with the same L/HBPEA ratio, while the 50 wt % SL-polymer was the stiffest material. Although all the

synthesized polymers adhered to the glass surface, each of them was recovered as a rubbery layer of variable flexibility. In contrast, the removal of the 50 wt % SL-HBPEA from the petri dish required intense efforts and resulted in glass rupture, denoting a strong adhesion force to the glass. The different materials were purified by reflux in THF for 72 h. A solid purified L-HBPEA (purified L-HBPEA) and a THF-soluble (THF-sol) fraction were collected and the respective yields are reported in Table 5.2.

Table 5.2 *Yield of the THF purification step of the samples.*

Sample	THF-sol. fraction (wt %)
HBPEA	/
SL-HBPEA 20	18.0
BL-HBPEA 20	18.5
CL-HBPEA 20	17.9
SL-HBPEA 50	25.3

SL-, BL-, CL-HBPEA, 20 wt % of beech wood, bamboo and coconut lignin respectively in L-HBPEA; SL-HBPEA 50, 50 wt % beech wood lignin in SL-HBPEA.

5.3.1 Analytical characterization of the L-HBPEA purified fractions

In this paragraph, we will show that the THF-soluble fractions, obtained by purification of the polymers, contain the unreacted lignin, unreacted HBPEA and small oligomers, which are generated from a non-complete condensation between the HBPEA and lignin. As observed in Table 5.2, in all the polymers with 20 wt % lignin content the THF soluble fraction represents about 18 wt %. A higher ratio of lignin in the polymer (up to 50 wt %) generates a higher content of THF soluble fraction recovered after purification. This is probably caused by the excess of lignin in comparison with HBPEA in the synthesis of the material. The excess of lignin does not crosslink with HBPEA therefore, the purification of the final polymer yielded a higher amount of THF-soluble fraction. Fig. 5.2 shows a FT-IR comparison of beech wood lignin starting material, HBPEA, SL-HBPEA and the fractions obtained by purification of the polymer (purified L-HBPEA and THF-sol).

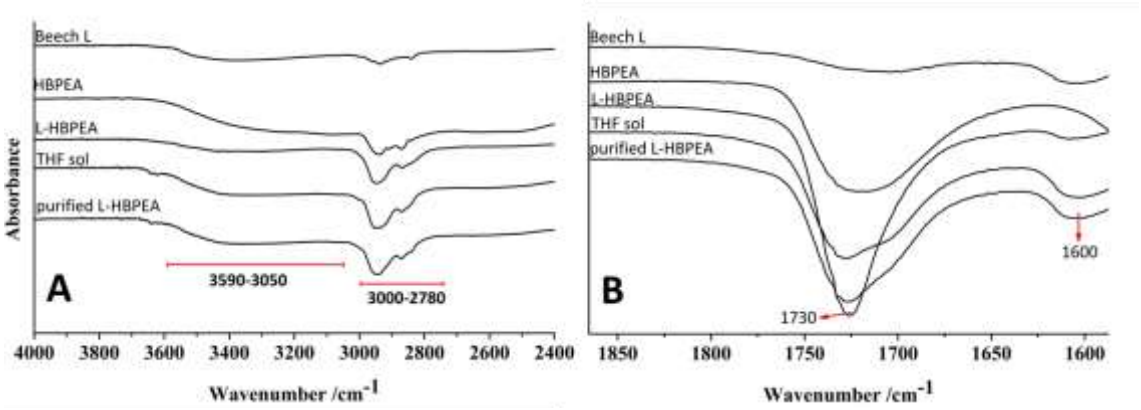

Figure 5.2 *FT-IR spectra of SL, HBPEA, L-HBPEA with a beech lignin-content of 20 wt % and of the two fractions obtained after polymer purification, SL-HBPEA THF soluble part (THF sol) and the purified L-HBPEA.* **A-** *from 2400 to 4000 cm^{-1}* **B-** *from 1850 to 1600 cm^{-1}*

Fig. 5.2A points out the different shape of the band in the range of 3590 and 3050 cm^{-1}, related to the hydroxyl groups. In the starting lignin this curve is more shifted towards higher wavenumbers, indeed the phenolic OH-stretch falls in the range of 3340-3490 cm^{-1}. HBPEA has free carboxylic hydroxyls, therefore the band is shifted at lower values (2500-3300 cm^{-1}).[214] The broader and less intense OH-stretch band in L-HBPEA denotes the occurred esterification with a consequent decrease of free hydroxyls and the change of the band shape. Moreover, the shape of the same band changes after purification of the polymer. This last observation can be indicative of hydrogen interactions between lignin and the HBPEA, which disappear after purification. The band in the region 2780-3000 cm^{-1} is related to the stretch of alkanes. Its increased intensity in all the fractions except for the starting lignin (SL) indicates the presence of the adipic acid alkyl chain. Moreover, the strong intensification of the carbonyl C=O stretch-peak at 1730 after condensation, gives an additional confirmation of the occurred esterification (Fig. 5.2B). The incorporation of lignin in the polymer is further proved by the appearance of a band at 1600 cm^{-1} in L-HBPEA, caused by the aromatic stretch (Table S2.1 in the SI).

Fig. 5.3 shows the ^{1}H-NMR spectra of HBPEA (A), HBPEA mixed with SL before polymerization (B) and THF-soluble fraction of SL-HBPEA after purification (C). In the spectrum A, the peaks at 4 ppm are related to –COO-CH_2-CH_2-N-protons, indicative of the ester bond formed during the condensation between AA and TEA. In B, in which lignin is only mixed with the prepolymer, we can observe the presence of lignin-methoxyl protons at 3.8 ppm. Fig. 5.3C confirms the performed condensation between lignin and HBPEA with the appearance of a new peak at 4.15 ppm. In fact, this peak is related to the –COO-CH_2-LIGNIN protons. This last observation represents a confirmation of the presence of small L-HBPEA oligomers in the THF-soluble fraction.

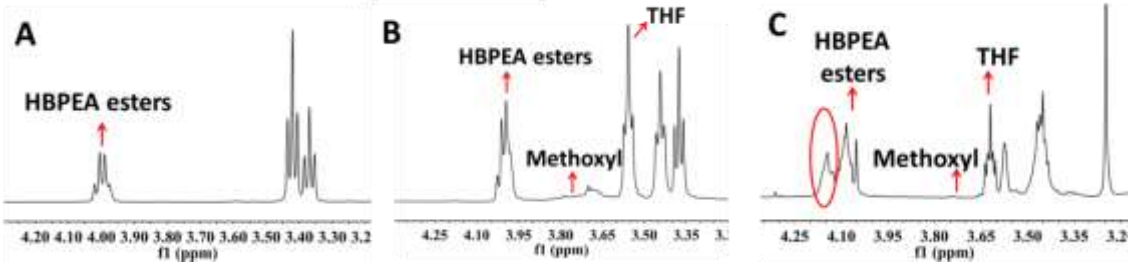

Figure 5.3 *^{1}H-NMR of* **A-** *HBPEA* **B-** *HBPEA mixed with beech lignin (SL)* **C-** *THF-soluble fraction of purified SL-HBPEA*

5.3.2 Comparison of SL-, BL- and CL-HBPEA

As mentioned, polymers synthesized employing lignins from coconut, bamboo and beech wood exhibited different mechanical properties. Nevertheless, the FT-IR analysis resulted in similar spectra (Fig.5.4 A), denoting the presence of same functional groups in all the materials. This is probably explained by the similar amount and nature of hydroxyl functionalities in SL, BL and CL, which were determined in chapter 2 (Table 5.1).

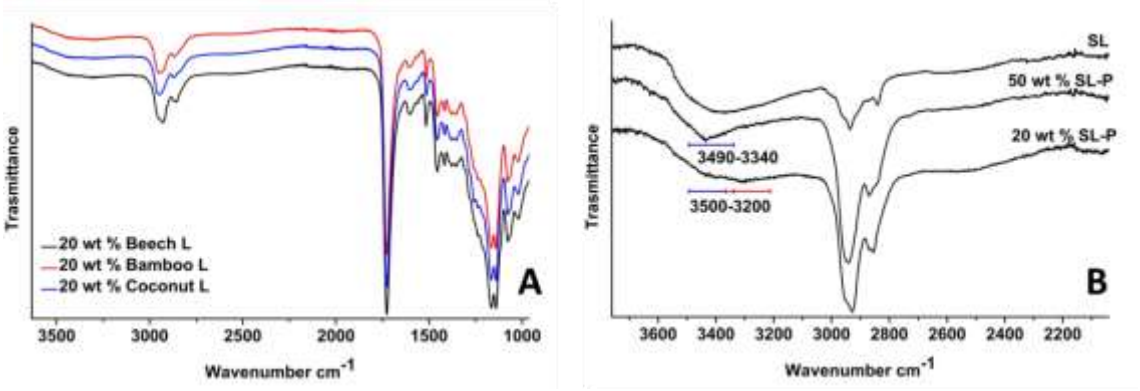

Figure 5.4 A- *FT-IR spectra of SL-HBPEA, BL-HBPEA and CL-HBPEA with a L/ HBPEA mass ratio of 20:80* **B-** *FT-IR spectra of SL, SL-HBPEA with 20 wt % of SL (20 wt % SL-P) and SL-HBPEA with 50 wt % of SL (50 wt % SL-P).*

On the other side, SL-HBPEA polymers with different lignin-content include a different amount of free phenolic OH. The FT-IR phenolic-OH stretch band fall in the range of 3490-3340 cm^{-1}. Therefore, in the FT-IR spectra (Fig. 5.4B) the band shape at 3500-3200 cm^{-1} is different for the two polymers. In detail, when the amount of lignin is higher (50 wt % SL-P) a more intense band in the region of phenolic OH stretch is observed. The SEM images of the four polymers (Fig 5.5) show the similarity of the material surfaces. As indicated by the presence of small particles, all the L-HBPEA materials have a non-homogeneous surface. The formation of only one final polymer is supported by differential scanning calorimetric (DSC) data,

which show always a single glass temperature point (Tg) (Table 5.3). In all cases the introduction of lignin increases the stiffness of the polymer. In line with this observation, a higher content of lignin causes a higher Tg. Moreover, the final material with higher lignin content displays higher residual mass at the TGA. In contrast, the source of lignin does not affect both Tg and residual mass. DSC and TGA measurements of the purified L-HBPEA and THF soluble fractions of the L-HBPEA were also performed. The DSC results show that purified polymers has a lower Tg in comparison with the corresponding non-purified material. These last consideration confirms that the lower amount of lignin in the purified L-HBPEA. (Table S5.1 in SI).

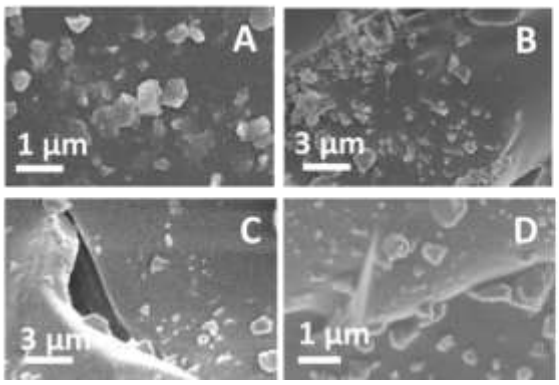

Sample	Tg, °C (DSC)	Residual mass (wt %) at 1000°C
HBPEA	-22.3	4.0
SL-HBPEA 20	- 9.1	12.1
BL-HBPEA 20	- 8.6	11.4
CL-HBPEA 20	- 8.5	13.6
SL-HBPEA 50	11.4	16.2

(Left) Figure 5.5 *SEM images of* **A-***20 wt % BL-HBPEA* **B-***20 wt % CL-HBPEA* **C-***20 wt % SL-HBPEA* **D-***50 wt % SL-HBPEA.* **(Right) Table 5.3** *Thermal analysis of the samples. The TGA analysis is conducted in nitrogen atmosphere. The temperature is increased from 30 to 1000 °C with a rate of 10 °C/min.*

5.4 Shear strength of L-HBPEA samples

This part of the project was made in collaboration with Dr. Michaela Eder and Nils Horbelt of the Max Planck biomaterial department.

As already mentioned, the pre-polymer made of lignin and HBPEA before their condensation can be described as a sticky viscous fluid. To characterize its gluing properties, we measured the shear stress of four different L-HBPEA samples named as:

- **S1**: 20 wt % SL-HBPEA
- **S2**: 20 wt % BL-HBPEA
- **S3**: 20 wt % CL-HBPEA
- **S4**: 50 wt % SL-HBPEA

This preliminary test on one sample each, was performed according to the European/German standard DIN EN 1465.

As shown in Fig.5.6A, the edges of aluminum bars (aluminum bars: 1 mm thick, 25 mm wide and 100 mm long) were covered on one side (12.5 mm) with a thin layer of L-HBPEA mixture. A second identical aluminum bar overlapped the first on the area covered by the L-HPBEA. A clamp was used to fix the bars position during the curing of the adhesive, at 120 °C in a vacuum oven for 20 h. After polymerization of the glue, the samples were clamped in a Zwick universal testing machine (scheme of the machine in Fig. 5.6 B) and tested with a constant feed rate of 0.6 mm min^{-1} until failure.

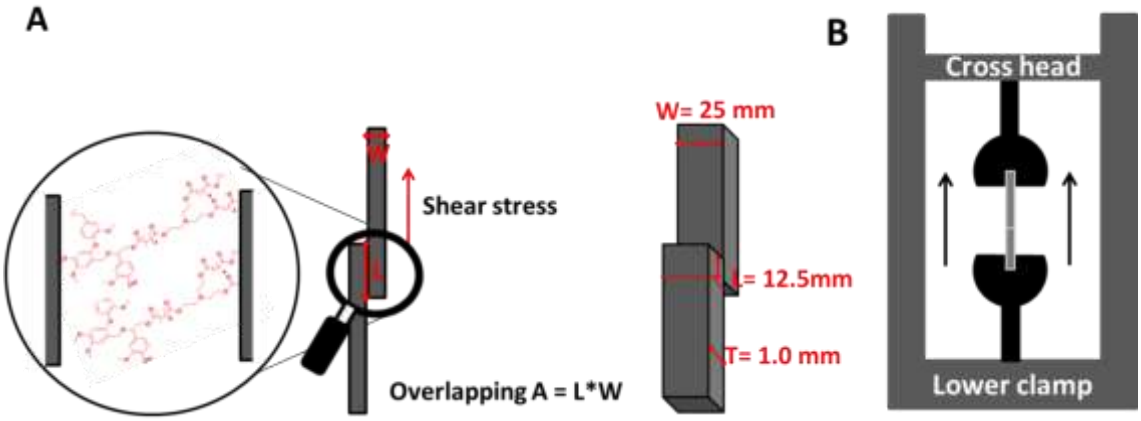

Figure 5.6 A- *Lap joint. The area occupied from L-HBPEA depends from the length of the adhesive layer (L) and the width of the bar (W).The thickness of the bars is indicated by the letter T.* **B-** *Scheme of the testing machine used for the measurement of the shear strength.*

The instrument records both the cross head displacement and the force necessary to break the joint. The shear stress was calculated based on the maximum force divided by the overlapping area, as described in equation 5.1.

Equation 5.1 *Calculation of the shear stress*

$$\sigma = F A^{-1}$$ **F:** applied force (N) **A:** adhesive area (m^2) **σ:** shear stress (Pa)

Due to our basic instrumentations, we could not accurately control the thickness of the adhesive layer. However, the performed test is suitable to obtain a fast and reliable comparison of the gluing properties of the different samples.
From the preliminary tests, we can assume that the lignin source does not influence the shearing strength. Indeed, samples S1, S2 and S3 with a lignin content of 20 wt %, break at similar stress levels (Table 5.4).
Sample S4, which contains 50 wt % of lignin, showed a higher value for shear strength.
Based on the preliminary findings, ten specimens with a lignin content of 50 wt % (S4) and other ten with a lignin content of 20 wt % (S1) were prepared. The data

related to the ten specimens of S1 gave rise to an average shearing strength of 5.7 MPa, with a standard deviation of 0.7 (Table 5.4, Fig. 5.8). The data obtained for S4 specimens showed a high standard deviation of 1.4 (Table 5.4, Fig 5.8). The low and high standard deviations between the samples S1 and S4, can be explained by the polymer distribution at the interface between the aluminum bars after the separation. In fact, the metal layers glued by specimens S1 showed a homogeneous film of polymer on both of the layers with an expected accumulation in the corners and at the border and a probably prevalent cohesive failure (Fig. 5.7, S1).

Figure 5.7 *Adhesive distribution at the failure after separation of the bars specimens of specimens S1, S4-A and S4-B groups.*

In contrast, the surface of the specimens of S4 exhibits a less reproducible distribution of adhesive (Fig. 5.7 S4-B). This can be attributed to the fact that the homogenous spreading of the prepolymer with a higher amount of lignin is more difficult. Hence, we identified two sub-groups, S4-A containing five specimens with homogenous polymer distribution and probably cohesive failure and S4-B with nonhomogeneous distribution and mixed (cohesive and adhesive) failure mode (Fig.5.7). Shear strength data are reported only for the first group of specimens S4-A.

Table 5.4 *Calculation of shear stress (σ) at the break by equation 5.1.*

Sample	σ at breaking (MPa)	σ standard deviation
S1	4.9	---
S2	5.7	---
S3	5.9	---
S4	7.2	---
S1 $_{10\ sp.}$	5.7*	0.7
S4 $_{10\ sp.}$	6.9*	1.4
S4-A $_{5\ sp.}$	8.1*	0.8

*Sp, specimens. *Average value.*

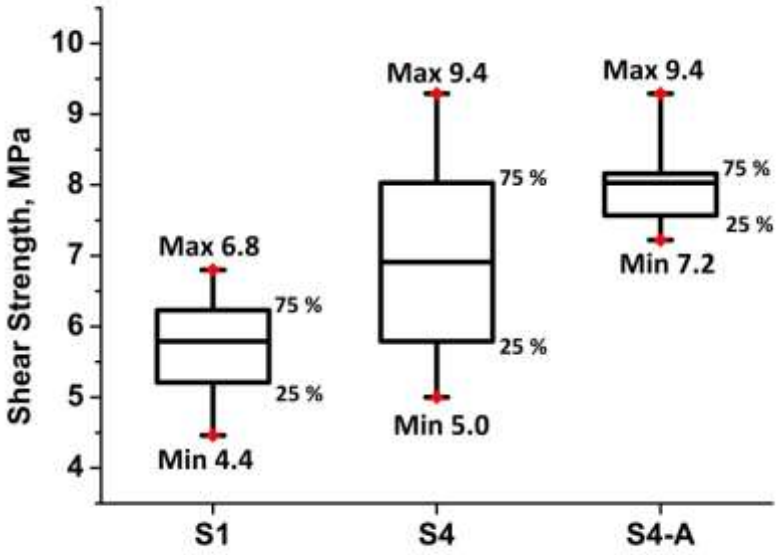

Figure 5.8 *Graphic representation of the statistical distribution of the shearing stress values of S1, S4 specimens and specimens group S4-A. The boxes include data between 75 and 25 % percentile.*

The groups named S4-A confirmed the trend of data obtained in the previous experiment, hence with relatively high average shear strength of 8.1 MPa. Moreover, the standard deviation of the values resulted strongly reduced to 0.8. Fig. 5.8 shows that 50 % of the S4-A-group specimens, have a shearing strength between 8.2 and 7.6 MPa, which means a smaller distribution of values in comparison with the other samples.

As an indicative comparison, Feldman et al.[215] reported the synthesis of lignin based epoxy-polymer as glue. They measured the shear strength of the adhesive containing 20 and 40 wt % of lignin, towards aluminum. The mechanical test was performed in conditions similar to our protocol. The results showed shear strength in the range of 10-12 MPa for a lignin content of 40 wt %.

Even though spreading the mixture homogenously is more difficult with higher lignin contents, the average shear stress of samples with homogenous films is increased by ~42 %. This could be explained with an adhesion mechanism based on the hydrogen interactions between free hydroxyl groups of the polymer and aluminum. Coconut lignin, bamboo lignin and beech lignin have a quite similar OH content therefore, once condensed with HBPEA in the same L/ HBPEA ratio, they showed just slight different adhesive strength.

5.5 L-HBPEA as adhesive: conclusion

A highly branched (ester-amino) polymer was synthesized by a two-steps-bulk condensation of adipic acid, which can be biomass derived, a nontoxic tertiary amine (TEA) and an unmodified lignin. The lignins, used as macromonomers in the reaction, were previously extracted from the corresponding raw material by soda-process and characterized for their chemical and thermal properties (chapter 2). A comparison of polymers containing lignin from several sources (coconut, beech wood and bamboo) and in different content (20 and 50 wt %), was performed. The different ratio of lignin and HBPEA in the polymer synthesis, resulted in remarkable thermo-mechanical differences of the final material. Indeed, higher amount of lignin increases the rigidity and thermal stability of the polymer. The gluing properties of the different samples were tested for the shearing strength. The test was performed by spreading the viscous mixture of lignin and HBPA between two aluminum plates and heating them in order to perform the polymerization. The resulting shear strength seems to not depend on the lignin source, but rather on the content. The synthesized lignin-based polymers showed a shear strength value up to 9 MPa for a 50 wt % lignin-content of the material. The shear strength of the glue synthesized in this work showed just a slightly lower value in comparison to epoxide lignin-base adhesives reported in literature. That indicates that a further optimization of the polymer synthesis could lead to an adhesive with stronger gluing properties. However, we showed that the synthesized adhesive can be prepared employing a wide variety of lignins, without affecting the gluing properties.

The same studies performed on aluminum surfaces, could be extended to wood materials in order to test the adhesive efficiency of the (amino-ester) lignin based-polymer towards wood.

6. CONCLUSION AND OUTLOOK

The need for alternative and non-fossil feedstocks within the production of chemical building blocks and materials drove our attention to the large possibilities offered by lignin. The aromatic polymer is well-known in the biomass field for its complex and variable structure. Indeed, the ratio of the different functionalities and linkages in lignin structure is heavily dependent on the utilized method to isolate it and on the biomass source. Additionally, the lignin application fields are affected by the structural features of the polymer. Therefore, the study of lignin structure is necessary for its possible valorization.

In this work lignin was extracted from beech wood by different isolation methods, such as alkaline hydrothermal treatments (using NaOH and $Ba(OH)_2$ as base) and organosolv process in acidic conditions. In a second approach, lignin was isolated from beech, coconut and bamboo by a soda pulping process. The aim of this study was to investigate the influence of the extraction process and the biomass source on lignin structure. Based on the structural features of the isolated lignins, a suitable application was suggested. Hence, the first part of this work consists of a detailed analytical comparison of the isolated lignins' main structural features by FT-IR, elemental analysis, GPC, ^{1}H, ^{31}P and 2D HSQC-NMR, TGA, DSC and the Klason test. By combining the different results, we concluded that the different isolation mechanisms mainly affect the Mw, the amount of phenolic hydroxyl groups and the intramolecular linkages of the structure. In detail, the alkaline treatments led to a high lignin deconstruction and consequently to a high content of hydroxyl groups in the polymer structure. In contrast, lignin extracted by acid organosolv method showed high Mw and structural complexity caused by the occurrence of more recombination reactions. As a consequence, organosolv lignin showed high thermal stability up to 700 °C. The biomass source strongly affects the monomer composition of lignin but not significantly the content of hydroxyl functions. Indeed, lignin extracted from coconut, beech and bamboo by the soda isolation process showed similar content of hydroxyl groups. The second part of the work focused on the applications of modified and unmodified lignin, considering the analytical results.

The topic of the 3rd chapter is the analytical characterization of mono- di-and polyaromatic molecules generated by lignin deconstruction. In detail, we developed a gas-chromatographic method which led to the separation of the aromatic mixture into three main groups. The molecules were differentiated on the basis of their volatility and each group was quantified by comparison with the calibration curve of three different reference standards. The analytical method was used to compare the yield and selectivity of heterogeneous–catalytic hydrogenolysis (HGL) of Kraft lignin. Firstly a comparison between three HGL catalysts, TiN-Ni, TiN-O_2 and Pd/C

under flow conditions was performed. The study showed a higher selectivity of the TiN-Ni catalyst towards guaiacol-like molecules. A second comparison was carried out between the products of the TiN-Ni catalyzed hydrogenolysis in batch condition at 150 and 175 °C. The reaction temperature showed a key-role in the tuning of the selectivity towards the molecules with lowest Mw. The developed analytical method appeared to be rather versatile; it was even used for the quantification of polyphenolic compounds extracted from olive leaves.

In the further sections, two different applications of the previously isolated and characterized lignins are reported. Lignin extracted by a hydrothermal alkaline process based on the use of $Ba(OH)_2$ as base, resulted in a low Mw and relatively soluble polymer. Therefore, the resulting lignin was nitrogen-functionalized with the purpose of synthesizing nitrogen-doped carbons (NDCs). A straightforward aromatic nitration was followed by reduction of the nitrolignin to achieve amino-lignin (AmL). Different NDCs were obtained by ionothermal carbonization of the lignin-derivatives in the presence of the eutectic salt melt $KCl/ZnCl_2$. We investigated the role of the nitrogen-functionalities inserted in the lignin-backbone towards the porosity and morphology of the resulting materials. NDC obtained using nitrolignin produced the best candidate for electrochemical applications. It showed high content of nitrogen and higher total pore volume. Thus, the NDCs were tested for the electrocatalytic activity towards the oxygen reduction reaction and the NDC derived from nitrolignin showed a catalytic activity comparable to the non-noble metal catalysts reported in the recent literature.

In the last project, described in 5^{th} chapter, lignin was used as a macromonomer in the condensation reaction with the prepolymer HBPEA. In this case, the presence of a relatively high number of hydroxyl groups in the lignin structure is required. For this reason, the lignins extracted by the soda process were utilized. In detail, coconut, bamboo and beech lignin, which showed a similar content of hydroxyl functionalities, were chosen as starting materials. The corresponding polymers showed gluing properties towards aluminum and therefore, their shear strengths were measured. Interestingly, the gluing properties appeared to be independent from the lignin type but were affected by the ratio of lignin contained in the polymer. Considering that, we suggested an adhesive mechanism based on the formation of hydrogen bonds between the polymer and the aluminum surface. Moreover, with this project we showed that lignin can be utilized in applications, in which the lignin structural variability does not represent a critical issue.

Considering the work reported here, we described a complete biorefinery scheme, from the extraction of the biomass to its applications (Fig. 6.1).

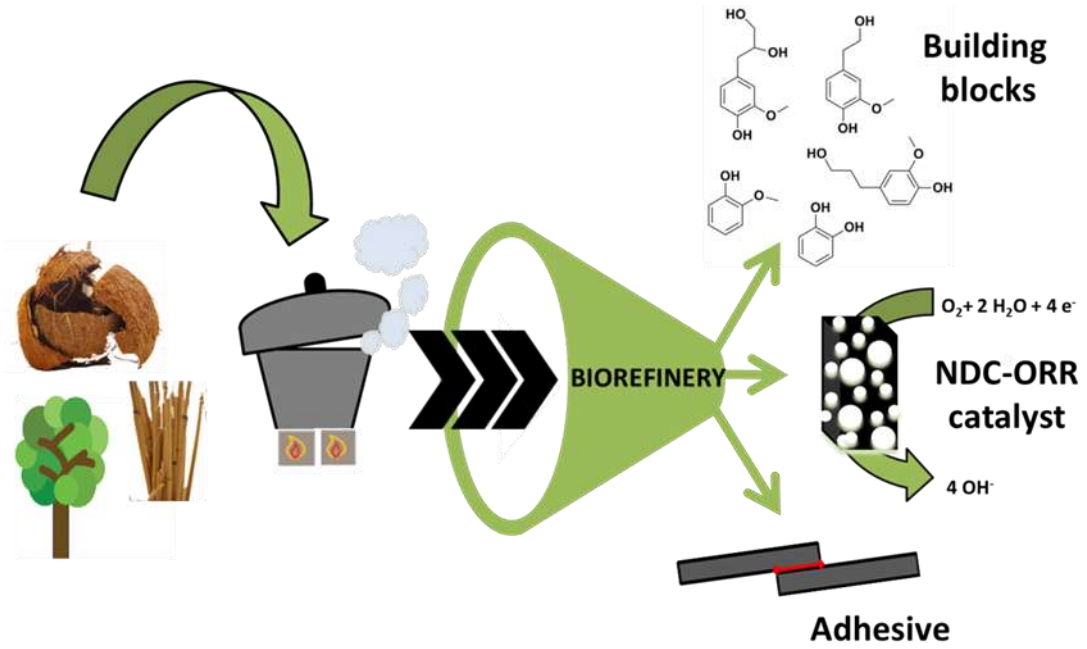

Figure 6.1 *Schematic summary of the project*

Interesting future outlooks can be suggested for each reported project.

The different groups of aromatic molecules obtained by lignin deconstruction could be separated and functionalized. The resulting compounds can be used as building blocks for the synthesis of pharmaceuticals and chemicals, which are currently mainly derived from fossil feedstock.

Regarding the synthesis of nitrogen doped mesoporous carbons; it would be interesting to test if the process developed here can be extended towards the use of lignin with different structural features. For instance, the investigation of the carbon properties obtained from the same process applied to lignins isolated from several sources and by different extraction methods could be an interesting investigation. Moreover, future studies will be directed towards the carbonization of sulfur-functionalized lignins to obtain N-X doped carbons.

Considering the results obtained from the application of lignin as a glue, the gluing properties of the polymer L-HBPEA towards wood should be investigated in future studies, with the purpose of satisfying the increasing demand for more sustainable and cheaper glues for the wood-industry.

A. MATERIALS AND METHODS

Materials

All the synthetic chemicals were of reagent grade and used as received, without further purifications. All the solvents and deutereted solvents were purchased by Sigma Aldrich and the solvents used for analysis were of analytical grade. sodium hydroxide pellets, potassium hydroxyde pellets, benzyl phenyl ether, barium hydroxide octahydrate, hydrochloric acid (1 M), ninhydrin, cyclohexanol, diphenyl ether, 2-methytetrahydrofuran, kraft lignin, 2-methoxy-4-propylphenol, vanillic acid, homovanillic acid, vanillin, 2-Methoxy-4-propylphenol (propylguaiacol), nitric acid, acetic anhydride, triethanolamine, adipic acid, sulfuric acid, sodium sulfate anhydrous, hydrochloric acid 37%¸ sodium hydrogencarbonate, pyridine and BSTFA were purchased by Sigma Aldrich. Beech wood chips were purchased by GOLDSPAN®. Olive leaves were purchased by Lexa.

Methods

Combustive elemental analysis

Combustive elemental analyses were performed using a Vario Micro device.
Specimens are burned in oxygen atmosphere, decompositions products (CO_2, H_2O, N_2, SOx ,NOx) are detected and N, S, H and C quantified.

Gel permeation chromatography (GPC)

GPC measurements are performed with the purpose to detect the mass average molecular weight (Mw) of a polymer. Mw is not directly measured but it is calculated by comparison of its hydrodynamic volume with a calibration standard, in the case of lignin polystyrene was utilized. The analysis is performed by a Thermo Separation Products apparatus equipped with an UV/RI detector. N-methyl-2-pyrrolidone was used as solvent to elute the samples at 70 °C through two PSS-GRAM columns in series (300 mm, 8 mm^2) with an average particle size of 7 µm and porosity between 100–1000 Å

Fourier transform-infrared spectroscopy (FT-IR)

FT-IR spectra were recorded on a Varian 1000-FT-IR spectrometer.
The measurement is based on the detection of the energy that a beam of infrared arrays need to induce the vibration of different chemical linkages. In this way,

structural information about chemical bonds and functional groups of the molecules can be obtained.

Gas chromatography-mass spectrometry (GC-MS) and flame ionization detector (GC-FID)

GC analysis were carried out on a Agilent Technologies 5975 gas chromatograph equipped with a MS detector (front) and a FID (back), two capillary columns both HP-5MS (30 m, 0.25 mm, 0.25 micron, front and back) and helium as carrier gas. The temperature program started with 50 °C kept for 2 minutes and then increased to 300 °C with a heating rate of 10 °C min^{-1}. The final temperature was maintained for 20 min. The injector and detector temperatures were set to 250 °C and 280 °C respectively. The autoinjector was used in a split modality, with a ratio of 1:100. The separation of the different molecules is based on their volatility.

Nuclear magnetic resonance

^{1}H-NMR monodimensional spectra were acquired on a Bruker Spectrospin 400 MHz Ultrashield Spectrometer in deuterated solvents. Chemical shifts of the components are referred to the solvent. The 2-methoxy-4-propylphenol utilized for lignin in the 4th section, its detivatives, conyferil alcohol and its hydrogenated form (about 20 mg) were dissolved in deuterated methanol or chloroform (0.6 mL). Bidimensional HSQC-NMR analyses were recorded using an Agilent 400 MHz device. Lignin and its derivatives were generally acetylated for the purpose of the analysis. Acetylated lignins (100-200 mg) were dissolved in deuterated chloroform (0.6 mL)

Nitrogen sorption measurements

Nitrogen adsorption measurements are performed by Quantachrome Quadrasorb device. The specimens were preliminary degassed for 20 h at 150 °C. The operative temperature is kept constant at 77 K, at which the adsorbate (nitrogen) is liquid. The volume of the gas adsorbed on the surface of the sample is recorded at different pressures and the data are processed by QuadraWin software. Information about specific surface area and pore properties are so obtained.

Scanning electron microscope (SEM)

Images were recorded using a LEO 1550 Gemini microscope. For L, NL, NDL and AmL and all their carbon-derivatives (Fig. 4.10 in chapter 4), the specimens are deposited on an aluminum holder coated by carbon and observed without any additional coating. During the analysis, a beam of electrons is directed onto the sample-

surface and the scattered electrons are detected. In order to obtain a 3D picture, the sample must be conductive, if not it is previously sputtered with a metal such as platinum or gold. Therefore, non-conductive L-HBPEA materials (Fig.5.5 in chapter 5) are preliminary sputtered with platinum.

Wide angle X-Ray diffraction (XRD)

XRD analysis was performed by the use of a Bruker D8 diffractometer equipped with a Cu-Kα source (λ = 0.154 nm) and a scintillation counter (KeveX Detector).
This technique is based on the diffraction of electromagnetic wavelengths incident on the sample. During the analysis, the angle θ between the diffracted wavelengths and the axis of the electromagnetic beam is detected. Diffracted waves interact between each other and only in the case of crystalline morphology the interactions are constructive and each peak has a position and intensity relative to a crystalline phase. Therefore this technique is useful for crystalline material and cannot supply information for amorphous polymers (i.e. lignin). Indeed in chapter 4 (Fig. S4.4 in the SI) XRD is applied to check the presence of residual salts after the ionothermal carbonization and the following washing of the carbons with water.

Thermogravimetric Analysis (TGA) and Differential Scanning Calorimetry (DSC)

TGA analyses were performed by TG 209F1 Libra TGA209F1D-0036-L instrument, in nitrogen atmosphere, with a heating ramp from 30 to 1000 °C and a heating rate of 10 K min^{-1} (Chapter 2) and 2.5 K min^{-1} (chapter 4) The sample-holders are made of platinum and the data were obtained by the NETZSCH Proteus software. During TGA analysis the sample is heated and the loss of weight is recorded with the increasing of the temperature. For lignin-derived samples (chapter 4), TGA was coupled with a Thermostar Mass spectrometer (TGA-MS) in order to study the nature of the products released by thermal decomposition.
DSC analysis was performed by the same instrument and without changing all the aforementioned parameters. During this experiment the sample is heated, as well as a reference and the heat necessary to maintain both of them at the same temperature is recorded. Through this measurement it is possible to investigate the phase-transitions of the sample at different temperature. Indeed, the heat required from the sample to increase the temperature is higher during a phase transition such as the melting.

X-ray photon spectroscopy (XPS)

XPS measurements were conducted by a Thermo-VG Scientific ESCALAB 250 X-ray photoelectron spectrometer (Thermo Electron, U.K.) using Al Kα X-ray source (1486.6 eV). The carbon peak served as internal reference and the high resolution N1 spectra was used for the quantification of the different N sites.

This is a non-destructive analytical technique in which the sample is subjected to a beam of high-energy photons that causes the release of electrons. The energy of the electrons is characteristic of each element, it is related to its respective amount and depend on the chemical and electronic environment. Therefore XPS measurement gives both qualitative and quantitative information about the elemental composition and the binding state of the elements. Nevertheless, XPS is a surface-sensitive analysis.

B. EXPERIMENTAL PART

B.1 Lignin acetylation

Procedure A- Lignin (450-550 mg) is dissolved in acetic anhydride (10 mL) and stirred at 100 °C for 3 h. The reaction is quenched by addition of H_2O (2 mL) and acetylated-lignin is extracted by $CHCl_3$ (2 x 25 mL). The organic phase is washed with a saturated $NaHCO_3$ aqueous solution (2 x 20 mL) and then with water to neutral pH. After anhydrification over anhydrous sodium sulfate, the $CHCl_3$ phase is concentrated by rotary evaporator and dried at 38 °C in vacuum atmosphere.

Procedure B-Lignin (500 mg) is stirred in a 1:1 acetic anhydride/pyridine solution (10 mL) over night at room temperature. The reaction is quenched by addition of water while cooling the flask. Acetylated-lignin is extracted by $CHCl_3$, dried over anhydrous sodium sulfate, concentrated by rotary evaporator and dried at 38 °C in vacuum atmosphere.

B.2 Determination of extractives in beech wood

Beech wood chips (10.5 g) dried at 45 °C for 48 h, are refluxed in Soxhlet apparatus with ethanol (300 mL) for 24 h. Thus, the flask is cooled at room temperature, the solid is recovered, dried and used for the total determination of lignin test. The ethanolic solution is concentrated by rotary evaporation and the residue dried at 38 °C overnight in vacuum yielding to 0.4 wt % (40.0 mg) of total extractives of the dried biomass.

B.3 Total solid in wood and lignin

Beech wood chips extractives-free and lignin samples (1.0 g) are dried at 105 °C overnight. The content of total solid is calculated as follow:

$$\% \text{ Total Solids} = (W_{ds} - W_h)/ W_s * 100$$

W_{ds}: weight of the dried sample+ weight of sample holder
W_h: weight of the sample holder
W_s: weight of the starting sample

B.4 Total determination of lignin content in biomass and of lignin purity

Beech wood chips extractives-free and lignin samples (300.0 mg) are suspended in a 72 v/v % H_2SO_4 aqueous solution (3.0 mL exactly measured) and stirred for 1 h at 30 °C. Deionized water (84 mL) is added to reach a final H_2SO_4 concentration of 4 V/V %. The suspension is vigorously shacked and filtrated in vacuum. The acid water is recovered and the UV absorbance at 240 nm (Abs_{240}) is measured with the purpose of quantify acid soluble lignin (ASL). The latter determination must be done within 6 hours of hydrolysis by diluting the acid solution with deionized water to bring Abs_{240} values in the range between 0.7 and 1.0. Deionized water is used as blank. The content of acid-soluble lignin (ASL) is calculated as follow:

$$ASL\ \% = (UVabs^* V_f^* D)^*100 /\varepsilon^*ODW\ ^*Pathlenght$$

UVabs: UV-Vis absorbance at 240 nm
V_f: volume of filtrate (86.73 mL)
D: dilution
ε: absorptivity of biomass at 240 nm (25 L g^{-1} cm^{-1})
Pathlenght: pathlenght of the UV-Vis cell (1 cm)
ODW (oven dry weigh)= W_s * % Total solid/ 100 (W_s: sample weight)

The weight percentage of acid insoluble lignin (AIL) was calculated after drying the solid, which is obtained by the afore described hydrolysis, at 105 °C overnight as follow:

$$AIL\ \%= (W_s - W_{ds} - W_h)/ ODW$$

W_s: weight of the starting sample
W_{ds}: weitght of the dried sample +weight of the holder
W_h: weight of the sample holder

B.5 Soda pulping process for beech wood (SL), coconut (CL) and bamboo treatment (BL)

The biomass source is treated with a 1.5 M NaOH aqueous solution in a solid/liquid ratio of 0.16 g/mL at 175 °C for 12 hours in autoclave. After cooling the system the mixture is filtrated, the pulp washed with water and the collected liquids acidified by HCl 4M to pH < 5. Lignin precipitated in the dark liquor is filtrated out and washed by water until neutral pH. The recovered lignin is dried in vacuum condition at 38 °C for 12 h.

B.6 $Ba(OH)_2$ hydrothermal alkaline extraction of lignin

Beech wood chips were treated with a 1.7 M $Ba(OH)_2$ aqueous solution in a solid/liquid ratio of 0.3 g/mL at 220 °C for 15 hours in autoclave. After cooling the system the mixture was filtrated and the pulp washed with HCl 1M and water until neutral pH is reached. The recovered L is dried overnight in vacuum at 38 °C. Tetrahydrofuran (THF) is added to the dried pulp and THF-soluble AL, recovered by concentration of the organic solvent is dried overnight at 38 °C in vacuum.

B.7 Acid-catalyzed OS extraction method

Beech wood chips were treated in the presence of 65 V/V % ethanol in H_2O and with a catalytic amount of sulfuric acid (0.01 mol) at 195 °C for 80 minutes in a sealed autoclave. The solid/liquid ratio was 0.15 g mL^{-1}. After cooling down the system the mixture was filtrated and the pulp washed with warm EtOH. A large amount of water was added to the collected liquids (dark liquor and washing EtOH) in order to precipitate L. OSL was washed by water and then dried overnight in vacuum at 38 °C. The extraction method is showed in Fig. 2.3.

B.8 Lignin phosphitylation

Solution A: a solution 0.1 mM of cyclohexanol (IST) and 0.01 mM of chromium(III) acetylacetonate (relaxation agent) in a 1:1 V/V mixture of anhydrous pyridine and N,N- dimethylformamide (DMF) is prepared .
Dried L (20 mg) is weighed directly in the NMR tube and dissolved in anhydrous DMF (200 µL). After complete dissolution of the powder, solution A (100 µL), TMDP (derivatizing agent, 50 µL) and deuterated chloroform (450 µL) are added, the solution is stirred at room temperature and subjected to analysis.

B.9 Kraft lignin hydrogenolysis in flow reactor

Hydrogenolysis is performed using the H-Cube Pro™ reactor. The filtered solution of KL in methanol (1.4 mg/mL) is flushed at a flow rate of 0.3 mL min^{-1} through a 70 mm column packed with the different catalysts, at 150 °C, in presence of H_2 and at a pressure of 25 bars. The collected sample is concentrated and dried overnight at 38 °C in vacuum oven.

B.10 Kraft lignin hydrogenolysis in batch reactor

The batch hydrogenolysis is conducted at 150-175 °C for 24 h in a stainless steel autoclave (Parr) while stirring. MeOH (400 mL) is added to KL (40 g), the autoclave is sealed and purged six times whit H_2 before filling it with the same gas at a pressure of 5 bars. After cooling the system at room temperature, the mixture is filtrated on paper and the liquid phase is concentrated by distillation of MeOH. The solid residue is dried overnight at 38 °C in vacuum atmosphere.

B.11 Liquid chromatography separation

A glass chromatographic column is filled with silica gel (6 g) and dried reacted KL (100 mg) is deposited and separated by elution of mobile phases having different polarity. The first solvent is a mixture 75/20/5 of n-hexane/isopropanol/methanol (300 mL), the second is pure ethanol (300 mL) and the last is pure methanol (300 mL). The fractions are collected, the solvent are distilled by rotary evaporator and the samples dried at 38 °C overnight in vacuum.

B.12 Silylation of chloroform soluble molecules

Depolymerized lignin (20-40 mg exactly weighted) is dissolved in chloroform (125 µL) and BSTFA (silylation agent, 250 µL) is then added. The solution is stirred and heated at 70 °C for 45 min. The solution is cooled down to room temperature and then injected in the GC.

B.13 Reduction of coniferyl alcohol

Hydrogenation of the commercial coniferyl alcohol is performed by H-Cube Pro™ reactor. A solution (0.7 mg mL^{-1}) of the sample in methanol is flushed at 0.5 mg mL^{-1} through a 70 mm column packed with Pd/C (10 %) in presence of H_2, at 30°C and 20 bars. The performed reaction is confirmed by GC-MS analysis, through comparison

with the NIST.5 library. Hydrogeneted coniferyl alcohol is concentrated by rotary evaporator and dried overnight at 38 °C in vacuum.

B.14 Preparation of calibration curves for quantification of depolymerized L-products

Guaiacol, hydrogenated-coniferyl alcohol and 3-phenoxyphenol are dissolved in three different flasks with $CHCl_3$ in a starting concentration of 5 mg mL^{-1} (mother solutions). The IST solution is prepared by dissolution of 2-methoxy-4-phenylphenol in $CHCl_3$ with a concentration of 5 mg mL^{-1}. Six specimens are prepared for each sample by $CHCl_3$ dilution of the mother solutions to a final concentration of 0.01, 0.05, 0.1, 0.2, 0.5, 1 mg mL^{-1}. The IST solution is added to each flask to reach a final IST-concentration of 1 mg mL^{-1}. Three calibration curves are obtained with a R^2> 0.995.

B.15 Phenols extraction from olive leaves

Olive leaves purchased by Lexa and a mixture 1:1 V/V of a 0.1 M oxalic acid in water and 2-MeTHF were stirred 1h at the considered temperature in a sealed autoclave in a ratio of 50 g/L of solid to liquid. At the end of the reaction the mixture is filtered and the two phases separated by the use of a separation funnel. The MeTHF phase is washed by water and then the solvent is distilled out. The dried residue is recovered in the yields reported in Table 3.6.

B.16 Nitration and derivatization of 2-methoxy-4-propylphenol

2-methoxy-3/5-nitro-4-propylphenyl acetate (S1)

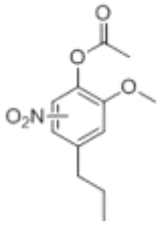

0.4 mL of nitric acid (9.6 mmol) are slowly added into a round bottom flask containing 1.2 mL of acetic anhydride (12.7 mmol) at 0°C. The so prepared mixture

is dropped to a solution of 2-methoxy-4-propylphenol (1.0 ml, 6.2 mmol) in acetic anhydride (20 ml, 0.21 mmol), followed by the addition of a catalytic amount of sulfuric acid (one drop). The reaction runs 1 h at room temperature under continuous stirring and is quenched by addition of ice. The pH is neutralized by KOH pellets and the product extracted by diethyl ether (200 ml). After drying the organic phase over anhydrous sodium sulfate and filtering the mixture, the solvent is removed by rotary evaporation. The product (S1) (567.8 mg, 3.4 mmol, 55 %) is obtained as a mixture of isomers (5-nitro/3-nitro1: 3) (Fig. S4.1)

^{1}H-NMR (400 MHz, Methanol-d4, δ): 7.79 (s, 1H), 7.21 (dd, J1 = 4 Hz, J2 = 8 Hz, 2H), 7.08 (s, 1H), 3.94 (s, 3H), 3.88 (s, 3H), 2.96 (t, J = 8 Hz, 2H), 2.54 (t, J = 8 Hz, 2H), 2.36 (s, 3H), 2.30 (s, 3H), 1.70 (m, 2H), 1.64 (m, 2H), 1.03 (t, J = 8 Hz, 3H), 0.96 (t, J = 8 Hz, 3H).

EI-MS (m/z): Mw calc. for $C_{12}H_{15}NO_5$: 253.25 g mol^{-1}, found: 253.1 g mol^{-1}.

2-methoxy-3/5-nitro-4-propylphenol (S2)

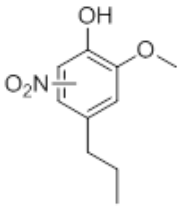

S1 (550 mg, 3.3 mmol) is dissolved in a methanolic solution of KOH (0.3 M, 25 ml) and stirred for 4h at 60 °C. Thus, it is cooled to room temperature and quenched by slow addition of 37 % hydrochloric acid to pH< 6. The product is extracted by diethyl ether (200 ml), the organic phase is dried over anhydrous sodium sulfate and the solvent removed by rotary evaporation. The residue is dried without further purification at 38 °C overnight in a vacuum oven. S2 (669 mg, 3.2 mmol) is achieved in 96 % yield as a mixture of isomers (5-nitro/3-nitro: 2.7).

^{1}H-NMR (400 MHz, Methanol-d4, δ); 7.44 (s, 1H), 6.92 (m, 2H), 6.86 (s, 1H), 3.93 (s, 3H), 3.85 (s, 3H), 2.83 (m, 2H), 2.41 (m, 2H), 1.62 (m, 2H), 1.56 (m, 2H), 0.98 (t, J = 7.4 Hz, 3H), 0.90 (t, J = 7.4 Hz, 3H).

EI-MS (m/z): Mw calc. for $C_{10}H_{13}NO_4$: 211.21g mol^{-1}, found: 211.1 g mol^{-1}.

3/5-amino-2-methoxy-4-propylphenyl acetate (S3)

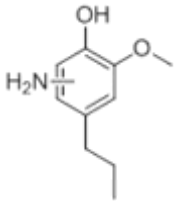

The continuous flow reduction is performed by a H-Cube Pro™ reactor equipped with a hydrogen (generated in situ) and a liquid feed. S2 is dissolved in methanol (0.05 M) and the solution is filtered and pumped with a flow of 0.3 ml/min by a HPLC pump through a 70 mm column packed with Raney-Nickel at 130 °C. H_2 is mixed with the eluent at a pressure of 6 Bar. The product is collected and dried at 38 °C in a vacuum oven overnight, yielding 95 % of S3.

^{1}H NMR (400 MHz, Methanol-d4, δ): 6.58 (s, 1H), 6.30 (s, 1H), 3.73 (s, 3H), 2.40 (m, 2H), 1.57 (m, 2H), 0.95 (t, J = 8 Hz, 3H).

EI-MS (m/z): Mw calc. for $C_{10}H_{15}NO_2$: 181.23, found: 181.1 g mol^{-1}.

B.17 Nitration and derivatization of Lignin

Nitro Lignin (NL)

A catalytic amount of sulfuric acid (three drops) is added to a solution of lignin (2.7 g) in acetic anhydride (20 ml, 0.21 mol). Thus, a solution of nitric acid (6 ml, 0.14 mol) in acetic anhydride (20 ml, 0.21 mol) is slowly added at 0 °C. After stirring the reaction for 3 h at room temperature, ice is added in order to quench it. KOH in pellets are used to neutralize the pH and nitrated lignin (NL) is extracted by 2-methyltetrahydrofuran (400 mL). After drying the organic phase over anhydrous sodium sulfate, the mixture is filtered and concentrated in a vacuum oven, yielding 75 wt % of NL (2.0 g).

Nitro Deacetylated Lignin (NDL)

NL (1.80 g) is dissolved in a 0.3 M solution of potassium hydroxide in MeOH (120 mL). The reaction runs at 60 °C for 4 h and after cooling the flask to room temperature, 37 % hydrochloric acid is slowly added to pH< 6.
The solvent is removed by rotary evaporation and the residue suspended in THF. The THF solution and the solid phase are separated by centrifugation, the organic solvent is removed in vacuum and NDL is collected and dried at 38 °C in a vacuum oven (1.1 g, 60 wt %).

Amino Lignin (AmL)

The continuous flow reduction of NDL to amino lignin (AmL) is performed by the H-Cube Pro™ reactor. NDL is dissolved in methanol (4 mg mL^{-1}), filtered and pumped with a flow-rate of 0.3 ml min^{-1} by a HPLC pump through a 70 mm column packed with Raney-Nickel at 130 °C. H_2 is mixed with the eluent at a pressure of 6 Bar. The sample is collected and dried at 38 °C in a vacuum oven overnight yielding 73 wt % of AmL.

B.18 Ninhydrin test

80 wt % of phenol in alcohol (few drops), pyridine (few drops) and a 5 v/v % of ninhydrin in ethanol (few drops) are added to the samples (AmL, NL, NDL and L) and the mixture is boiled for five minutes. Thus, the vial is cooled at room temperature and the color of the specimens is compared.

B.19 General Procedure for the synthesis of Mesoporous N-doped Carbon

Frozen L, NL and AmL (100 mg) are grinded in an agate mortar cooled in ice. A mixture of $KCl/ZnCl_2$ (500 mg) prepared under argon atmosphere and with a molar ratio of 51:49, is blended with the obtained lignin-powder. The mixture is heated under nitrogen up to 850 °C using the following temperature program: 2 h at 25 °C, heating rate of 3 °C/min to 240 °C, 240 °C for 2 hours and then heating rate of 1 °C/min to 850°C. The final temperature of 850 °C is kept for two hours. After cooling the system at room temperature, the powder is suspended in water, stirred overnight to remove the salts and finally filtered. This procedure is repeated twice. Samples are dried in a vacuum oven at 60 °C overnight.

B.20 Synthesis and purification of L-HBPEA polymers

Adipic acid (2.5 g, 0.017 mol) is added in a round bottom flask to triethanolamine (1.5 g, 0.01 mol) and stirred under vacuum, at 100 °C for 4h. A solution of lignin in THF (10 mL, 0.1 g mL^{-1}) is added to the viscous liquid and the system is stirred at 100 °C for few minutes. Hence THF is removed by rotary evaporator and the still fluid mixture is polymerized in a vacuum oven at 120 °C for 20 h.
Polymer purification: the solid polymer is suspended in THF in a ratio solid/liquid of 20 mg mL^{-1} and refluxed for 72 h. The solution turns light brown for the dissolution of non-reacted L, HBPEA and of small oligomers. After percolation both the phases are dried under vacuum at 40 °C and weighted.

C. SUPPLEMENTARY INFORMATION

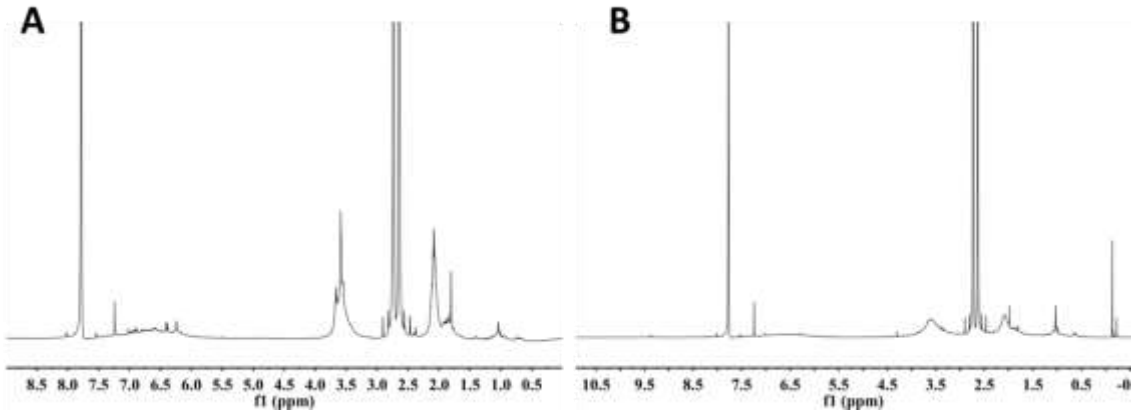

Figure S2.1 *^{1}H-NMR spectra of* **A-***soda lignin (SL),* **B-** *organosolv lignin (OSL) with DMF as internal standard*

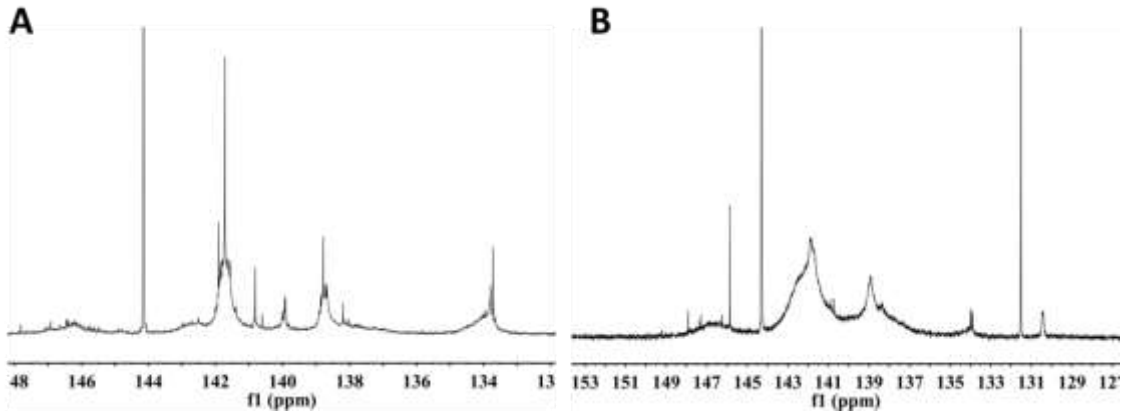

Figure S2.2 *^{31}P-NMR spectra of* **A-***soda lignin (SL),* **B-***organosolv lignin (OSL) with ciclohexanol as IST*

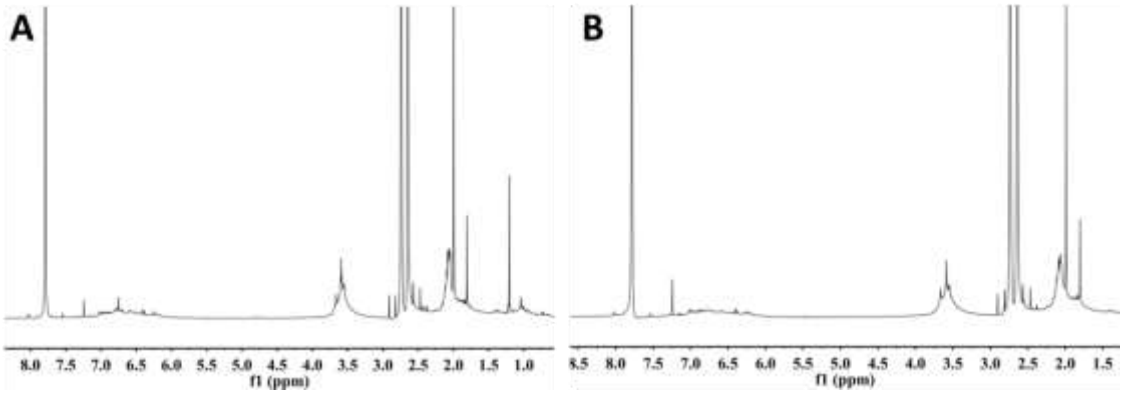

Figure S2.3 *^{1}H-NMR spectra of* **A-** *bamboo lignin (BL)* **B-** *coconut lignin with DMF as IST*

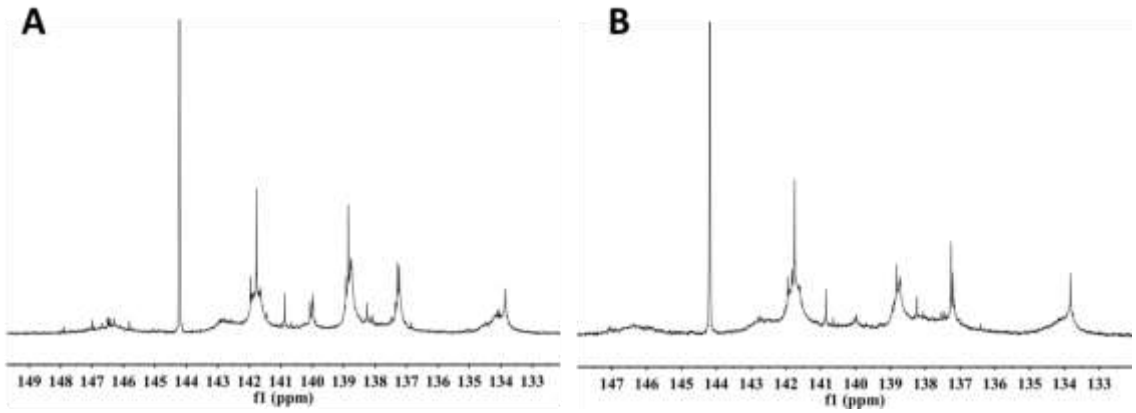

Figure S2.4 *^{31}P-NMR spectra of* **A**-*bamboo lignin (BL),* **B**-*coconut lignin (CL) with ciclohexanol as IST*

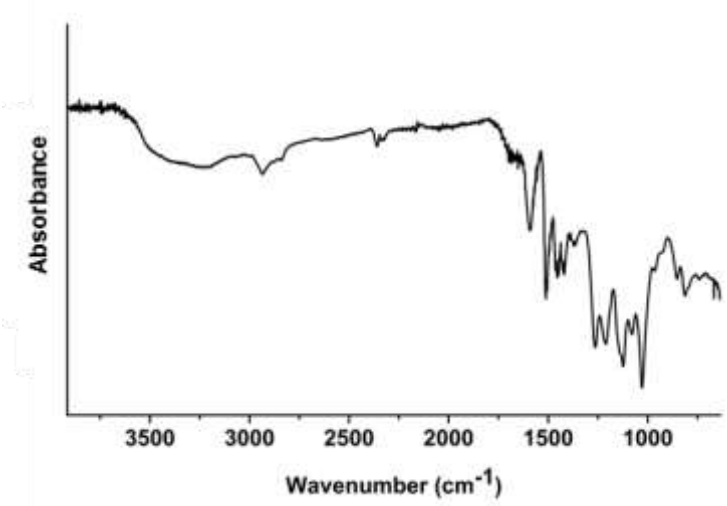

Figure S3.1 *FT-IR of Kraft lignin (KL)*

*Reprinted with the permission from Graglia, M., Pampel, J., Hantke, T., Fellinger, T.-P., Esposito, D., Nitro Lignin-Derived Nitrogen-Doped Carbon as an Efficient and Sustainable Electrocatalyst for Oxygen Reduction. ACS Nano **2016,** 10, 4364-4371. Copyright (2016) American Chemical Society.

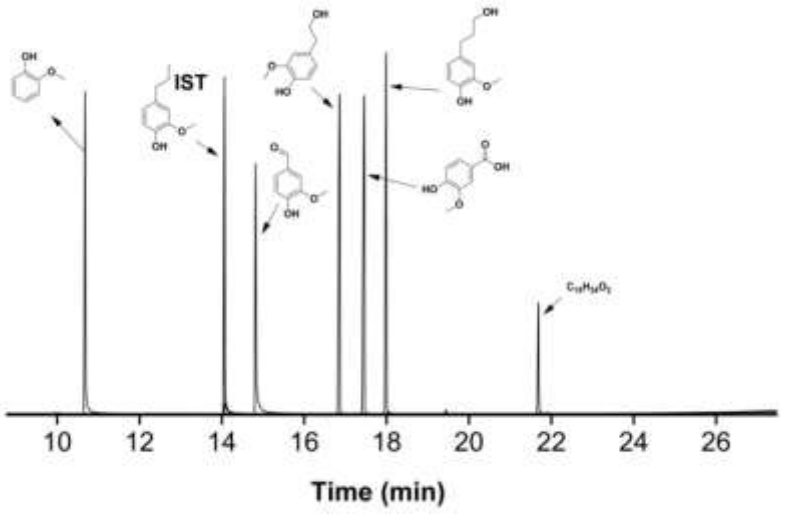

Figure S3.2 *GC-MS chromatogram of the reference standards used for the identification of molecules obtained by lignin-HGL. In order of retention time: guaiacol, 2-methoxy-4-propylphenol (IST) vanillin, homovanillyl alcohol, vanillic acid, hydrogenated conifer alcohol and oleic acid*

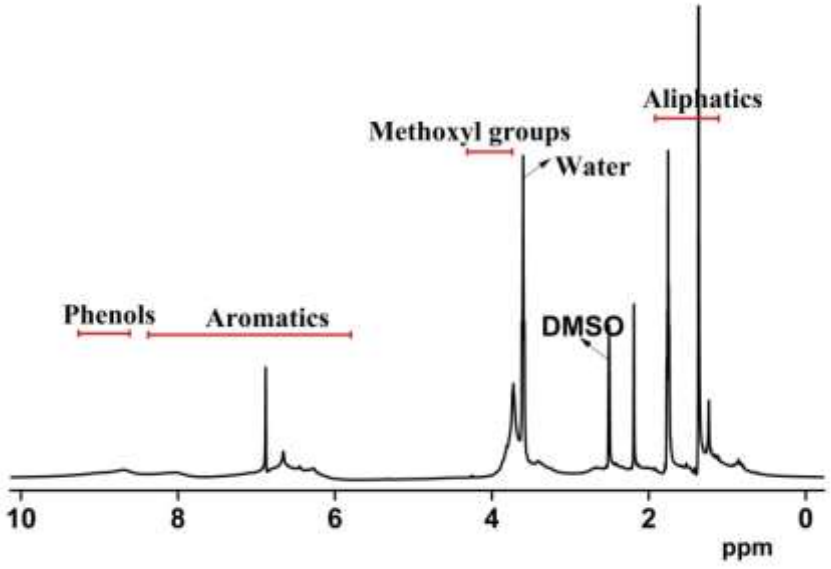

Figure S4.1 *^{1}H-NMR spectrum of alkaline lignin extracted by treating beech wood chips at 220 °C, 15 h in the presence of $Ba(OH)_2$ in water.*[*]

*Reprinted with the permission from Graglia, M., Pampel, J., Hantke, T., Fellinger, T.-P., Esposito, D., Nitro Lignin-Derived Nitrogen-Doped Carbon as an Efficient and Sustainable Electrocatalyst for Oxygen Reduction. ACS Nano **2016,** 10, 4364-4371. Copyright (2016) American Chemical Society.

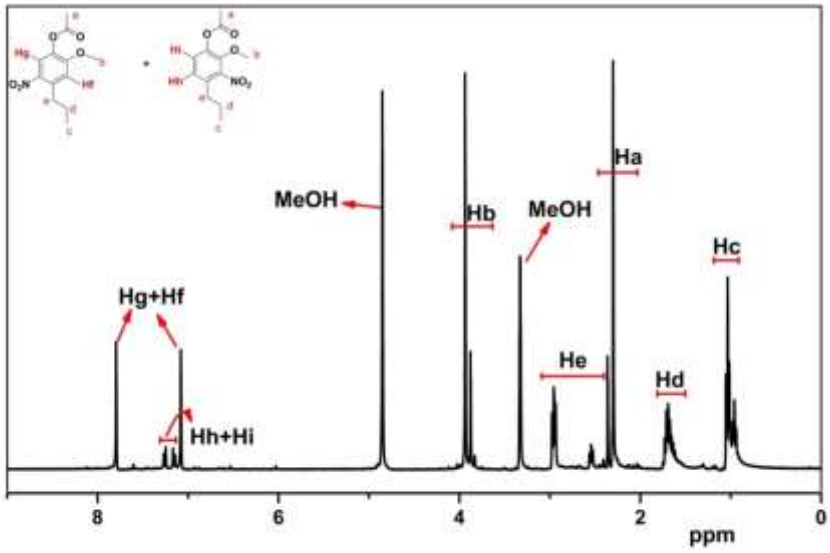

Figure S4.2 *^{1}H-NMR of 2-methoxy-3/5-nitro-4-propylphenyl acetate**

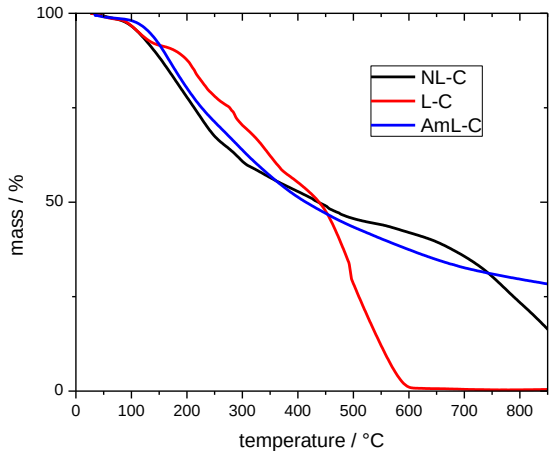

Figure S4.3 *Thermal gravimetric analysis of L-C, NL-C, AmL-C. The analysis is conducted in nitrogen atmosphere. The temperature is increased from 30° to 1000° C with a rate of 2.5 K/min.**

*Reprinted with the permission from Graglia, M., Pampel, J., Hantke, T., Fellinger, T.-P., Esposito, D., Nitro Lignin-Derived Nitrogen-Doped Carbon as an Efficient and Sustainable Electrocatalyst for Oxygen Reduction. ACS Nano **2016,** 10, 4364-4371. Copyright (2016) American Chemical Society.

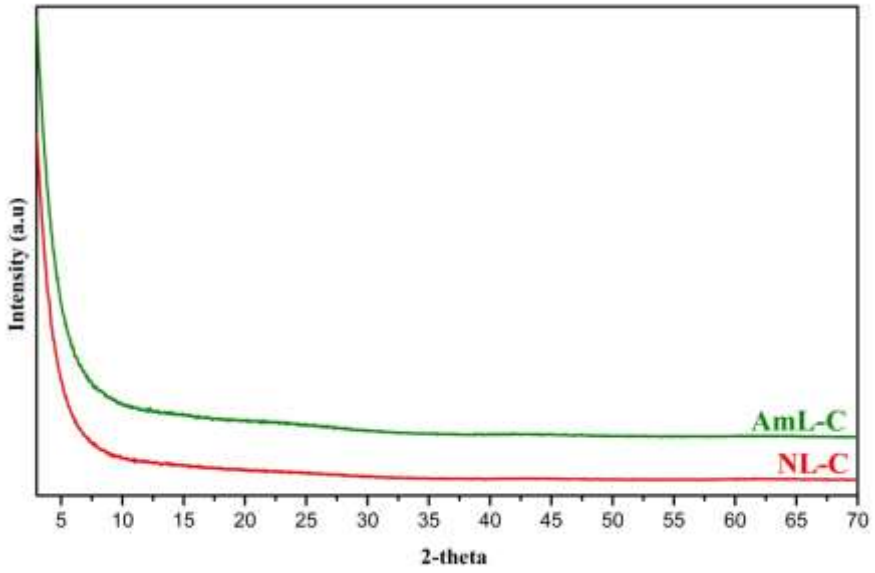

Figure S4.4 *XRD Pattern of Nitro-Lignin (NL-C) and Amino-Lignin (AmL) after carbonization*[103]*

Table S2.1 *FT-IR adsorption bands of lignins*

Absorption	Band
3450-3400	OH stretching
2940-2820	OH stretching
1715-1710	C=O stretching (nonconjugated)
1675-1660	C=O stretching (conjugated to aromatic ring))
1605-1600/ 1515-1505	Aromatic ring vibrations
1470-1460	C-H deformations, asymmetric
1430-1425	Aromatic ring vibrations
1370-1365	C-H deformations, symmetric
1330-1325	Syringyl ring breathing
1270-1275	Guaiacil ring breathing
1085-1030	C-H and C-O deformations

*Reprinted with the permission from Graglia, M., Pampel, J., Hantke, T., Fellinger, T.-P., Esposito, D., Nitro Lignin-Derived Nitrogen-Doped Carbon as an Efficient and Sustainable Electrocatalyst for Oxygen Reduction. ACS Nano **2016,** 10, 4364-4371. Copyright (2016) American Chemical Society.

Table S3.1 *Solubility of Kraft lignin. Lignin is stirred in the solvent, in a ratio of 2 mg mL^{-1}. After 48 h the mixture is filtrated, the liquid phase is concentrated and the residue weighted.*

Solvent	Concentration (mg mL^{-1})
MeOH	1.4
H_2O	0.23
EtOH	0.83
THF	1.4

Table S4.1 *Elemental composition (derived by combustion analyses) and N_2-physisorption data of the samples prepared with eutectic NaCl/$ZnCl_2$-mixture*

Sample	N-content (wt %)	C-content (wt %)	S_{BET} ($m^2 g^{-1}$)	V_{tot} ($cm^3 g^{-1}$)	Total yield (wt %)	Carbon yield (wt %)
AmL-C	4.4	80.8	1240	1.00	15.6	19.0
NDL-C	4.3	73.5	1640	0.99	13.6	15.1
NL-C	4.0	77.1	1610	1.00	10.0	11.6

Table S5.1 *DSC and TGA data of SL-, BL-, CL-HBPEA with a 20 wt % of L , pre and post THF purification (gel-phase)*

Sample	Tg, °C (DSC)		Residual mass (wt %) at 1000°C	
	L-HBPEA	Purified L-HBPEA	L-HBPEA	Purified L-HBPEA
SL-HBPEA 20	- 9.1	-16.3	12.1	9.9
BL-HBPEA 20	- 8.6	-17.7	11.4	4.8
CL-HBPEA 20	- 8.5	-17.4	13.6	13.7

*Reprinted with the permission from Graglia, M., Pampel, J., Hantke, T., Fellinger, T.-P., Esposito, D., Nitro Lignin-Derived Nitrogen-Doped Carbon as an Efficient and Sustainable Electrocatalyst for Oxygen Reduction. ACS Nano **2016,** 10, 4364-4371. Copyright (2016) American Chemical Society.

D. ABBREVIATIONS

LgC	Lignocellulose
C	Cellulose
HmC	Hemicellulose
L	Lignin
LCCs	Lignin-carbohydrate complexes
KL	Kraft lignin
ILs	Ionic liquids
PU	Polyurethane
PEG	Polyethylenglycol
HBPEA	Hyperbranched poly(ester-amine)
NDC	Nitrogen-doped carbon
MC	Mesoporous carbon
ORR	Oxygen reduction reaction
PF	Phenol formaldehyde
HGL	Hydrogenolysis
HDO	Hydrodeoxygenation
NIST	National Institute of Standards and Technology
RT	Retention time
NMR	Nuclear magnetic resonance
Mw	Mass average molar mass
Mn	Number average molar mass
D	Dispersity
GPC	gel permeation chromatography
NMP	Methyl-2-pyrrolidone
THF	Tetrahydrofuran
MeOH	Methanol
EtOH	Ethanol
2-MeTHF	methyltetrahydrofuran

DMF	Dimethylformamide
DMSO	Dimethylsulfoxid
$CHCl_3$	Chloroform
$CDCl_3$	Deuterated chloroform
OS	Organosolv
BET	Brunauer-Emmett-Teller
TGA	Thermogravimetric analysis
FT-IR	Fourier Transform Infrared Spectroscopy
AL	Alkali lignin
OSL	Organosolv lignin
BL	Bamboo lignin
CL	Coconut lignin
AIL	Acid insoluble lignin
ASL	Acid soluble lignin
TMDP	2–chloro–4,4,5,5–tetramethyl–1,3,2–dioxaphospholane
DSC	Differential scanning calorimetry
T_{md}	Temperature of maximum decomposition
Tg	Glass temperature
BSTFA	N,O-Bis(trimethylsilyl)trifluoroacetamide

E. PUBLICATIONS

Graglia, M., Kanna, N., Esposito, D. Lignin Refinery: *Towards the Preparation of Renewable Aromatic Building Blocks* ChemBioEng Rev. **2015**,2,37710.1002/cben.20150001

Graglia, M., Pampel, J., Hantke, T., Fellinger, T.P., Esposito, D. *Nitro Lignin-Derived Nitrogen-Doped Carbon as an Efficient and Sustainable Electrocatalyst for Oxygen Reduction.* A*CS Nano*, **2016,** DOI**:** 10.1021/acsnano.5b08040

Molinari, V.; Clavel, G.; Graglia, M.; Antonietti, M.; Esposito, D., *Mild continuous hydrogenolysis of Kraft lignin over titanium nitride-nickel catalyst*, ACS catalysis, **2016**, DOI: 10.1021/acscatal.5b01926

F. ACKNOWLEDGEMENTS

I would like to thank several people, who played an important role for me during this period at the Max-Planck Institute.
First of all I thank Prof. Antonietti who offered me the opportunity to discover the pleasure of making science.
I thank the Max Planck society for the financial resources that it invests in the scientific education and growth of young scientists.
I thank Prof. Strauch, Prof. Taubert, Prof. Tauer, Prof. Schlaad and Dr. Rinaldi for the time they dedicate to review my thesis and discuss my work.
I would like to thank Dr. Esposito because he directed my projects guiding me through my scientific growth and because he always reminded me that “coraggio, coraggio, dopo aprile vien sempre maggio”.
I would also like to thank all the people that contributed to the projects reported in this work, Jonas, Dr. Fellinger, Tina, Dr. Molinari, Dr. Eder and Nils Horbelt.
Now I would like to thank a lot of other special people. It is known that office colleagues are very important for working with a good mood, but I was lucky because they are also friends. So many thanks to Roberto, Binshen, Narasimharao and especially to Vale and Max, we worked, ate, did sport, had discussions, scientific and personal, we were stressed and we enjoyed moments together.
Thanks to Gianpaolo and again Vale for our “alternative German class” and for the support. Thank to Elliot, Afro, Max, Vale and Jonas for the time they dedicate to help me with the writing of the thesis. A huge thanks to Irina because she was always available and nice. A special acknowledgment is for Sylvia, Marlies, Heike and Olaf, their work is essential for all the scientific projects.
Thanks to the running crew, Max, Menny, Karoline, and Tom, it was such a nice time.
Thanks to all the people who were around me, because they created a nice atmosphere. Therefore, many thanks to Mark, Jonas, Martina, Martin, Llorenz, Steffen and a lot of others.
It will not be enough just to say thanks to Afro and Max, friends, colleagues and Berliner family.
E ovviamente non dimentico chi ha sempre creduto in me incoraggiandomi ed insegnandomi con l´esempio, che ogni risultato richiede grande impegno. Perciò grazie alla mia mamma, al mio papà, a mio fratello, alla nonna, ad Ale, Giuse ed a tutta la mia famiglia.
And thanks to Axel, because he always encourages and trusts me.

DECLARATION

Die vorliegende Dissertation entstand in dem Zeitraum zwischen Juni 2014 und September 2016 am Max-Planck-Institut für Kolloid- und Grenzflächenforschung, unter der Betreuung von Prof. Dr. Markus Antonietti.
Hiermit erkläre ich, dass die vorliegende Arbeit selbstständig angefertigt und keine anderen als die angegebenen Hilfsmittel und Quellen verwendet wurden.

Micaela Graglia
Potsdam, 19-09-2016

REFERENCES

1. Keim, W., Fossil Feedstocks–What Comes After? In Bertau, M., Offermanns, H., Plass, L., Schmidt, F., Wernicke, H.-J., eds.Methanol: The Basic Chemical and Energy Feedstock of the Future: Asinger's Vision Today, Springer Berlin Heidelberg: Berlin, Heidelberg, 2014; pp 23-37.
2. Vakkilainen, E., Kaparinen, K., Heinimö, J., Large industrial users of energy biomass. IEA Bioenergy Task 40 **2013**.
3. (BGR), F.I.f.G.a.N.R., Reserves, Resources and Availability of Energy Resources 2010. **2010**.
4. OPEC schare of world crude oil reserves 2014. http://www.opec.org/opec_web/en/data_graphs/330.htm.
5. Jong, E.J., Higson, A., Walsh, P., Wellisch, M., Value Added Products from Biorefineries. IEA Bioeenergy **2015**.
6. What is BIOMASS? biomassenergycentre.org.uk.
7. Hosler, D., Burkett, S.L., Tarkanian, M.J., Prehistoric Polymers: Rubber Processing in Ancient Mesoamerica. Science **1999,** 284, 1988-1991.
8. Worden, E.C., Nitrocellulose Industry: a Compendium of the History, Chemistry, Manufacture, Commercial Application, and Analysis of Nitrates, Acetates, and Xanthates of Cellulose as Applied to the Peaceful Arts; with a Chapter on Gun-Cotton, Smokeless Powder, and Explosive Cellulose Nitrates. Nature **1911,** 88, 69-70.
9. Neal, A.L.A.a.M.A., Applications and societal benefits of plastics. Philosophical transactions of the royal society **2009,** 1977-1984.
10. Cherubini, F., The biorefinery concept: Using biomass instead of oil for producing energy and chemicals. Energy Conversion and Management **2010,** 51, 1412-1421.
11. Esposito, D., Antonietti, M., Redefining biorefinery: the search for unconventional building blocks for materials. Chem Soc Rev **2015,** 44, 5821-35.
12. Strassberger, Z., Tanase, S., Rothenberg, G., The pros and cons of lignin valorisation in an integrated biorefinery. RSC Adv. **2014,** 4, 25310-25318.
13. Heredia, A., Jimenez, A., Guillen, R., Composition of plant cell walls. Zeitschrift fur Lebensmittel-Untersuchung und -Forschung **1995,** 200, 24-31.
14. Espinoza-Acosta, J.L., Torres-Chávez, P.I., Carvajal-Millán, E., Ramírez-Wong, B., Bello-Pérez, L.A., Montaño-Leyva, B., Ionic Liquids and Organic Solvents for Recovering Lignin from Lignocellulosic Biomass. **2014**.
15. Calvo-Flores, F.G., Dobado, J.A., Lignin as renewable raw material. ChemSusChem **2010,** 3, 1227-35.
16. Brandt, A., Grasvik, J., Hallett, J.P., Welton, T., Deconstruction of lignocellulosic biomass with ionic liquids. Green. Chem. **2013,** 15, 550-583.
17. Keegstra, K., Plant Cell Walls. Plant Physiology **2010,** 154, 483-486.
18. Alberts B, J.A., Lewis J, et al. , The Plant Cell Wall. Molecular Biology of the Cell. **2002,** http://www.ncbi.nlm.nih.gov/books/NBK26928/
19. Brett, C., Waldron, K., Cell-wall formation. Physiology and Biochemistry of Plant Cell Walls, Springer Netherlands: Dordrecht, 1990; pp 58-88.
20. SI., F., Lignin in materials. Appl Polym Symp **1975,** 1, 247-257.
21. Zakzeski, J., Bruijnincx, P.C.A., Jongerius, A.L., Weckhuysen, B.M., The Catalytic Valorization of Lignin for the Production of Renewable Chemicals. Chemical Reviews **2010,** 110, 3552-3599.
22. Li, X., Chapple, C., Understanding Lignification: Challenges Beyond Monolignol Biosynthesis. Plant Physiology **2010,** 154, 449-452.

23. Calvo-Flores, F.G., Dobado, J.A., Isac-García, J., Martín-MartíNez, F.J., Structure and Physicochemical Properties. Lignin and Lignans as Renewable Raw Materials, John Wiley & Sons, Ltd: 2015; pp 9-48.
24. Thakur, V.K., Thakur, M.K., Raghavan, P., Kessler, M.R., Progress in Green Polymer Composites from Lignin for Multifunctional Applications: A Review. ACS Sustainable Chemistry & Engineering **2014,** 2, 1072-1092.
25. Ralph, J., Helm, R.F., Quideau, S., Hatfield, R.D., Lignin-feruloyl ester cross-links in grasses. Part 1. Incorporation of feruloyl esters into coniferyl alcohol dehydrogenation polymers. Journal of the Chemical Society, Perkin Transactions 1 **1992,** 2961-2969.
26. Lawoko, M., Henriksson, G., Gellerstedt, G., Characterisation of lignin-carbohydrate complexes (LCCs) of spruce wood (Picea abies L.) isolated with two methods. Holzforschung, 2006; Vol. 60, p 156.
27. Knaggs, A.R., The biosynthesis of shikimate metabolites. Natural Product Reports **2003,** 20, 119-136.
28. Humphreys, J.M., Chapple, C., Rewriting the lignin roadmap. Current Opinion in Plant Biology **2002,** 5, 224-229.
29. Sibout, R., Höfte, H., Plant Cell Biology: The ABC of Monolignol Transport. Current Biology **2012,** 22, R533-R535.
30. Calvo-Flores, F.G., Dobado, J.A., Isac-García, J., Martín-MartíNez, F.J., Biosynthesis of Lignin. Lignin and Lignans as Renewable Raw Materials, John Wiley & Sons, Ltd: 2015; pp 75-112.
31. Laurichesse, S., Avérous, L., Chemical modification of lignins: Towards biobased polymers. Progress in Polymer Science **2014,** 39, 1266-1290.
32. Graglia, M., Kanna, N., Esposito, D., Lignin Refinery: Towards the Preparation of Renewable Aromatic Building Blocks. ChemBioEng Reviews **2015,** 2, 377-392.
33. Doherty, W.O.S., Mousavioun, P., Fellows, C.M., Value-adding to cellulosic ethanol: Lignin polymers. Industrial Crops and Products **2011,** 33, 259-276.
34. Perez-Cantu, L., Schreiber, A., Schütt, F., Saake, B., Kirsch, C., Smirnova, I., Comparison of pretreatment methods for rye straw in the second generation biorefinery: Effect on cellulose, hemicellulose and lignin recovery. Bioresource Technology **2013,** 142, 428-435.
35. Roberts, V.M., Stein, V., Reiner, T., Lemonidou , A., Li, X., Lercher, J.A., Towards Quantitative Catalytic Lignin Depolymerization. Chem. - Eur. J. **2011,** 17, 5939-5948.
36. Li, J., Gellerstedt, G., Improved lignin properties and reactivity by modifications in the autohydrolysis process of aspen wood. Industrial Crops and Products **2008,** 27, 175-181.
37. da Costa Sousa, L., Chundawat, S.P.S., Balan, V., Dale, B.E., 'Cradle-to-grave' assessment of existing lignocellulose pretreatment technologies. Current Opinion in Biotechnology **2009,** 20, 339-347.
38. Calvo-Flores, F.G., Dobado, J.A., Isac-García, J., Martín-MartíNez, F.J., Isolation of Lignins. Lignin and Lignans as Renewable Raw Materials, John Wiley & Sons, Ltd: 2015; pp 113-144.
39. Gratzl, J.S., Chen, C.-L., Chemistry of Pulping: Lignin Reactions. Lignin: Historical, Biological, and Materials Perspectives, American Chemical Society: 1999; Vol. 742, pp 392-421.
40. S.Y.Lin , C.W.D., Methods in Lignin Chemistry. Springer-Verlag Berlin Heildeberg, Springer Series in Wood Science **1992,** 75-76.
41. Vishtal, A.G., Kraslawski, A., CHALLENGES IN INDUSTRIAL APPLICATIONS OF TECHNICAL LIGNINS. BioResources **2011**.
42. Chakar, F.S., Ragauskas, A.J., Review of current and future softwood kraft lignin process chemistry. Industrial Crops and Products **2004,** 20, 131-141.

43. Ragauskas, A.J., Beckham, G.T., Biddy, M.J., Chandra, R., Chen, F., Davis, M.F., Davison, B.H., Dixon, R.A., Gilna, P., Keller, M., Langan, P., Naskar, A.K., Saddler, J.N., Tschaplinski, T.J., Tuskan, G.A., Wyman, C.E., Lignin Valorization: Improving Lignin Processing in the Biorefinery. Science **2014,** 344.
44. Sánchez, C., Egüés, I., García, A., Llano-Ponte, R., Labidi, J., Lactic acid production by alkaline hydrothermal treatment of corn cobs. Chemical Engineering Journal **2012,** 181–182, 655-660.
45. Esposito, D., Antonietti, M., Chemical Conversion of Sugars to Lactic Acid by Alkaline Hydrothermal Processes. ChemSusChem **2013,** 6, 989-992.
46. Graglia, M., Pampel, J., Hantke, T., Fellinger, T.-P., Esposito, D., Nitro Lignin-Derived Nitrogen-Doped Carbon as an Efficient and Sustainable Electrocatalyst for Oxygen Reduction. ACS Nano **2016,** 10, 4364-4371.
47. Wörmeyer, K., Ingram, T., Saake, B., Brunner, G., Smirnova, I., Comparison of different pretreatment methods for lignocellulosic materials. Part II: Influence of pretreatment on the properties of rye straw lignin. Bioresource Technology **2011,** 102, 4157-4164.
48. Haghighi Mood, S., Hossein Golfeshan, A., Tabatabaei, M., Salehi Jouzani, G., Najafi, G.H., Gholami, M., Ardjmand, M., Lignocellulosic biomass to bioethanol, a comprehensive review with a focus on pretreatment. Renewable and Sustainable Energy Reviews **2013,** 27, 77-93.
49. Gandini, A., The irruption of polymers from renewable resources on the scene of macromolecular science and technology. Green Chemistry **2011,** 13, 1061-1083.
50. Shimada, K., Hosoya, S., Ikeda, T., Condensation Reactions of Softwood and Hardwood Lignin Model Compounds Under Organic Acid Cooking Conditions. Journal of Wood Chemistry and Technology **1997,** 17, 57-72.
51. Li, J., Henriksson, G., Gellerstedt, G., Lignin depolymerization/repolymerization and its critical role for delignification of aspen wood by steam explosion. Bioresource Technology **2007,** 98, 3061-3068.
52. Erdocia, X., Prado, R., Corcuera, M.Á., Labidi, J., Effect of different organosolv treatments on the structure and properties of olive tree pruning lignin. Journal of Industrial and Engineering Chemistry **2014,** 20, 1103-1108.
53. Constant, S., Basset, C., Dumas, C., Di Renzo, F., Robitzer, M., Barakat, A., Quignard, F., Reactive organosolv lignin extraction from wheat straw: Influence of Lewis acid catalysts on structural and chemical properties of lignins. Industrial Crops and Products **2015,** 65, 180-189.
54. Grande, P.M., Viell, J., Theyssen, N., Marquardt, W., Dominguez de Maria, P., Leitner, W., Fractionation of lignocellulosic biomass using the OrganoCat process. Green Chemistry **2015,** 17, 3533-3539.
55. Luterbacher, J.S., Rand, J.M., Alonso, D.M., Han, J., Youngquist, J.T., Maravelias, C.T., Pfleger, B.F., Dumesic, J.A., Nonenzymatic Sugar Production from Biomass Using Biomass-Derived γ-Valerolactone. Science **2014,** 343, 277-280.
56. Pinkert, A., Goeke, D.F., Marsh, K.N., Pang, S., Extracting wood lignin without dissolving or degrading cellulose: investigations on the use of food additive-derived ionic liquids. Green Chemistry **2011,** 13, 3124-3136.
57. Achinivu, E.C., Howard, R.M., Li, G., Gracz, H., Henderson, W.A., Lignin extraction from biomass with protic ionic liquids. Green Chemistry **2014,** 16, 1114-1119.
58. Nitsos, C.K., Matis, K.A., Triantafyllidis, K.S., Optimization of Hydrothermal Pretreatment of Lignocellulosic Biomass in the Bioethanol Production Process. ChemSusChem **2013,** 6, 110-122.

59. Sun, S.-L., Wen, J.-L., Ma, M.-G., Sun, R.-C., Structural Elucidation of Sorghum Lignins from an Integrated Biorefinery Process Based on Hydrothermal and Alkaline Treatments. Journal of agricultural and food chemistry **2014,** 62, 8120-8128.
60. Azadi, P., Inderwildi, O.R., Farnood, R., King, D.A., Liquid fuels, hydrogen and chemicals from lignin: A critical review. Renewable Sustainable Energy Rev. **2013,** 21, 506-523.
61. Balat, H., Kırtay, E., Hydrogen from biomass – Present scenario and future prospects. International Journal of Hydrogen Energy **2010,** 35, 7416-7426.
62. Strassberger, Z., Tanase, S., Rothenberg, G., The pros and cons of lignin valorisation in an integrated biorefinery. RSC Advances **2014,** 4, 25310-25318.
63. Calvo-Flores, F.G., Dobado, J.A., Isac-García, J., Martín-MartíNez, F.J., Applications of Modified and Unmodified Lignins. Lignin and Lignans as Renewable Raw Materials, John Wiley & Sons, Ltd: 2015; pp 247-288.
64. Laus, R., Costa, T.G., Szpoganicz, B., Fávere, V.T., Adsorption and desorption of Cu(II), Cd(II) and Pb(II) ions using chitosan crosslinked with epichlorohydrin-triphosphate as the adsorbent. Journal of Hazardous Materials **2010,** 183, 233-241.
65. Finch, C.A., Advanced wood adhesives technology. A. Pizzi. Marcel dekker, New York, Basel, 1994. pp. viii + 289, price US$115.00. ISBN 0-8247-9266-1. Polymer International **1996,** 39, 78-78.
66. Thanh Binh, N.T., Luong, N.D., Kim, D.O., Lee, S.H., Kim, B.J., Lee, Y.S., Nam, J.-D., Synthesis of Lignin-Based Thermoplastic Copolyester Using Kraft Lignin as a Macromonomer. Composite Interfaces **2009,** 16, 923-935.
67. Sivasankarapillai, G., McDonald, A.G., Synthesis and properties of lignin-highly branched poly (ester-amine) polymeric systems. Biomass and Bioenergy **2011,** 35, 919-931.
68. Chahar, S., Dastidar, M.G., Choudhary, V., Sharma, D.K., Synthesis and characterisation of polyurethanes derived from waste black liquor lignin. Journal of Adhesion Science and Technology **2004,** 18, 169-179.
69. E. S. Stevens, A.K., G. M. GlE. S. Stevens, A. Klamczynski, G. M. Glenn Starch-lignin foams. eXPRESS Polymer Letters **2010,** 4, 311-320.
70. Hatakeyama, H., Nakayachi, A., Hatakeyama, T., Thermal and mechanical properties of polyurethane-based geocomposites derived from lignin and molasses. Composites Part A: Applied Science and Manufacturing **2005,** 36, 698-704.
71. Nägele, H., Pfitzer, J., Nägele, E., Inone, E.R., Eisenreich, N., Eckl, W., Eyerer, P., Arboform® - A Thermoplastic, Processable Material from Lignin and Natural Fibers. In Hu, T.Q., ed.Chemical Modification, Properties, and Usage of Lignin, Springer US: Boston, MA, 2002; pp 101-119.
72. Ciolacu, D., Oprea, A.M., Anghel, N., Cazacu, G., Cazacu, M., New cellulose–lignin hydrogels and their application in controlled release of polyphenols. Materials Science and Engineering: C **2012,** 32, 452-463.
73. Fang, R., Cheng, X., Xu, X., Synthesis of lignin-base cationic flocculant and its application in removing anionic azo-dyes from simulated wastewater. Bioresource Technology **2010,** 101, 7323-7329.
74. Dos Santos, D.A., Rudnitskaya, A., Evtuguin, D.V., Modified kraft lignin for bioremediation applications. Journal of environmental science and health. Part A, Toxic/hazardous substances & environmental engineering **2012,** 47, 298-307.
75. Katsumata, K., Meshitsuka, G., Modified Kraft Lignin and Its Use for Soil Preservation. In Hu, T.Q., ed.Chemical Modification, Properties, and Usage of Lignin, Springer US: Boston, MA, 2002; pp 151-165.

76. Gonzalez-Serrano, E., Cordero, T., Rodriguez-Mirasol, J., Cotoruelo, L., Rodriguez, J.J., Removal of water pollutants with activated carbons prepared from H3PO4 activation of lignin from kraft black liquors. Water Research **2004,** 38, 3043-3050.
77. Hu, L., Pan, H., Zhou, Y., Zhang, M., METHODS TO IMPROVE LIGNIN'S REACTIVITY AS A PHENOL SUBSTITUTE AND AS REPLACEMENT FOR OTHER PHENOLIC COMPOUNDS: A BRIEF REVIEW. **2011**.
78. Malutan, T., Nicu, R., Popa, V.I., CONTRIBUTION TO THE STUDY OF HYDROXYMETYLATION REACTION OF ALKALI LIGNIN. **2007**.
79. Sturgeon, M.R., O'Brien, M.H., Ciesielski, P.N., Katahira, R., Kruger, J.S., Chmely, S.C., Hamlin, J., Lawrence, K., Hunsinger, G.B., Foust, T.D., Baldwin, R.M., Biddy, M.J., Beckham, G.T., Lignin depolymerisation by nickel supported layered-double hydroxide catalysts. Green Chemistry **2014,** 16, 824-835.
80. Calvo-Flores, F.G., Dobado, J.A., Isac-García, J., Martín-MartíNez, F.J., High-Value Chemical Products. Lignin and Lignans as Renewable Raw Materials, John Wiley & Sons, Ltd: 2015; pp 289-312.
81. Gasser, C., Hommes, G., Schäffer, A., Corvini, P.X., Multi-catalysis reactions: new prospects and challenges of biotechnology to valorize lignin. Appl. Microbiol. Biotechnol. **2012,** 95, 1115-1134.
82. Yan, N., Zhao, C., Dyson, P.J., Wang, C., Liu, L.-t., Kou, Y., Selective Degradation of Wood Lignin over Noble-Metal Catalysts in a Two-Step Process. ChemSusChem **2008,** 1, 626-629.
83. Van den Bosch, S., Schutyser, W., Koelewijn, S.F., Renders, T., Courtin, C.M., Sels, B.F., Tuning the lignin oil OH-content with Ru and Pd catalysts during lignin hydrogenolysis on birch wood. Chemical Communications **2015,** 51, 13158-13161.
84. Liu, F., Liu, Q., Wang, A., Zhang, T., Direct Catalytic Hydrogenolysis of Kraft Lignin to Phenols in Choline-Derived Ionic Liquids. ACS Sustainable Chemistry & Engineering **2016,** 4, 3850-3856.
85. Loubinoux, B., Heitz, M., Coudert, G., Guillaumet, G., Hydrogenolysis of lignins : nickel boride catalyst. Tetrahedron Letters **1980,** 21, 4991-4994.
86. Meier, D., Ante, R., Faix, O., Catalytic hydropyrolysis of lignin: Influence of reaction conditions on the formation and composition of liquid products. Bioresource Technology **1992,** 40, 171-177.
87. Wang, X., Rinaldi, R., A Route for Lignin and Bio-Oil Conversion: Dehydroxylation of Phenols into Arenes by Catalytic Tandem Reactions. Angewandte Chemie International Edition **2013,** 52, 11499-11503.
88. Molinari, V., Giordano, C., Antonietti, M., Esposito, D., Titanium Nitride-Nickel Nanocomposite as Heterogeneous Catalyst for the Hydrogenolysis of Aryl Ethers. Journal of the American Chemical Society **2014,** 136, 1758-1761.
89. Zhang, J., Teo, J., Chen, X., Asakura, H., Tanaka, T., Teramura, K., Yan, N., A Series of NiM (M = Ru, Rh, and Pd) Bimetallic Catalysts for Effective Lignin Hydrogenolysis in Water. ACS Catalysis **2014,** 4, 1574-1583.
90. Fargues, C., Mathias, Á., Rodrigues, A., Kinetics of Vanillin Production from Kraft Lignin Oxidation. Industrial & Engineering Chemistry Research **1996,** 35, 28-36.
91. Cui, F., Dolphin, D., Metallophthalocyanines as possible lignin peroxidase models. Bioorganic & Medicinal Chemistry **1995,** 3, 471-477.
92. Sales, F.G., Maranhão, L.C.A., Filho, N.M.L., Abreu, C.A.M., Experimental evaluation and continuous catalytic process for fine aldehyde production from lignin. Chemical Engineering Science **2007,** 62, 5386-5391.

93. Ji, N., Wang, X., Weidenthaler, C., Spliethoff, B., Rinaldi, R., Iron(II) Disulfides as Precursors of Highly Selective Catalysts for Hydrodeoxygenation of Dibenzyl Ether into Toluene. ChemCatChem **2015,** 7, 960-966.
94. Zhao, C., Kou, Y., Lemonidou, A.A., Li, X., Lercher, J.A., Hydrodeoxygenation of bio-derived phenols to hydrocarbons using RANEY[registered sign] Ni and Nafion/SiO2 catalysts. Chemical Communications **2010,** 46, 412-414.
95. Mu, W., Ben, H., Du, X., Zhang, X., Hu, F., Liu, W., Ragauskas, A.J., Deng, Y., Noble metal catalyzed aqueous phase hydrogenation and hydrodeoxygenation of lignin-derived pyrolysis oil and related model compounds. Bioresource Technology **2014,** 173, 6-10.
96. Saidi, M., Samimi, F., Karimipourfard, D., Nimmanwudipong, T., Gates, B.C., Rahimpour, M.R., Upgrading of lignin-derived bio-oils by catalytic hydrodeoxygenation. Energy & Environmental Science **2014,** 7, 103-129.
97. Bu, Q., Lei, H., Zacher, A.H., Wang, L., Ren, S., Liang, J., Wei, Y., Liu, Y., Tang, J., Zhang, Q., Ruan, R., A review of catalytic hydrodeoxygenation of lignin-derived phenols from biomass pyrolysis. Bioresource Technology **2012,** 124, 470-477.
98. Dence, C.W., The Determination of Lignin. In Lin, S.Y., Dence, C.W., eds.Methods in Lignin Chemistry, Springer Berlin Heidelberg: Berlin, Heidelberg, 1992; pp 33-61.
99. Lupoi, J.S., Singh, S., Parthasarathi, R., Simmons, B.A., Henry, R.J., Recent innovations in analytical methods for the qualitative and quantitative assessment of lignin. Renewable and Sustainable Energy Reviews **2015,** 49, 871-906.
100. DANIEL J. NICHOLSON, A.T.L.a.R.C.F., A THREE-STAGE KLASON METHOD FOR MORE ACCURATE DETERMINATIONS OF HARDWOOD LIGNIN CONTENT. Cellulose Chem. Technol. **2014,** 48, 53-59.
101. A. Sluiter, B.H., R. Ruiz, C. Scarlata, J. Sluiter, D. Templeton, and D. Crocker, Determination of Structural Carbohydrates and Lignin in Biomass: Laboratory Analytical Procedure (LAP) NREL, national renewable energy laboratory **2012**.
102. A. Sluiter, R.R., C. Scarlata, J. Sluiter, and D. Templeton, Determination of Extractives in Biomass: Laboratory Analytical Procedure (LAP). NREL, national renewable energy laboratory **2005**.
103. Calvo-Flores, F.G., Dobado, J.A., Isac-García, J., Martín-MartíNez, F.J., Functional and Spectroscopic Characterization of Lignins. Lignin and Lignans as Renewable Raw Materials, John Wiley & Sons, Ltd: 2015; pp 145-188.
104. Gellerstedt, G., Gel Permeation Chromatography. In Lin, S.Y., Dence, C.W., eds.Methods in Lignin Chemistry, Springer Berlin Heidelberg: Berlin, Heidelberg, 1992; pp 487-497.
105. Ringena, O., Lebioda, S., Lehnen, R., Saake, B., Size-exclusion chromatography of technical lignins in dimethyl sulfoxide/water and dimethylacetamide. Journal of Chromatography A **2006,** 1102, 154-163.
106. Xu, F., Sun, J.-X., Sun, R., Fowler, P., Baird, M.S., Comparative study of organosolv lignins from wheat straw. Industrial Crops and Products **2006,** 23, 180-193.
107. VASILE, M.B.a.C., THERMAL DEGRADATION OF LIGNIN – A REVIEW. CELLULOSE CHEMISTRY AND TECHNOLOGY **2010,** 44, 353-363.
108. Lundquist, K., Proton (1H) NMR Spectroscopy. In Lin, S.Y., Dence, C.W., eds.Methods in Lignin Chemistry, Springer Berlin Heidelberg: Berlin, Heidelberg, 1992; pp 242-249.
109. Lundquist, K., 1H NMR spectral studies on lignin. Nordic Pulp and Paper Research Journal **1992,** 3, 141-146.
110. Faix, O., Argyropoulos Dimitris, S., Robert, D., Neirinck, V., Determination of Hydroxyl Groups in Lignins Evaluation of 1H-, 13C-, 31P-NMR, FTIR and Wet Chemical

Methods. Holzforschung - International Journal of the Biology, Chemistry, Physics and Technology of Wood, 1994; Vol. 48, p 387.
111. Tiainen, E., Drakenberg, T., Tamminen, T., Kataja, K., Hase, A., Determination of Phenolic Hydroxyl Groups in Lignin by Combined Use of 1H NMR and UV Spectroscopy. Holzforschung, 1999; Vol. 53, p 529.
112. Robert, D., Carbon-13 Nuclear Magnetic Resonance Spectrometry. In Lin, S.Y., Dence, C.W., eds.Methods in Lignin Chemistry, Springer Berlin Heidelberg: Berlin, Heidelberg, 1992; pp 250-273.
113. Dimitris, S.A., Heteronuclear NMR Spectroscopy of Lignins. Lignin and Lignans, CRC Press: 2010; pp 245-265.
114. Sette, M., Wechselberger, R., Crestini, C., Elucidation of Lignin Structure by Quantitative 2D NMR. Chemistry – A European Journal **2011,** 17, 9529-9535.
115. Sun, S.L., Wen, J.L., Ma, M.G., Sun, R.C., Structural elucidation of sorghum lignins from an integrated biorefinery process based on hydrothermal and alkaline treatments. Journal of agricultural and food chemistry **2014,** 62, 8120-8.
116. Pu, Y., Cao, S., Ragauskas, A.J., Application of quantitative 31P NMR in biomass lignin and biofuel precursors characterization. Energy & Environmental Science **2011,** 4, 3154-3166.
117. B. Hames, R.R., C. Scarlata, A. Sluiter, J. Sluiter, and D. Templeton, Preparation of Samples for Compositional Analysis. NREL **2008**.
118. A. Sluiter, B.H., D. Hyman, C. Payne, R. Ruiz, C. Scarlata, J. Sluiter, D. Templeton, and J. Wolfe, Determination of Total Solids in Biomass and Total Dissolved Solids in Liquid Process Samples. **2008**.
119. A. Sluiter, B.H., R. Ruiz, C. Scarlata, J. Sluiter, and D. Templeton, Determination of Ash in Biomass. NREL **2005**.
120. Pan, X., Gilkes, N., Kadla, J., Pye, K., Saka, S., Gregg, D., Ehara, K., Xie, D., Lam, D., Saddler, J., Bioconversion of hybrid poplar to ethanol and co-products using an organosolv fractionation process: optimization of process yields. Biotechnology and bioengineering **2006,** 94, 851-61.
121. Glasser, W.G., Davé, V., Frazier, C.E., Molecular Weight Distribution of (Semi-) Commercial Lignin Derivatives. Journal of Wood Chemistry and Technology **1993,** 13, 545-559.
122. Tolbert, A., Akinosho, H., Khunsupat, R., Naskar, A.K., Ragauskas, A.J., Characterization and analysis of the molecular weight of lignin for biorefining studies. Biofuels, Bioproducts and Biorefining **2014,** 8, 836-856.
123. El Mansouri, N.E., Yuan, Q., Huang, F., CHARACTERIZATION OF ALKALINE LIGNINS FOR USE IN PHENOL-FORMALDEHYDE AND EPOXY RESINS. **2011**.
124. Santos, R.B., Hart, P., Jameel, H., Chang, H.-m., Wood Based Lignin Reactions Important to the Biorefinery and Pulp and Paper Industries. **2013**.
125. Nada, A.-A.M.A., Yousef, M.A., Shaffei, K.A., Salah, A.M., Infrared spectroscopy of some treated lignins. Polymer Degradation and Stability **1998,** 62, 157-163.
126. John, R., Larry, L.L., NMR of Lignins. Lignin and Lignans, CRC Press: 2010; pp 137-243.
127. Jakab, E., Faix, O., Till, F., Székely, T., Proceedings of the 10th International Conference on Fundamental Aspects, Processes and Applications of PyrolysisThe effect of cations on the thermal decomposition of lignins. Journal of Analytical and Applied Pyrolysis **1993,** 25, 185-194.
128. Ribas Batalha, L.A., Colodette, J.L., Gomide, J.L., Barbosa, L.C.A., Maltha, C.R.A., Borges Gomes, F.J., DISSOLVING PULP PRODUCTION FROM BAMBOO. **2011**.

129. Huang, C., He, J., Du, L., Min, D., Yong, Q., Structural Characterization of the Lignins from the Green and Yellow Bamboo of Bamboo Culm (Phyllostachys pubescens). Journal of Wood Chemistry and Technology **2016,** 36, 157-172.
130. Mendu, V., Shearin, T., Campbell, J.E., Stork, J., Jae, J., Crocker, M., Huber, G., DeBolt, S., Global bioenergy potential from high-lignin agricultural residue. Proceedings of the National Academy of Sciences **2012,** 109, 4014-4019.
131. Váquez-Torres, H., Canché-Escamilla, G., Cruz-Ramos, C.A., Coconut husk lignin. I. Extraction and characterization. Journal of Applied Polymer Science **1992,** 45, 633-644.
132. Wen, J.-L., Sun, S.-L., Xue, B.-L., Sun, R.-C., Quantitative structural characterization of the lignins from the stem and pith of bamboo (Phyllostachys pubescens). Holzforschung, 2013; Vol. 67, p 613.
133. Szmant, H.H., Organic Building Blocks of the Chemical Industry. **1989,** 3-7.
134. Briante, R., Patumi, M., Febbraio, F., Nucci, R., Production of highly purified hydroxytyrosol from Olea europaea leaf extract biotransformed by hyperthermophilic β-glycosidase. Journal of Biotechnology **2004,** 111, 67-77.
135. Wang, X., Rinaldi, R., Solvent Effects on the Hydrogenolysis of Diphenyl Ether with Raney Nickel and their Implications for the Conversion of Lignin. ChemSusChem **2012,** 5, 1455-1466.
136. Sergeev, A.G., Hartwig, J.F., Selective, Nickel-Catalyzed Hydrogenolysis of Aryl Ethers. Science **2011,** 332, 439-443.
137. Song, Q., Wang, F., Cai, J., Wang, Y., Zhang, J., Yu, W., Xu, J., Lignin depolymerization (LDP) in alcohol over nickel-based catalysts via a fragmentation-hydrogenolysis process. Energy & Environmental Science **2013,** 6, 994-1007.
138. Galkin, M.V., Samec, J.S.M., Selective Route to 2-Propenyl Aryls Directly from Wood by a Tandem Organosolv and Palladium-Catalysed Transfer Hydrogenolysis. ChemSusChem **2014,** 7, 2154-2158.
139. Zhang, J., Asakura, H., van Rijn, J., Yang, J., Duchesne, P., Zhang, B., Chen, X., Zhang, P., Saeys, M., Yan, N., Highly efficient, NiAu-catalyzed hydrogenolysis of lignin into phenolic chemicals. Green Chemistry **2014,** 16, 2432-2437.
140. Molinari, V. Ni-based materials for the catalytic conversion of lignocellulosic biomass into valuable products. phd phd, Universität Potsdam, Potsdam, 2015.
141. Song, Q., Wang, F., Xu, J., Hydrogenolysis of lignosulfonate into phenols over heterogeneous nickel catalysts. Chemical Communications **2012,** 48, 7019-7021.
142. Molinari, V., Clavel, G., Graglia, M., Antonietti, M., Esposito, D., Mild Continuous Hydrogenolysis of Kraft Lignin over Titanium Nitride–Nickel Catalyst. ACS Catalysis **2016,** 6, 1663-1670.
143. Thring, R.W., Chornet, E., Overend, R.P., Analysis of phenols from lignin depolymerization by capillary gas chromatography. Journal of Chromatography A **1989,** 467, 441-446.
144. Deepa, A.K., Dhepe, P.L., Lignin Depolymerization into Aromatic Monomers over Solid Acid Catalysts. ACS Catalysis **2015,** 5, 365-379.
145. Proestos, C., Komaitis, M., Analysis of Naturally Occurring Phenolic Compounds in Aromatic Plants by RP-HPLC Coupled to Diode Array Detector (DAD) and GC-MS after Silylation. Foods **2013,** 2, 90.
146. Coscia, C.J., Schubert, W.J., Nord, F.F., Investigations on Lignins and Lignification. XXIV.1a,b The Application of Hydrogenation, Hydrogenolysis, and Vapor Phase Chromatography in the Study of Lignin Structure. The Journal of Organic Chemistry **1961,** 26, 5085-5091.

147. Pepper, J.M., Lee, Y.W., Lignin and related compounds. II. Studies using ruthenium and Raney nickel as catalysts for lignin hydrogenolysis. Canadian Journal of Chemistry **1970,** 48, 477-479.
148. Pepper, J.M., Lee, Y.W., Lignin and related compounds. I. A comparative study of catalysts for lignin hydrogenolysis. Canadian Journal of Chemistry **1969,** 47, 723-727.
149. Pepper, J.M., Steck, W., THE EFFECT OF TIME AND TEMPERATURE ON THE HYDROGENATION OF ASPEN LIGNIN. Canadian Journal of Chemistry **1963,** 41, 2867-2875.
150. Barta, K., Matson, T.D., Fettig, M.L., Scott, S.L., Iretskii, A.V., Ford, P.C., Catalytic disassembly of an organosolv lignin via hydrogen transfer from supercritical methanol. Green Chemistry **2010,** 12, 1640-1647.
151. Jiang, Z., He, T., Li, J., Hu, C., Selective conversion of lignin in corncob residue to monophenols with high yield and selectivity. Green. Chem. **2014,** 16, 4257-4265.
152. Pecina, R., Burtscher, P., Bonn, G., Bobleter, O., GC-MS and HPLC analyses of lignin degradation products in biomass hydrolyzates. Fresenius' Zeitschrift für analytische Chemie **1986,** 325, 461-465.
153. Xie, P.-j., Huang, L.-x., Zhang, C.-h., Zhang, Y.-l., Phenolic compositions, and antioxidant performance of olive leaf and fruit (Olea europaea L.) extracts and their structure–activity relationships. Journal of Functional Foods **2015,** 16, 460-471.
154. Manach, C., Scalbert, A., Morand, C., Rémésy, C., Jiménez, L., Polyphenols: food sources and bioavailability. The American Journal of Clinical Nutrition **2004,** 79, 727-747.
155. De Leonardis, A., Aretini, A., Alfano, G., Macciola, V., Ranalli, G., Isolation of a hydroxytyrosol-rich extract from olive leaves (Olea Europaea L.) and evaluation of its antioxidant properties and bioactivity. European Food Research and Technology **2008,** 226, 653-659.
156. Guinda, Á., Castellano, J.M., Santos-Lozano, J.M., Delgado-Hervás, T., Gutiérrez-Adánez, P., Rada, M., Determination of major bioactive compounds from olive leaf. LWT - Food Science and Technology **2015,** 64, 431-438.
157. Paiva-Martins, F., Pinto, M., Isolation and characterization of a new hydroxytyrosol derivative from olive (Olea europaea) leaves. Journal of agricultural and food chemistry **2008,** 56, 5582-8.
158. Bouallagui, Z., Han, J., Isoda, H., Sayadi, S., Hydroxytyrosol rich extract from olive leaves modulates cell cycle progression in MCF-7 human breast cancer cells. Food and chemical toxicology : an international journal published for the British Industrial Biological Research Association **2011,** 49, 179-84.
159. Jemai, H., Bouaziz, M., Fki, I., El Feki, A., Sayadi, S., Hypolipidimic and antioxidant activities of oleuropein and its hydrolysis derivative-rich extracts from Chemlali olive leaves. Chemico-Biological Interactions **2008,** 176, 88-98.
160. Jemai, H., El Feki, A., Sayadi, S., Antidiabetic and Antioxidant Effects of Hydroxytyrosol and Oleuropein from Olive Leaves in Alloxan-Diabetic Rats. Journal of agricultural and food chemistry **2009,** 57, 8798-8804.
161. Pereira, A., Ferreira, I., Marcelino, F., Valentão, P., Andrade, P., Seabra, R., Estevinho, L., Bento, A., Pereira, J., Phenolic Compounds and Antimicrobial Activity of Olive (Olea europaea L. Cv. Cobrançosa) Leaves. Molecules **2007,** 12, 1153.
162. Le Floch, F., Tena, M.T., Ríos, A., Valcárcel, M., Supercritical fluid extraction of phenol compounds from olive leaves. Talanta **1998,** 46, 1123-1130.
163. Omar, S.H., Oleuropein in Olive and its Pharmacological Effects. Scientia Pharmaceutica **2010,** 78, 133-154.
164. Rigane, G., Bouaziz, M., Baccar, N., Abidi, S., Sayadi, S., Ben Salem, R., Recovery of hydroxytyrosol rich extract from two-phase Chemlali olive pomace by chemical treatment. Journal of food science **2012,** 77, C1077-83.

165. Strasser, H., Burgstaller, W., Schinner, F., High-yield production of oxalic acid for metal leaching processes by Aspergillus niger. FEMS Microbiology Letters **1994,** 119, 365-370.
166. Pace, V., Hoyos, P., Castoldi, L., Dominguez de Maria, P., Alcantara, A.R., 2-Methyltetrahydrofuran (2-MeTHF): a biomass-derived solvent with broad application in organic chemistry. ChemSusChem **2012,** 5, 1369-79.
167. Briante, R., Patumi, M., Terenziani, S., Bismuto, E., Febbraio, F., Nucci, R., Olea europaea L. Leaf Extract and Derivatives: Antioxidant Properties. Journal of agricultural and food chemistry **2002,** 50, 4934-4940.
168. Chang, Y., Antonietti, M., Fellinger, T.-P., Synthesis of Nanostructured Carbon through Ionothermal Carbonization of Common Organic Solvents and Solutions. Angewandte Chemie International Edition **2015,** 54, 5507-5512.
169. Shang, H., Lu, Y., Zhao, F., Chao, C., Zhang, B., Zhang, H., Preparing high surface area porous carbon from biomass by carbonization in a molten salt medium. RSC Advances **2015,** 5, 75728-75734.
170. Chieffi, G., Fechler, N., Esposito, D., Valorization of lignin waste from hydrothermal treatment of biomass: towards porous carbonaceous composites for continuous hydrogenation. RSC Advances **2015,** 5, 63691-63696.
171. Ma, Z., Zhang, H., Yang, Z., Zhang, Y., Yu, B., Liu, Z., Highly mesoporous carbons derived from biomass feedstocks templated with eutectic salt ZnCl2/KCl. Journal of Materials Chemistry A **2014,** 2, 19324-19329.
172. Porada, S., Schipper, F., Aslan, M., Antonietti, M., Presser, V., Fellinger, T.P., Capacitive Deionization using Biomass-based Microporous Salt-Templated Heteroatom-Doped Carbons. ChemSusChem **2015,** 8, 1867-74.
173. Liu, X., Zhou, Y., Zhou, W., Li, L., Huang, S., Chen, S., Biomass-derived nitrogen self-doped porous carbon as effective metal-free catalysts for oxygen reduction reaction. Nanoscale **2015,** 7, 6136-42.
174. Fechler, N. Salts as Highly Diverse Porogens: Functional Ionic Liquid-Derived Carbons and Carbon-Based Composites for Energy-Related Applications. phd phd, Universität Potsdam, Potsdam, 2012.
175. Sing, K.S.W., Everett, D.H., Haul, R.A.W., Moscou, L., Pierotti, R.A., Rouquerol, J., Siemieniewska, T., REPORTING PHYSISORPTION DATA FOR GAS SOLID SYSTEMS WITH SPECIAL REFERENCE TO THE DETERMINATION OF SURFACE-AREA AND POROSITY (RECOMMENDATIONS 1984). Pure and Applied Chemistry **1985,** 57, 603-619.
176. Saha, D., Li, Y., Bi, Z., Chen, J., Keum, J.K., Hensley, D.K., Grappe, H.A., Meyer, H.M., 3rd, Dai, S., Paranthaman, M.P., Naskar, A.K., Studies on supercapacitor electrode material from activated lignin-derived mesoporous carbon. Langmuir : the ACS journal of surfaces and colloids **2014,** 30, 900-10.
177. Saha, D., Payzant, E.A., Kumbhar, A.S., Naskar, A.K., Sustainable mesoporous carbons as storage and controlled-delivery media for functional molecules. ACS Appl Mater Interfaces **2013,** 5, 5868-74.
178. Roldán, L., Marco, Y., García-Bordejé, E., Bio-sourced mesoporous carbon doped with heteroatoms (N,S) synthesised using one-step hydrothermal process for water remediation. Microporous and Mesoporous Materials **2016,** 222, 55-62.
179. Fechler, N., Fellinger, T.-P., Antonietti, M., "Salt Templating": A Simple and Sustainable Pathway toward Highly Porous Functional Carbons from Ionic Liquids. Advanced Materials **2013,** 25, 75-79.
180. Pampel, J., Denton, C., Fellinger, T.-P., Glucose derived ionothermal carbons with tailor-made porosity. Carbon **2016,** 107, 288-296.

181. Yang, W., Fellinger, T.-P., Antonietti, M., Efficient Metal-Free Oxygen Reduction in Alkaline Medium on High-Surface-Area Mesoporous Nitrogen-Doped Carbons Made from Ionic Liquids and Nucleobases. Journal of the American Chemical Society **2011,** 133, 206-209.
182. Huang, M.-C., Teng, H., Nitrogen-containing carbons from phenol–formaldehyde resins and their catalytic activity in NO reduction with NH3. Carbon **2003,** 41, 951-957.
183. Burg, P., Fydrych, P., Cagniant, D., Nanse, G., Bimer, J., Jankowska, A., The characterization of nitrogen-enriched activated carbons by IR, XPS and LSER methods. Carbon **2002,** 40, 1521-1531.
184. Zhao, L., Baccile, N., Gross, S., Zhang, Y., Wei, W., Sun, Y., Antonietti, M., Titirici, M.-M., Sustainable nitrogen-doped carbonaceous materials from biomass derivatives. Carbon **2010,** 48, 3778-3787.
185. Yuan, H., Deng, L., Cai, X., Zhou, S., Chen, Y., Yuan, Y., Nitrogen-doped carbon sheets derived from chitin as non-metal bifunctional electrocatalysts for oxygen reduction and evolution. RSC Advances **2015,** 5, 56121-56129.
186. Gao, S., Chen, Y., Fan, H., Wei, X., Hu, C., Luo, H., Qu, L., Large scale production of biomass-derived N-doped porous carbon spheres for oxygen reduction and supercapacitors. Journal of Materials Chemistry A **2014,** 2, 3317-3324.
187. Dizhbite, T., Telysheva, G., Jurkjane, V., Viesturs, U., Characterization of the radical scavenging activity of lignins—natural antioxidants. Bioresource Technology **2004,** 95, 309-317.
188. Meng, Q.B., Weber, J., Lignin-based microporous materials as selective adsorbents for carbon dioxide separation. ChemSusChem **2014,** 7, 3312-8.
189. Suhas, Carrott, P.J., Ribeiro Carrott, M.M., Lignin--from natural adsorbent to activated carbon: a review. Bioresour Technol **2007,** 98, 2301-12.
190. Reed, A.R., Williams, P.T., Thermal processing of biomass natural fibre wastes by pyrolysis. International Journal of Energy Research **2004,** 28, 131-145.
191. Jeon, J.W., Zhang, L., Lutkenhaus, J.L., Laskar, D.D., Lemmon, J.P., Choi, D., Nandasiri, M.I., Hashmi, A., Xu, J., Motkuri, R.K., Fernandez, C.A., Liu, J., Tucker, M.P., McGrail, P.B., Yang, B., Nune, S.K., Controlling porosity in lignin-derived nanoporous carbon for supercapacitor applications. ChemSusChem **2015,** 8, 428-32.
192. Bouxin, F.P., David Jackson, S., Jarvis, M.C., Isolation of high quality lignin as a by-product from ammonia percolation pretreatment of poplar wood. Bioresource Technology **2014,** 162, 236-242.
193. Zhang, W., Zhang, J., Ren, S., Liu, Y., Palladium-catalyzed aromatic C-H bond nitration using removable directing groups: regiospecific synthesis of substituted o-nitrophenols from related phenols. J Org Chem **2014,** 79, 11508-16.
194. Lalitha, A., Sivakumar, K., Zeolite H-Y–Supported Copper(II) Nitrate: A Simple and Effective Solid-Supported Reagent for Nitration of Phenols and Their Derivatives. Synthetic Communications **2008,** 38, 1745-1752.
195. Wang, B., Recent development of non-platinum catalysts for oxygen reduction reaction. Journal of Power Sources **2005,** 152, 1-15.
196. Xing, T., Zheng, Y., Li, L.H., Cowie, B.C.C., Gunzelmann, D., Qiao, S.Z., Huang, S., Chen, Y., Observation of Active Sites for Oxygen Reduction Reaction on Nitrogen-Doped Multilayer Graphene. ACS Nano **2014,** 8, 6856-6862.
197. Upton, B.M., Kasko, A.M., Strategies for the Conversion of Lignin to High-Value Polymeric Materials: Review and Perspective. Chemical Reviews **2016,** 116, 2275-2306.
198. Pucciariello, R., Bonini, C., D'Auria, M., Villani, V., Giammarino, G., Gorrasi, G., Polymer blends of steam-explosion lignin and poly(ε-caprolactone) by high-energy ball milling. Journal of Applied Polymer Science **2008,** 109, 309-313.

199. Guo, Z.-X., Gandini, A., Pla, F., Polyesters from lignin. 1. The reaction of kraft lignin with dicarboxylic acid chlorides. Polymer International **1992,** 27, 17-22.
200. Guo, Z.-X., Gandini, A., Polyesters from lignin—2. The copolyesterification of kraft lignin and polyethylene glycols with dicarboxylic acid chlorides. European Polymer Journal **1991,** 27, 1177-1180.
201. Sivasankarapillai, G., McDonald, A.G., Li, H., Lignin valorization by forming toughened lignin-co-polymers: Development of hyperbranched prepolymers for cross-linking. Biomass and Bioenergy **2012,** 47, 99-108.
202. Van de Vyver, S., Roman-Leshkov, Y., Emerging catalytic processes for the production of adipic acid. Catalysis Science & Technology **2013,** 3, 1465-1479.
203. Voit, B., Beyerlein, D., Eichhorn, K.J., Grundke, K., Schmaljohann, D., Loontjens, T., Functional Hyper-Branched Polyesters for Application in Blends, Coatings, and Thin Films. Chemical Engineering & Technology **2002,** 25, 704-707.
204. Dunky, M., Urea–formaldehyde (UF) adhesive resins for wood. International Journal of Adhesion and Adhesives **1998,** 18, 95-107.
205. Pizzi, A., Orovan, E., Cameron, F.A., Cold-set tannin-resorcinol-formaldehyde adhesives of lower resorcinol content. Holz als Roh- und Werkstoff **1988,** 46, 67-71.
206. Steiner, P.R., Phenol–formaldehyde wood adhesive characterization by proton magnetic resonance spectroscopy. Journal of Applied Polymer Science **1975,** 19, 215-225.
207. Pizzi, A., Tannery row – The story of some natural and synthetic wood adhesives. Wood Science and Technology **2000,** 34, 277-316.
208. Stewart, D., Lignin as a base material for materials applications: Chemistry, application and economics. Industrial Crops and Products **2008,** 27, 202-207.
209. Mancera, C., El Mansouri, N.-E., Vilaseca, F., Ferrando, F., Salvado, J., THE EFFECT OF LIGNIN AS A NATURAL ADHESIVE ON THE PHYSICO-MECHANICAL PROPERTIES OF VITIS VINIFERA FIBERBOARDS. **2011**.
210. Mansouri, N.E.E., Pizzi, A., Salvado, J., Lignin-based polycondensation resins for wood adhesives. Journal of Applied Polymer Science **2007,** 103, 1690-1699.
211. Shiraishi, N., Recent Progress in Wood Dissolution and Adhesives from Kraft Lignin. Lignin, American Chemical Society: 1989; Vol. 397, pp 488-495.
212. Quanfu Yin, W.Y., Chengjun Sun, Mingwei Di, PREPARATION AND PROPERTIES OF LIGNIN-EPOXY RESIN COMPOSITE. BioResources **2012,** 7, 5737-5748.
213. Hiroo ITO, N.S., Epoxy Resin Adhesives from Thiolignin Mokuzai Gakkaishi **1987,** 33.
214. Umesh, P.A., Rajai, H.A., Vibrational Spectroscopy. Lignin and Lignans, CRC Press: 2010; pp 103-136.
215. Wang, J., Banu, D., Feldman, D., Epoxy-lignin polyblends: effects of various components on adhesive properties. Journal of Adhesion Science and Technology **1992,** 6, 587-598.